ON THE DESIGN OF AN ACOUSTICALLY ISOLATING BUBBLE SCREEN FOR THE CARR INLET ACOUSTIC RANGE

Kenneth William Marr

NAVAL POSTGRADUATE SCHOOL
Monterey, California

THESIS

ON THE DESIGN OF
AN ACOUSTICALLY ISOLATING BUBBLE SCREEN
FOR THE CARR INLET ACOUSTIC RANGE

by

Kenneth William Marr

June 1981

Thesis Advisor: J. V. Sanders

Approved for public release; distribution unlimited

REPORT DOCUMENTATION PAGE

READ INSTRUCTIONS BEFORE COMPLETING FORM

1. REPORT NUMBER

2. GOVT ACCESSION NO.

3. RECIPIENT'S CATALOG NUMBER

4. TITLE (and Subtitle)
On the Design of an Acoustically Isolating Bubble Screen for the Carr Inlet Acoustic Range

5. TYPE OF REPORT & PERIOD COVERED
Master's Thesis
June 1981

6. PERFORMING ORG. REPORT NUMBER

7. AUTHOR(s)
Kenneth William Marr

8. CONTRACT OR GRANT NUMBER(s)

9. PERFORMING ORGANIZATION NAME AND ADDRESS
Naval Postgraduate School
Monterey, California 93940

10. PROGRAM ELEMENT, PROJECT, TASK AREA & WORK UNIT NUMBERS

11. CONTROLLING OFFICE NAME AND ADDRESS
Naval Postgraduate School
Monterey, California 93940

12. REPORT DATE
June 1981

13. NUMBER OF PAGES
93

14. MONITORING AGENCY NAME & ADDRESS(if different from Controlling Office)

15. SECURITY CLASS. (of this report)
Unclassified

15a. DECLASSIFICATION/DOWNGRADING SCHEDULE

16. DISTRIBUTION STATEMENT (of this Report)
Approved for public release; distribution unlimited

17. DISTRIBUTION STATEMENT (of the abstract entered in Block 20, if different from Report)

18. SUPPLEMENTARY NOTES

19. KEY WORDS (Continue on reverse side if necessary and identify by block number)
acoustic isolation
acoustic reflection
bubble screen

20. ABSTRACT (Continue on reverse side if necessary and identify by block number)
The theoretical acoustic behavior of an underwater bubble screen was examined using Rayleigh reflection theory. A microcomputer model simulates the acoustic impedance mismatch at the interfaces of an ideal, bubble screen. A sensitivity analysis indicates that the angle of incidence of sound energy and the speed of sound in the layer are the most important screen properties for predicting the insulating capability of a bubble screen. In the neighborhood of

frequencies for which the screen thickness is an integral number of half wavelengths, the interference results in a reduced reflection coefficient and a corresponding increase in transmission through the screen. So that for a broad band spectrum wide enough to cover a number of such frequencies, the attenuation to be expected exceeds 10 dB only over about 90 percent of the spectrum. The interest for this work came from the need for a noise insulating screen at the Carr Inlet Acoustic Range.

Approved for public release; distribution unlimited

On the Design of an Acoustically Isolating Bubble Screen for the Carr Inlet Acoustic Range

by

Kenneth William Marr
Lieutenant, United States Navy
B.S., United States Naval Academy, 1974

Submitted in partial Fullfillment of the requirements for the degree of

MASTER OF SCIENCE IN ENGINEERING ACOUSTICS

from the

NAVAL POSTGRADUATE SCHOOL
June 1981

ABSTRACT

The theoretical acoustic behavior of an underwater bubble screen was examined using Rayleigh reflection theory. A microcomputer model simulates the acoustic impedance mismatch at the interfaces of an ideal, bubble screen. A sensitivity analysis indicates that the angle of incidence of sound energy and the speed of sound in the layer are the most important screen properties for predicting the insulating capability of a bubble screen. In the neighborhood of frequencies for which the screen thickness is an integral number of half wavelengths, the interference results in a reduced reflection coefficient and a corresponding increase in transmission through the screen. So that for a broad band spectrum wide enough to cover a number of such frequencies, the attenuation to be expected exceeds 10 dB only over about 90 percent of the spectrum. The interest for this work came from the need for a noise insulating screen at the Carr Inlet Acoustic Range.

TABLE OF CONTENTS

LIST OF TABLES

LIST OF FIGURES

I. INTRODUCTION

Acoustic trials of ships and submarines are conducted by Puget Sound Naval Shipyard (PSNS) at the Carr Inlet Acoustic Range in the state of Washington. According to Mr. John Kriebel of PSNS (personal communication) the measurements are often contaminated by noise generated by ship traffic in adjacent waters. One method which may offer noise isolation is a bubble screen located between the range and the offending noise source. Mr. Kriebel suggested that a feasibility study be conducted.

This thesis is one part of the study and has the objective of examining the theoretical benefits of a bubble screen, using a computer model based on Rayleigh reflection theory for an homogeneous layer. Recommendations and conclusions are made based on a literature search and a sensitivity analysis of the computer model. A companion thesis by LT Kelley examines the noise generated by the bubbles themselves.

The writer wishes to acknowledge the interest and support from the PSNS Carr Inlet Acoustic Range during this study.

II. BACKGROUND

A. RESONANCE BUBBLE THEORY

Experimental studies of the acoustic behavior of bubbles in water have been conducted for many years. Normally, when a single bubble is being studied, the resonance theory of gas bubble pulsations proposed by Minnaert in 1933 [Ref. 1] is considered. This theory shows that a gas bubble in water is capable of vibrations which become large at an exciting frequency, f, in hertz given by

$$f_{res} = \frac{1}{2\pi r}\sqrt{\frac{3\gamma P}{\rho}}$$

where,

γ = ratio of the specific heats of the gas
P = ambient hydrostatic pressure in pascals
ρ = density of water medium in kilograms per cubic meter
r = radius of the bubbles in meters

Table I shows the radius of a resonant bubble as a function of frequency f and depth z of concern at Carr Inlet.

TABLE I

Resonant Bubble Sizes

f \ z	0 m	50 m	100 m	150 m	200 m
10 Hz	0.32 m	0.79 m	1.08 m	1.3 m	1.5 m
100	0.032 m	0.079 m	0.108 m	0.13 m	0.15 m
1000	3.2 mm	7.9 mm	10.8 mm	13 mm	15 mm
10,000	0.32 mm	0.79 mm	1.08 mm	1.3 mm	1.5 mm

where $\rho = 1.03 \times 10^3$ kg/m^3
$P = 10^5 (1 + 0.1z)$ pascal
$\gamma = 1.40$

Carstenson and Foldy [Ref. 2] examined certain acoustic properties of bubble screens and demonstrated reasonable experimental agreement with the theory of resonance of bubbles in water.

Although resonance theory predicts very large attenuations of incident sound energy for bubbles in water, this attenuation is a very strong function of the bubble size. "75 percent of the energy lost by the sound wave is due to bubbles of radii within 10 percent of the resonant radii." [Ref. 3: p.13] A parameter used to describe bubble behavior is its extinction cross section (σ_e), the ratio of the energy lost from the sound wave to the intensity incident on the bubble. [Ref. 4] σ_e is made up of both absorption cross section (σ_a) and scattering cross section (σ_s) where

$$\sigma_e = \sigma_a + \sigma_s$$

For a plane wave propagating in a bubbly mixture, the attenuation, a, for bubbles of uniform radius r is [Ref. 5: p.615]

$$a = 4.34 \cdot \sigma_e \cdot n(r) \quad \text{in dB per meter}$$

where n(r) = number of bubbles per cubic meter of radius r

Medwin [Ref. 6] has indicated that "...at a resonance, the scattering and absorption cross sections of a typical bubble at sea are of the order 1000 times its geometric cross section."

Several points should be made here.

1. The sensitivity of attenuation on bubble sizes requires a precise control of bubble size.

2. As will be discussed later, even if bubbles of radius greater than 1 to 2 cm could be produced, these bubbles will rapidly become unstable and break up.

3. A bubble will expand monotonically as it rises to accomodate the decrease in hydrostatic pressure. A bubble of 1 mm radius at 100 m will expand to 3.2 mm at the surface and its resonance frequency will vary from 10 kHz to 1.0 kHz during its ascent.

4. MacPherson [Ref. 7] indicates that it is difficult to produce bubbles of a given size. Consequently, it is difficult to predict the attenuation obtainable from given bubble production mechanisms.

B. RAYLEIGH REFLECTION THEORY

For the above reasons and because of the difficulty of producing bubble resonance at low frequencies, this paper proposes to view the bubble screen as an homogeneous layer separating semi-infinite layers of bubble free water. Rayleigh reflection theory predicts that attenuation of sound energy by the layer of bubbles will be a function of layer width, angle of incidence, frequency, and the acoustic properties of the bubble layer. A layer of constant width will be used to simulate the bubble screen.

A sensitivity analysis will then indicate which parameters are of greatest concern in bubble layer design. The sound power transmission coefficient, α_T, will be the measure used to analyze these parameters. α_T is related to the sound power reflection coefficient α_R by the equation,

$$\alpha_T + \alpha_R = 1$$

C. MANUFACTURING BUBBLES

In the past, researchers used a variety of techniques to control the size of bubbles in screens. The methods attempted include electrolysis, [Ref. 8] microdispersers, [Ref. 9] porous porcelain filters, [Ref. 10] and perforated pipes. Exact bubble size was important to determine acoustic characteristics of scattering cross section, extinction cross section, resonance frequency, and other parameters. Several papers concerning bubble generation [Refs. 11, 12, 13, 14] indicate that some of the many factors controlling bubble size for perforated pipes include:

1. orifice size
2. pressure drop across the orifice
3. wetting of the orifice
4. contaminants in the media
5. angle of inclination of the orifice
6. rate of bubble formation

Uncertainties in these factors are the primary factors which will prevent accurate bubble size prediction for a bubble screen installation on a large scale such as at Carr Inlet.

D. BUBBLE HYDRODYNAMICS

Air bubbles in water exhibit complex hydrodynamic characteristics. However, their behavior can be categorized generally with respect to the bubble size. Initial bubble motion has been analyzed by Walters and Davidson [Refs. 15 and 16] and Bachhuber and Sanford [Ref. 17]. Gas diffusion from bubble affects bubble behavior significantly when the bubble diameter is small. The gas diffusion effect depends on the rate of ascent, the radius of the bubble and the difference between the gas concentrations across the bubble liquid interface. [Ref. 18: p. 714] There are two critical radii:

R_a = the radius above which the bubble grows monotonically in size as it ascends; gas leakage is not predominant

R_b = the radius below which the bubbles shrink and collapse bubbles whose radii lie between Ra and Rb are unpredictable.

Two bubbles of the same gas and size produced at the same depth can be affected differently by surfactants, causing one of the bubbles to grow and the other to shrink and collapse.

Bubbles of interest for a screen at Carr Inlet are in the 1-10 mm diameter range. This size has proven to be the easiest to produce via a perforated pipe. This method is also by far the most convenient and cost effective.

"Hydrostatic head has very little influence on the relation between the rate of formation and the size of the

bubble." [Ref. 19: p.17] VanKrevelen and Hoftijzer [Ref. 20: p.30] showed that "...the diameter of the bubbles is independent of flow rate and increases with the cube root of the orifice diameter." This statement breaks down at higher flow rates when gas jetting effects begin.

Crump [Ref. 21] suggests a differential pressure of 2-3 psi be established between pipe line pressure and hydrostatic water pressure. This should make the desired bubbles for forming the bubble screen. A bubble of radius 1mm will expand monotonically due to decreased hydrostatic pressure and will not be affected to a significant amount by gas diffusion and temperature effects. A 1 mm diameter bubble at 150 m depth will increase in size to 2.5 mm in ascending isothermally to the surface.

A sample calculation of this effect is shown in Table II and shows that this bubble will shift its resonant frequency by several kilohertz during its ascent.

TABLE II

Typical Bubble Size Expansion

RADIUS in mm (600 ft.)	RADIUS in mm (surface)	RESONANCE FREQUENCY in kHz (600 ft.)	(surface)
.200	.5	70.4	16.0
.500	1.23	28.2	6.4
1.0	2.5	14.1	3.2
2.0	4.9	7.0	1.6
10.0	24.6	1.4	.13

E. RISE OF BUBBLES

The rate of rise of bubbles has been thoroughly documented. [Refs. 22, 23, 24, 25] The speed at which a bubble rises depends primarily upon the size and shape of the bubble, and can be categorized as in Table III. [Ref. 26: p. 72]

TABLE III

Characteristics of Rising Bubbles

SHAPE	DIAMETER in MM	SPEED in cm/s	Re NUMBER	MOTION
spherical	.5	5-10	< 200	rectilinear
ellipsoidal	1-15	10-30	200<Re<4700	zig-zag helical oscillating
spherical-capped	>15	30-40	>4700	erratic unstable

Increasing bubble size causes:

1. increased coefficient of drag
2. increased vertical speed
3. nonlinear motion
4. oscillating motion
5. wake shedding

Turbulence seems to be the controlling factor in the motion of bubbles larger than 1.200 mm. [Ref. 27: p. 121] "Bubbles smaller than about 0.1 cm in water rise along smooth paths and do not generate any measureable sound when rising." [Ref. 28: p. 25]

Surface contaminants affect bubble behavior in many ways. These surfactants [Ref. 29] will have their greatest effect on the terminal speed of a bubble by affecting transition from rectilinear motion to oscillating motion. The bubble's wake structure is changed causing delayed boundary layer separation, delayed vortex shedding and smaller bubble wakes.

Terminal speed will be a function of bubble diameter, surfactants and Reynold's number. Approximate increase in vertical speed due to multiple bubbles range up to a factor of 1.5 times the single bubble velocities. [Ref. 30]

F. BUBBLE NOISE

Previous investigations [Ref. 31] show that greater than 90 percent of sound produced by bubbles in water occurs during bubble formation.

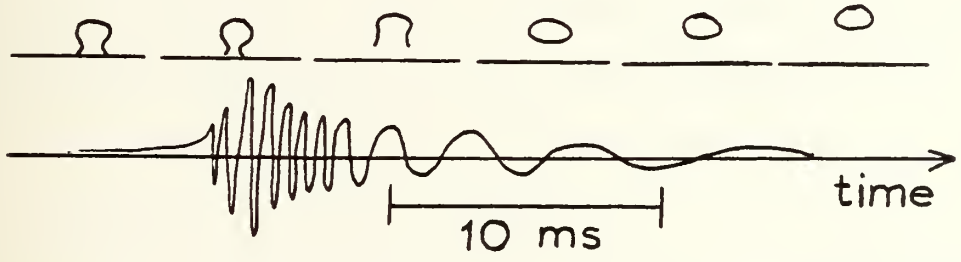

Figure 1. Sound produced by a bubble at an orifice

This sketch [Ref. 32: p. 23] correlates the process of an individual bubble leaving an orifice with the observed time variation of the radiant noise. The peak sound pressure occurs at the time the bubble separates from the orifice.

Strasberg [Ref. 33: p.24] predicted the peak sound pressure at distance d to be,

$$P_{rms} = \frac{1}{2d}\left(\frac{\rho c P_+ \dot{v} \delta_s}{\pi \delta}\right)^{1/2}$$

where, δ = total dissipation constant

δ_s = .014 for an air bubble in water

$\dot{v}$ = total volume rate of bubble formation

P_+ = excess pressure

This works out to be,

$$\simeq 132 \text{ dB re } 1 \mu\text{Pa at } 1 \text{ m.}$$

for a bubble rate of 10/sec for f = 1.0 kHz

After separation, larger bubbles generate continuous sound levels of relatively small amplitude (46 to 66 dB re 1 μPa at 1m). [Ref. 34: p.25]
This is apparently due to oscillations induced by their irregular flow path. Smaller bubbles produce less or immeasurable sound when rising. The coalescing of bubbles cause one tenth the sound of bubble formation.

G. PROPERTIES OF BUBBLE SCREENS

Studies on the acoustic theory of bubbles and bubble screens were done during World War II. [Refs. 35, 36, 37] Efforts in the United States were concentrated through the National Defense Research Committee (NDRC) under a broad research program supported by the Office of Scientific Research and Development (OSRD). The prominent NDRC organizations whose findings were published by the U.S.

Navy after the war as NDRC Summary Technical Reports were the University of California Division of War Research (UCDWR), the Columbia University Division of War Research, the Columbia University Sonar Analysis Group, and the Woods Hole Oceanographic Institution. The UCDWR was the largest of the associated groups and came to be known as the Sonar Data Division, accounting for a significant amount of empirical studies on ship's wakes, scattering and absorption of bubbles, and sound transmission through bubble screens. Carstenson and Foldy were part of this effort and in 1947 they published their study of the propagation of sound through a bubble screen. Their screen was approximately 17 in. long and 10 ft. high with thickness varying from 3 in. to 6 in. The pulsed screen was analyzed as if bubbles were uniformly distributed between two infinite parallel planes and the speed of sound in the screen was assumed to be approximately the same as that of water.

For the case of continuous - flow screens, the bubbles were of varying sizes and speed of sound in the layer considerably different from that in water.

Their results supported the resonant bubble theory for pulse screens at frequencies from 15 kHz to 35 kHz. However, their data from 5 kHz to 45 kHz for continuous flow screens of bubbles of varying sizes were not very satisfactory.

Throughout their study, the thickness of the screen was assumed to be the arithmetic average of the observed layer width. The density of the screen was based on observations of the average number of bubbles present per unit volume and of the average bubble size.

For the continuous flow case, the screen had a "..fairly sharply defined core of larger bubbles...but in front and back there is a gradually tapering distribution of smaller bubbles." [Ref. 38: p.501] As a result, the speed of sound was a gradually changing function of the distance normal to the layer interface plane causing reduced reflections of sound.

Wood and Spitzer [Refs. 39,40] proposed theoretical sound speeds which would occur for given concentrations of air by volume in water. Figure 2 illustrates those results and experimental verification by others. [Refs. 41, 42] For concentrations between 10^{-2} and 10^{-3}, readily obtainable in the laboratory or in the field, sound speeds as low as 100 - 300 m/sec are found.

H. APPLICATIONS OF LAYERS

There are extensive studies of the reflection and transmission of energy in layered media. [Refs. 45, 46] Numerous applications of the use of layers range from reflection reduction for optical lens coatings to absorbent materials for architectural acoustics. The ratio of layer thickness to the wavelength of the energy in the layer is a very significant parameter due to the standing wave pattern produced.

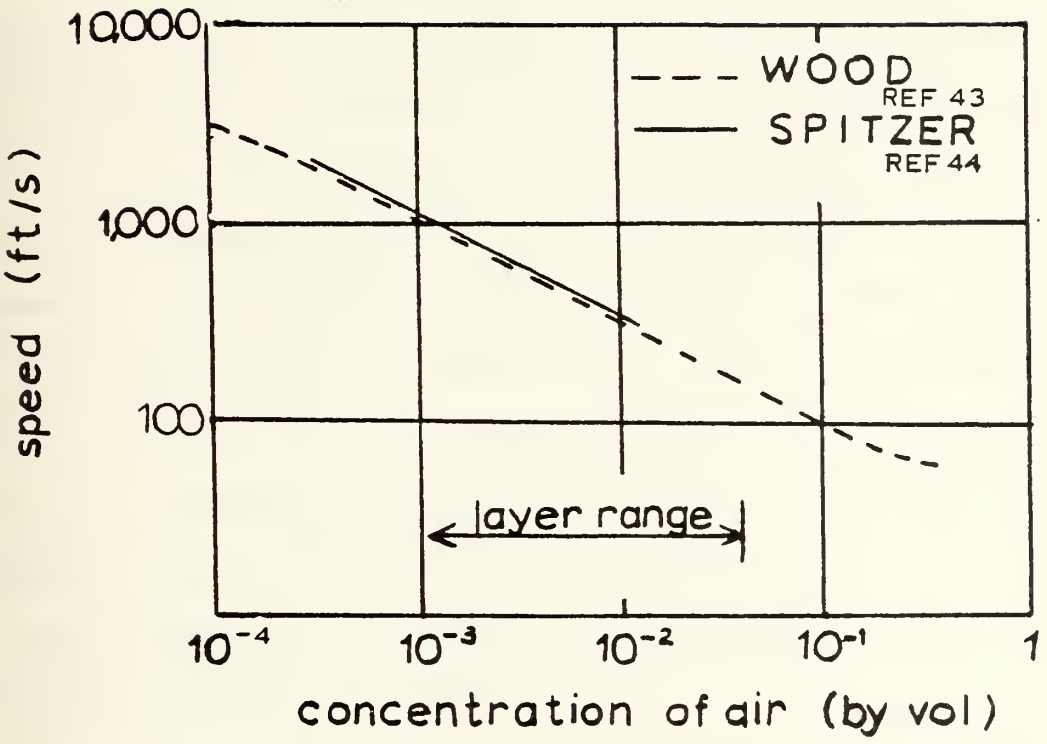

Figure 2. Sound speed in air-water mixtures

III. BUBBLE LAYER AT CARR INLET

A. OCEANOGRAPHIC CHARACTERISTICS

The chart of Carr Inlet Acoustic Range in Appendix A indicates a large, irregularly shaped area surrounding the test site. The site is roughly 5 nm long and 3 nm wide. It is proposed to consider in this study a bubble screen crossing the mouth of the inlet, a distance of approximately 2900 m. This position places the screen directly between commercial boat traffic to the southeast and the test site.

The water depth at this position varies from approximately 450 ft. at the relatively level bottom at the middle of the inlet, to relatively steep shore gradients approaching Fox Island and McNeil Island as shown in Figure 3.

The frequencies of interest for attenuation will be broadband (100 Hz to 10 kHz+).

Oceanographic studies [Ref. 47] at Carr Inlet indicate that the tides and currents which are likely to be encountered will be variable but less than one-half kt. There is no significant evidence for underground springs or bottom currents which would cause any significant salinity or temperature gradients. Seasonal variations in water temperature and salinity occur due to the annual air temperature cycles and rain runoff. However, no significant

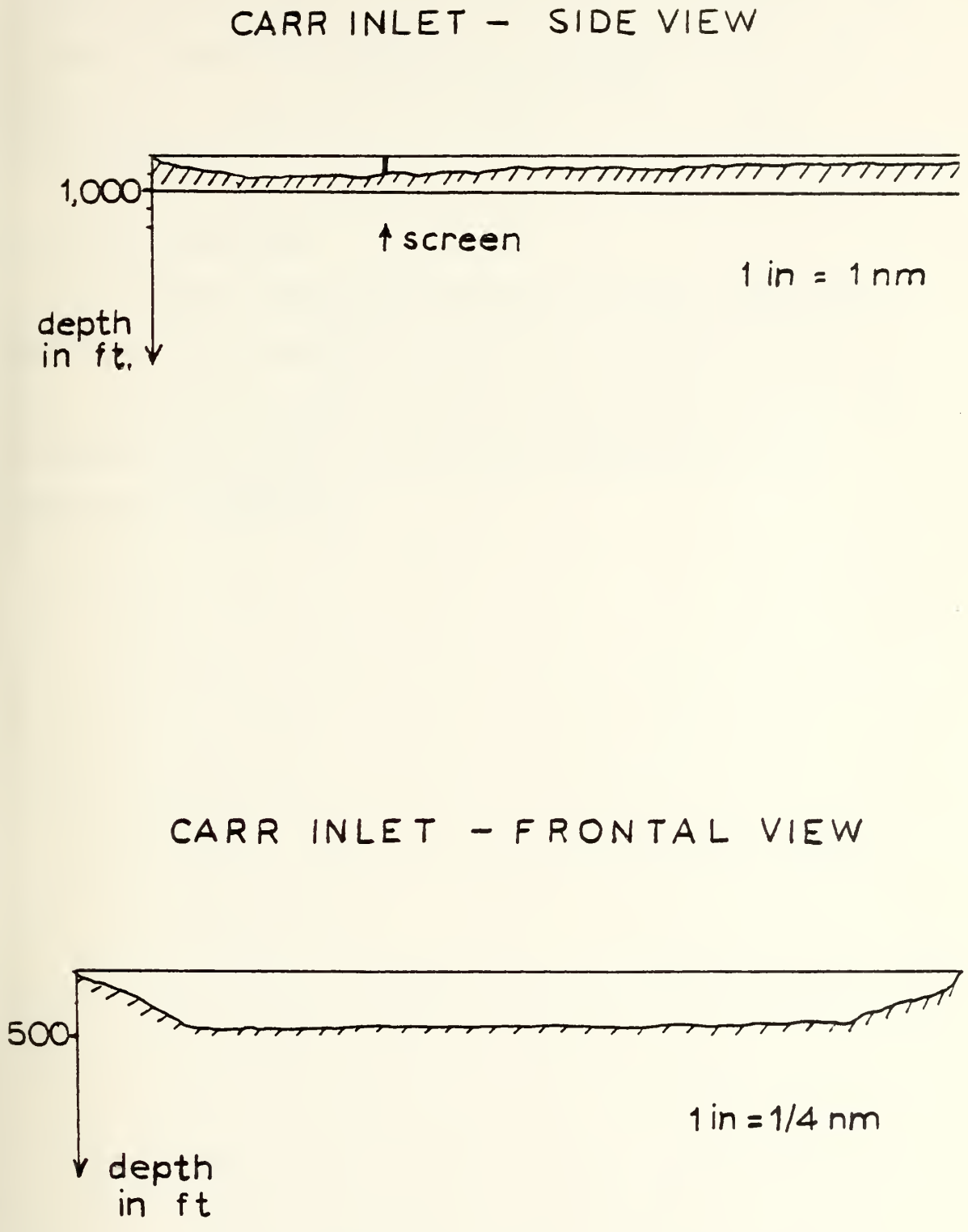

Figure 3. Position of bubble screen in sensitivity analysis.

impact is anticipated on the sound velocity profile. So, for the distances encountered in this application, the sound speed in water will be assumed to be constant (C = 1500 m/s).

B. SCREEN POSITION

Considering these oceanographic factors, the bubble screen will be assumed to be produced at the bottom of the inlet and to rise vertically with constant width. An estimation for actual layer width spreading will be presented in Chapter V.

IV. SENSITIVITY ANALYSIS

A. THEORY

At frequencies removed from the resonant frequency of the bubbles, a bubble layer is expected to reflect sound as a result of two interrelated effects on the acoustic properties of the medium. [Ref. 48: P.925] First, the compressibility of the water is changed with the introduction of the bubbles which in turn changes the sound speed in the layer. Second, density will be changed. For the bubble concentrations considered in this thesis, this latter change is small and the principal acoustic characteristic of the bubble layer will be its sound speed. The sound speed in bubble layers was addressed by Wood [Ref. 49] whose work was confirmed experimentally by Silberman. [Ref. 50: p.90]

In the present work, the acoustic effect of a bubble screen will be analyzed in terms of the sound power transmission coefficient using a computer simulation of the bubble screen. As indicated earlier, this computer simulation will be based on Rayleigh reflection theory for an homogeneous layer of bubbly water with constant thickness.

Rayleigh reflection theory is based on a solution of a system of acoustic equations, describing the conditions that must be satisfied at each boundary of the layer.

The boundary conditions at the interfaces are continuity of the acoustic pressure and of the normal component of the particle velocity.

For oblique incidence and when the media in front and behind the layer are the same, the sound power transmission coefficient α_T reduces to [Ref. 51],

$$\alpha_T = \frac{1}{\left(\cos^2(b_2 h) + \frac{(m_1+m_2)^2}{4}\sin^2(b_2 h)\right)} \qquad (1)$$

This coefficient represents the ratio of the intensity of the transmitted sound to the intensity of the incident sound.

The geometry of the problem is shown in Figure 4, and

$$m_1 = \frac{\rho_2 c_2 \cos\theta_1}{\rho_1 c_1 \cos\theta_2}$$

$$m_2 = \frac{\rho_3 c_3 \cos\theta_2}{\rho_2 c_2 \cos\theta_3}$$

$$b_2 = 2\pi f \frac{\cos\theta_2}{c_2}$$

θ_n measured from normal to interface, n = 1,2,3

1....incident layer

2....screen layer

3....exit layer

h = layer thickness

$$\rho_1 = \rho_3 \simeq \rho_2$$

and by Snell's law:

$$\frac{c_1}{c_2} = \frac{\sin\theta_1}{\sin\theta_2}$$

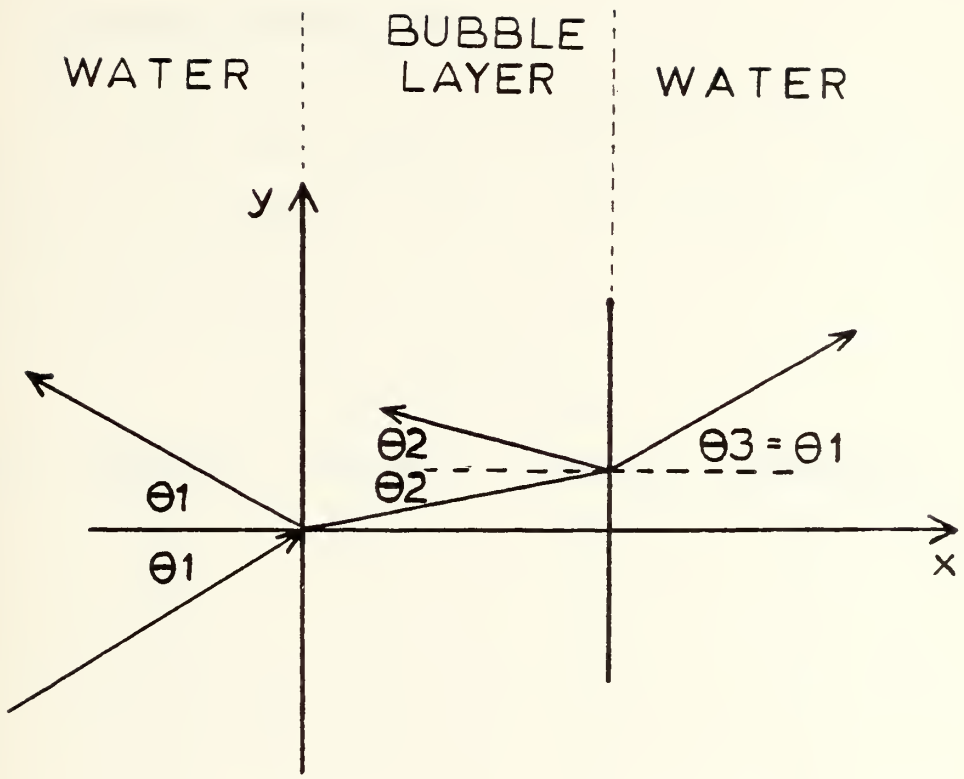

Figure 4. Bubble layer reflection geometry

α_T is a function of width and acoustic impedance of the layer and depends on the angle of incidence and frequency of the incident sound.

The subsequent sensitivity analysis will indicate the theoretical performance expected when parameters vary.

B. SENSITIVITY ANALYSIS RESULTS

1. Parameter description

Data were taken using the options in Table IV. A change in symbols was required for use in the computer model. The new symbols used to represent the parameters are also listed for the options in Table IV.

TABLE IV

Analysis Options

OPTION	ORDINATE	ABSCISSA	CONSTANT	PARAMETER
1	T3	L2	A1	A
2	T3	A1	L2	A
3	T3	A1	A	L2
4	T3	L2	A	A1
5	T3	A	L2	A1
6	T3	A	A1	L2

where,

T3 = sound power transmission coefficient

L2 = layer width divided by the wavelength in layer

A1 = incident angle

A = sound speed ratio C_{layer} / C_{water}

Each of these options will be addressed in the following analysis. Values of A and their corresponding fraction volume of air bubbles are shown in Table V.

TABLE V

Sound speed ratios for given air concentrations

A	Fraction by volume of air in water
0.5	2×10^{-4}
0.4	5×10^{-4}
0.3	8×10^{-4}
0.2	2×10^{-3}
0.1	8×10^{-3}

These values of A may reasonably be expected in a practical bubble screen.

The value of L2 was obtained by incorporating a normalization factor which forced the data to repeat itself after L2 reached a value of 1.0. This was done for ease in plotting and clarity in data presentation. The normalization factor L1 is found by noting that in Eq. (1),

$$\alpha_T = 1, \quad \text{for} \quad b_2 h = n\pi \qquad n = 0, 1, 2, \ldots$$

for what values of layer width/wavelength $\left(\frac{h}{\lambda_{(\text{in layer})}}\right)$?

$$\frac{2\pi f}{c_2} h \cos\theta_2 = n\pi$$

Let n = 1,

$$\frac{2f}{f\lambda_2} h \cos\theta_2 = 1$$

where $L1 = \frac{h}{\lambda_2}$ and, by Snell's Law, $\cos\theta_2 = \sqrt{1 - A^2 \sin^2\theta_1}$

Therefore, $L1 = 1/(2\sqrt{1 - A^2 \sin^2\theta_1})$ and $L2 = \frac{h}{\lambda_2 L1}$

2. The Computer Program

The WANG SYSTEM 2200S desk top computer was used to run the analysis and provide data output. The program, "OPT6", was written in BASIC language and provides a definition of the variables and symbols at the beginning of the program.

The plotting option is selected when the program is executed. Each option has its own subroutine which interrogates the operator for the bubble screen parameters required to produce the selected data output. Step sizes for all the parameters are pre-selected. The sound power transmission coefficient is plotted vertically against the changing option parameters.

3. Option 1

When the sound power transmission coefficient is plotted against the normalized layer ratio, T3 cycles between maxima and minima. Minimum sound power is transmitted through the layer at odd integer multiples of one-quarter wavelengths. Figures 5 to 10 show the dependence of T3 on L2 of a fixed A1 for a variety of values of A.

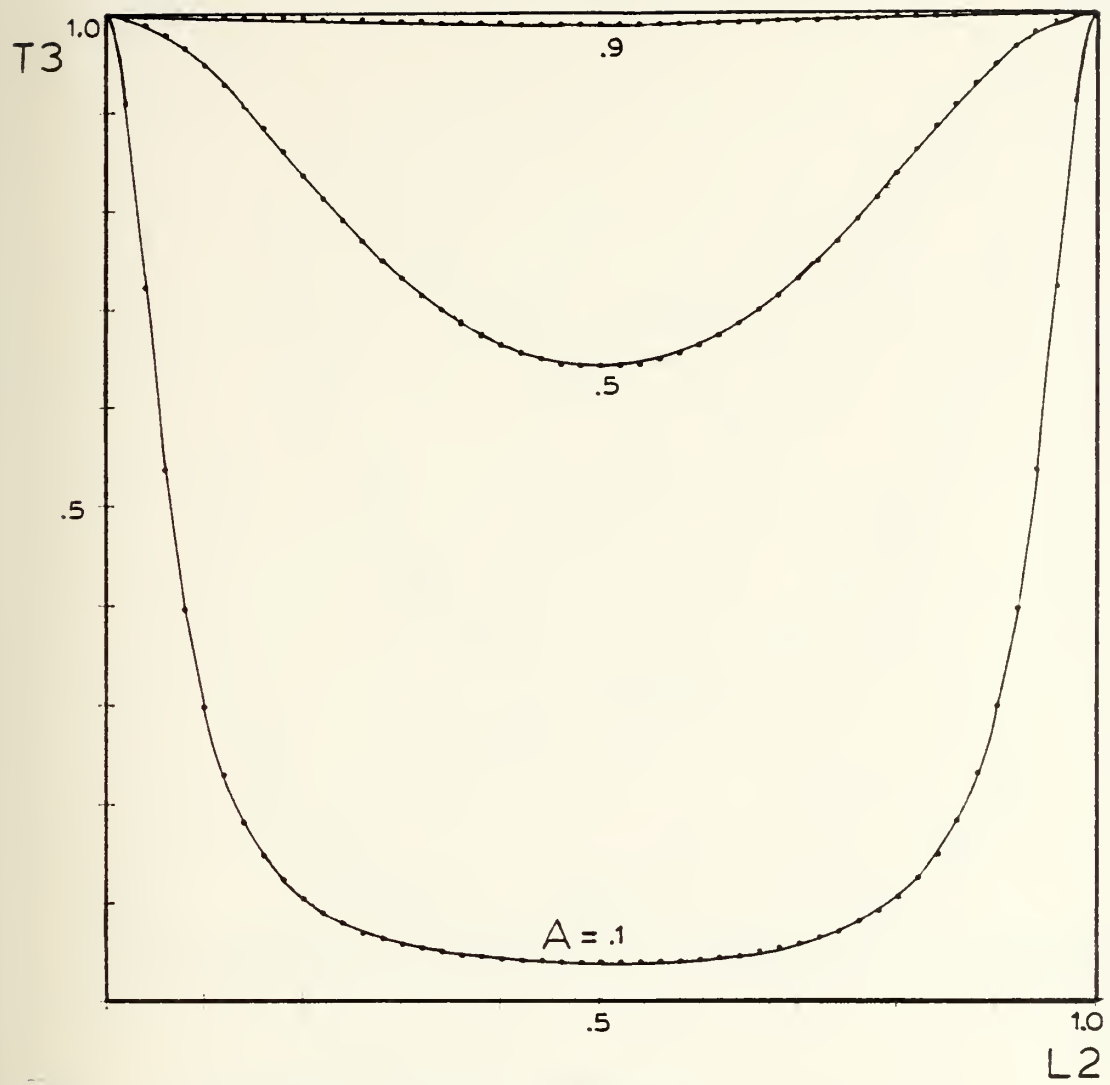

A = SOUND SPEED RATIO

A1 = INCIDENT ANGLE

L2 = LAYER WIDTH/WAVELENGTH RATIO

T3 = SOUND POWER TRANSMISSION COEFFICIENT

Figure 5. Sound power transmission coefficient vs. layer ratio, parameter A for constant A1 = 0^{o}

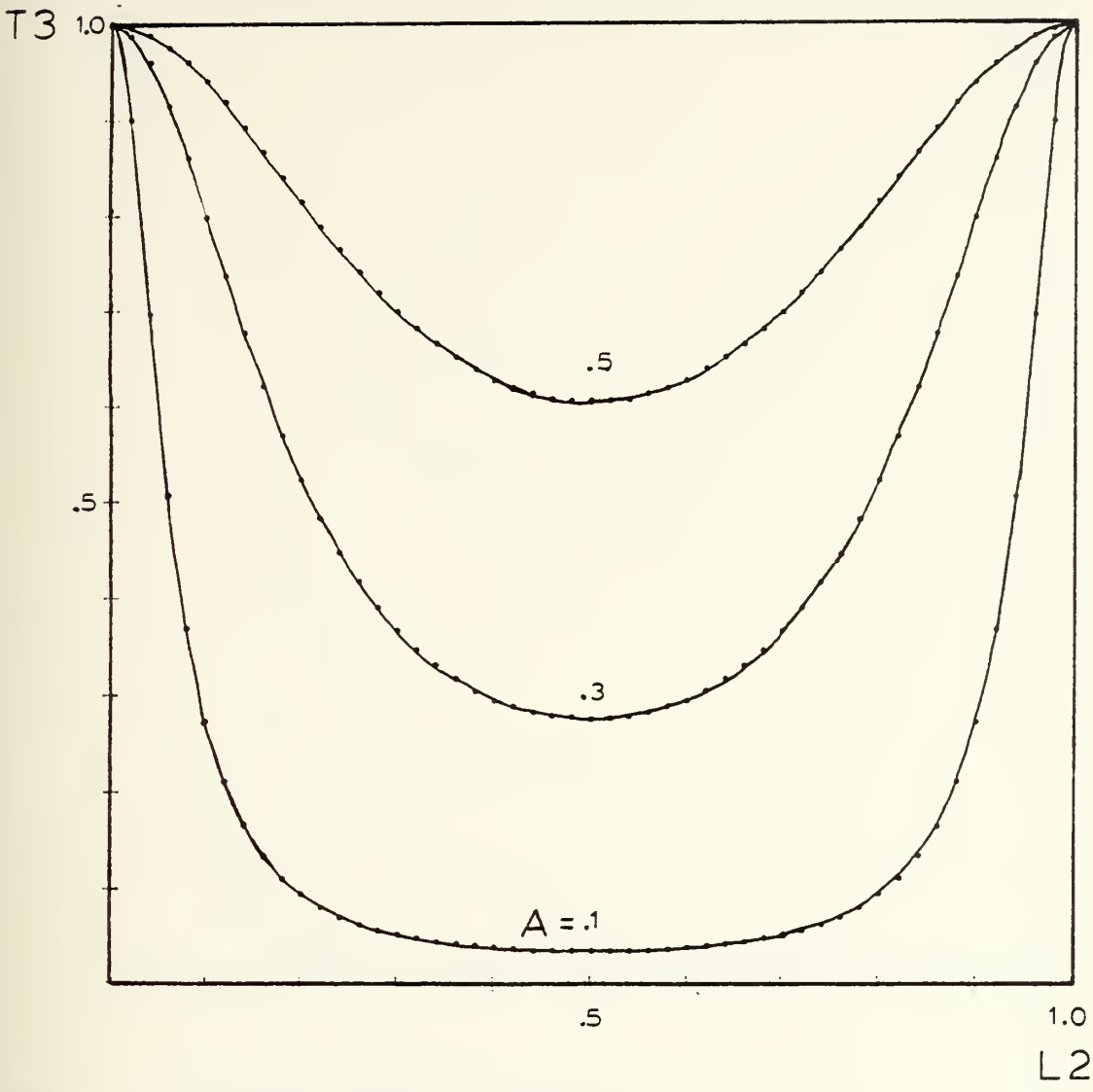

A = SOUND SPEED RATIO

A1 = INCIDENT ANGLE

L2 = LAYER WIDTH/WAVELENGTH RATIO

T3 = SOUND POWER TRANSMISSION COEFFICIENT

Figure 6. Sound power transmission coefficient vs. layer ratio, parameter A for constant A1 = 20°

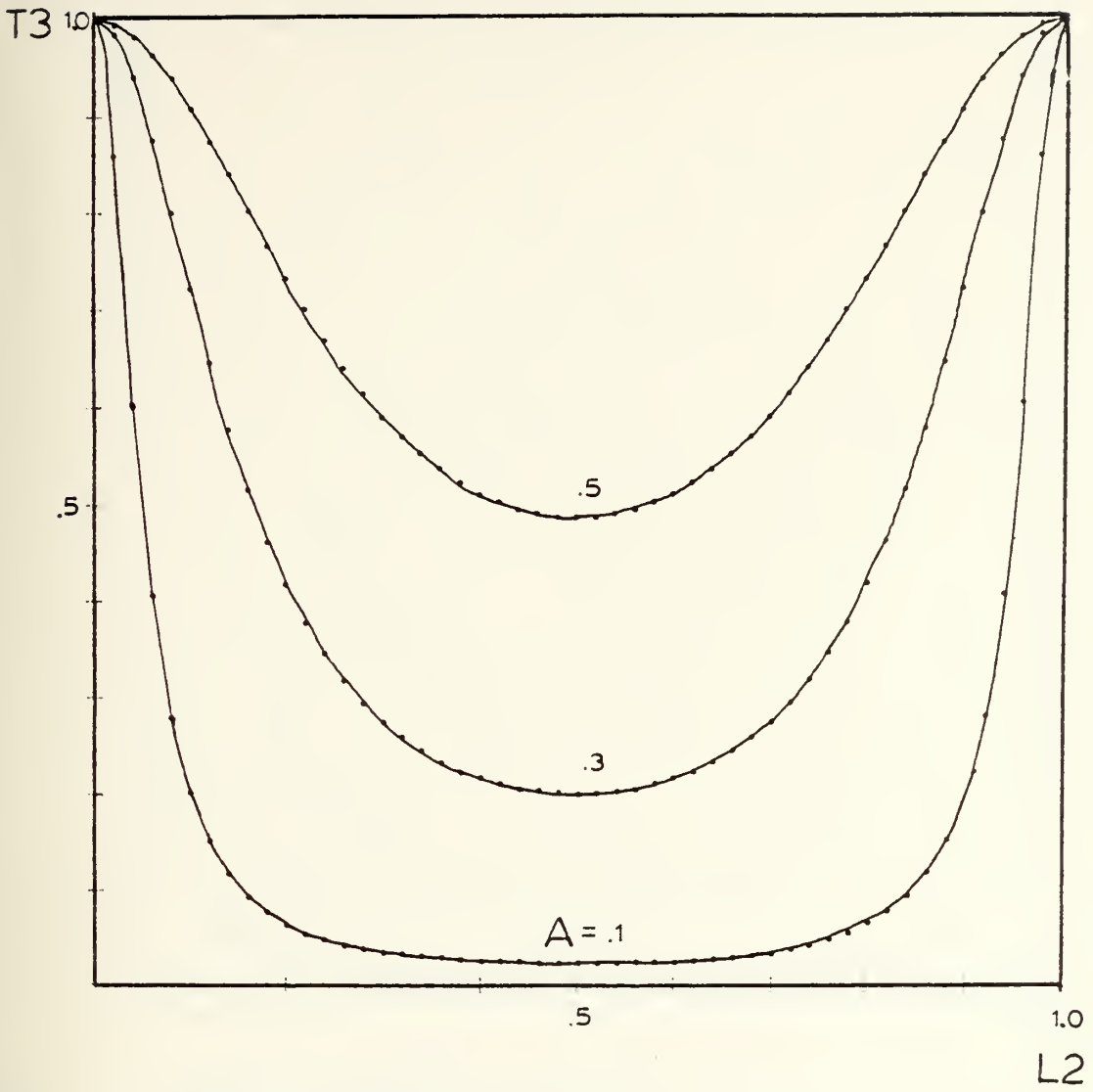

A = SOUND SPEED RATIO

A1 = INCIDENT ANGLE

L2 = LAYER WIDTH/WAVELENGTH RATIO

T3 = SOUND POWER TRANSMISSION COEFFICIENT

Figure 7. Sound power, transmission coefficient vs. layer ratio, parameter A for constant A1 = 40°

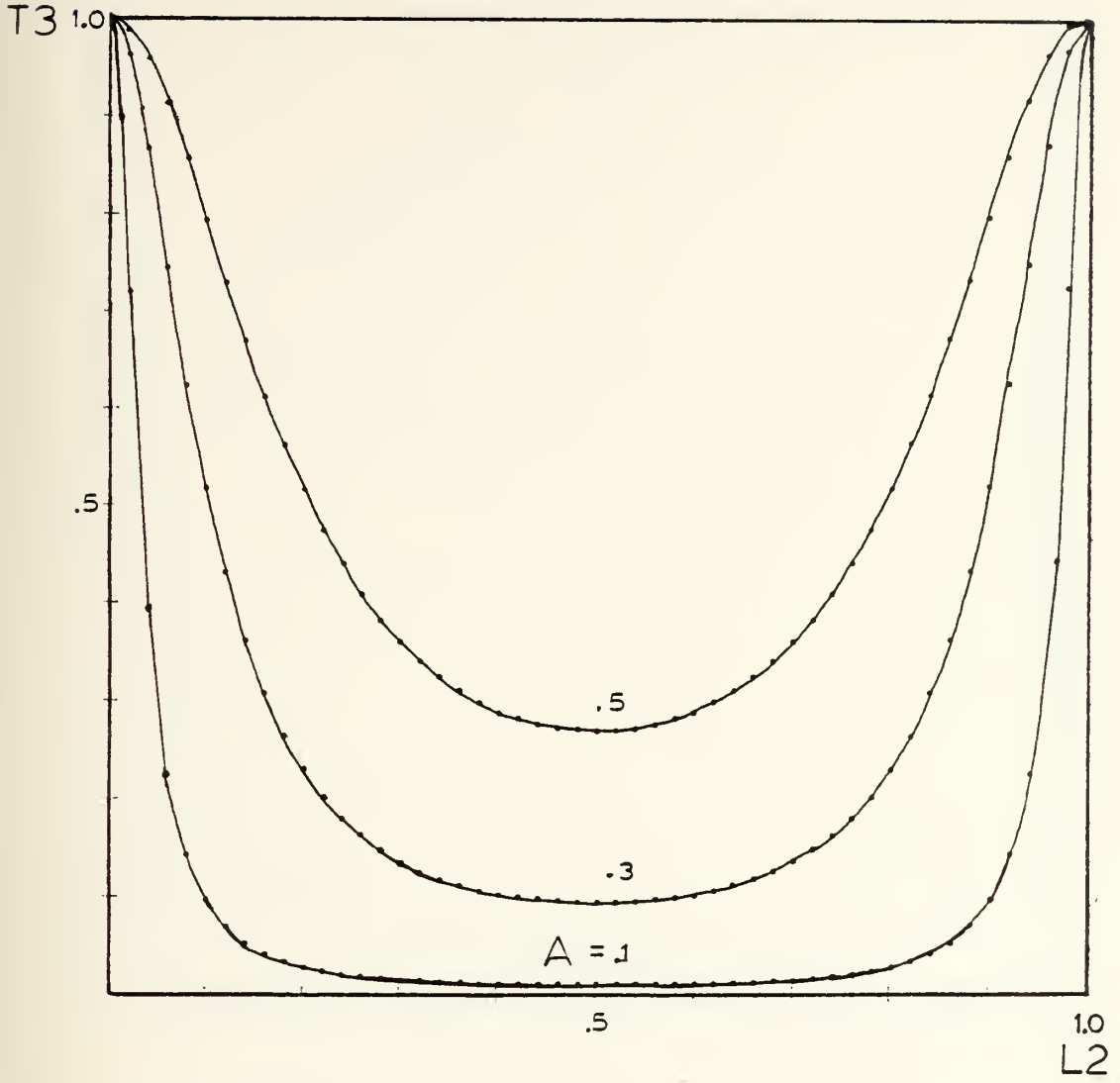

A = SOUND SPEED RATIO

A1 = INCIDENT ANGLE

L2 = LAYER WIDTH/WAVELENGTH RATIO

T3 = SOUND POWER TRANSMISSION COEFFICIENT

Figure 8. Sound power transmission coefficient vs. layer ratio, parameter A for constant A1 = 60°

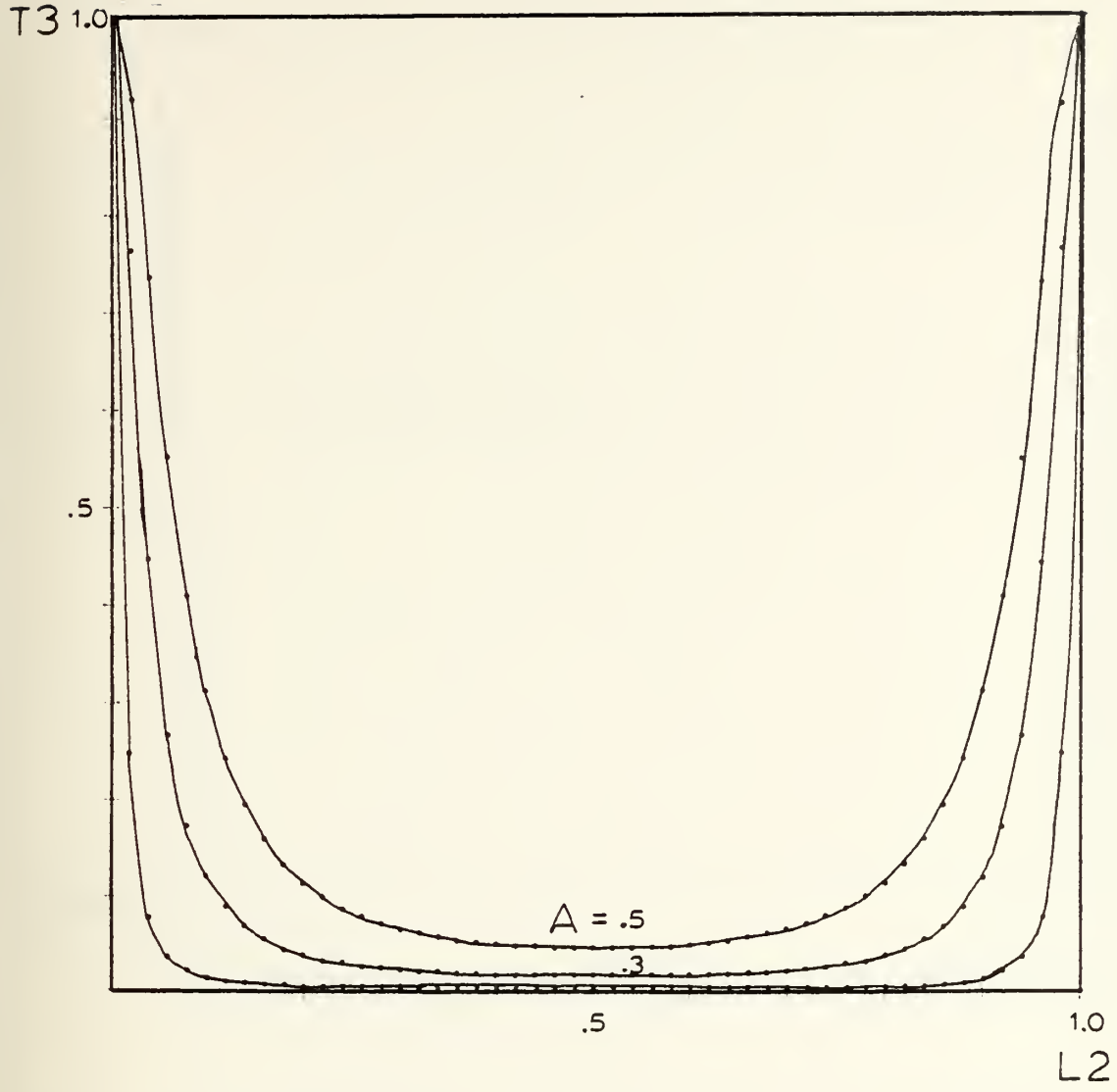

A = SOUND SPEED RATIO

A1 = INCIDENT ANGLE

L2 = LAYER WIDTH/WAVELENGTH RATIO

T3 = SOUND POWER TRANSMISSION COEFFICIENT

Figure 9. Sound power, transmission coefficient vs. layer ratio, parameter A for constant A1 = 80°

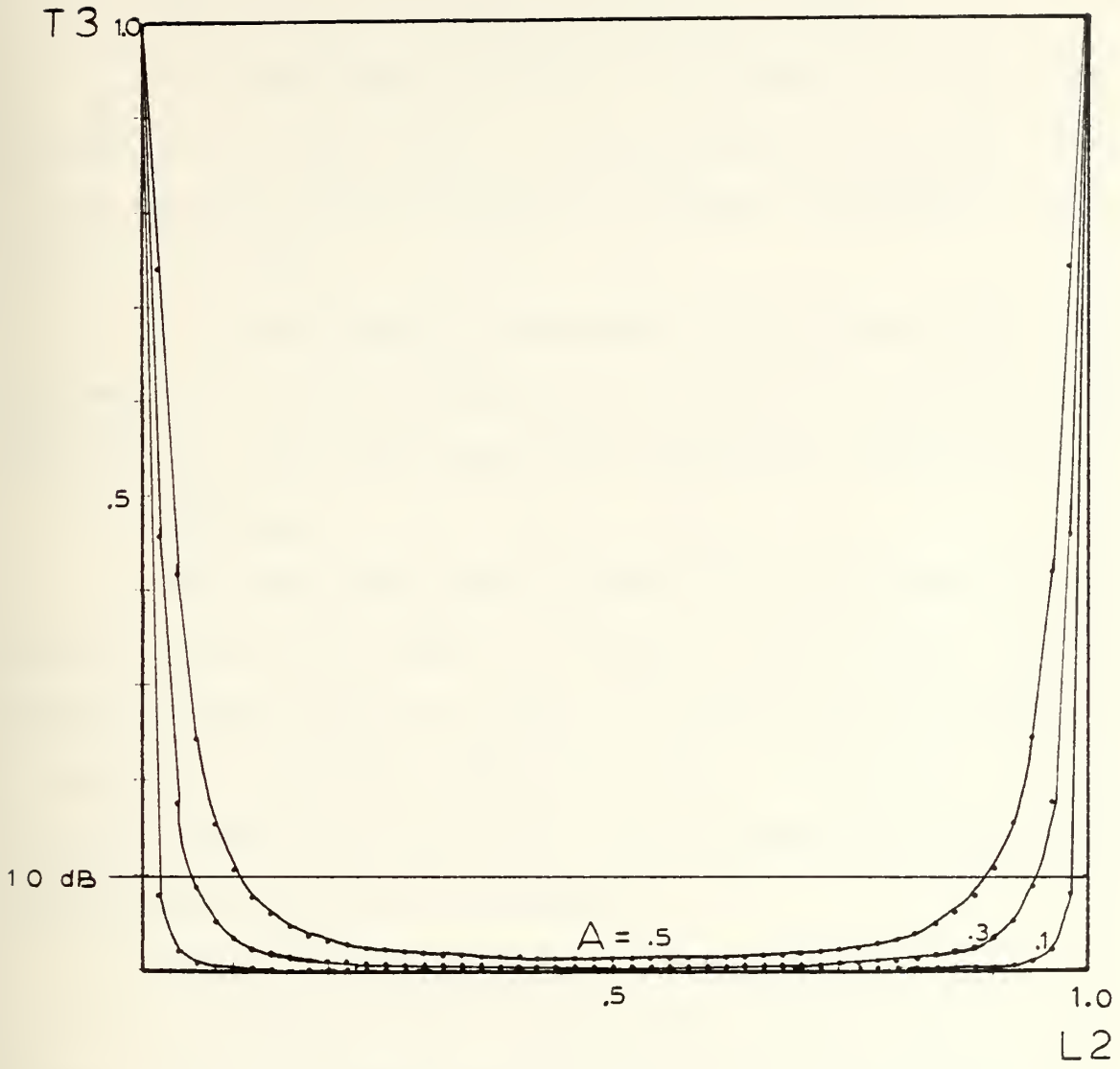

A = SOUND SPEED RATIO

A1 = INCIDENT ANGLE

L2 = LAYER WIDTH/WAVELENGTH RATIO

T3 = SOUND POWER TRANSMISSION COEFFICIENT

Figure 10. Sound power transmission coefficient vs. layer ratio, parameter A for constant A1 = 85°

The following observations can be made:

a. Regardless of angle of incidence, if the sound speed ratio is less than 0.1, attenuation of at least 10dB can be expected over at least the middle 75 percent of the layer ratio range.

b. Regardless of the sound ratio or the angle of incidence, there will always be at least 5-10 percent of the layer ratio which will have only negligible attenuation.

4. Option 2

When the sound power transmission coefficient is plotted against the angle of incidence, the maximum transmission always occurs at normal incidence and the minimum transmission at angles approaching 90^{o}. Figures 11 to 16 are plots with the layer ratio held constant and the sound speed ratio varied as a parameter.

The following observations can be made:

a. When the sound speed ratio reaches 0.1, at least 10dB attenuation can be expected over all angles of incidence and over at least 75 percent of the layer ratio range.

b. The only values of sound speed which will give a uniform value of attenuation over all angles of incidence are speed ratios of less than 0.1. This situation would require the bubble screen to maintain a volume fraction of air to water of greater than approximately 10^{-2}.

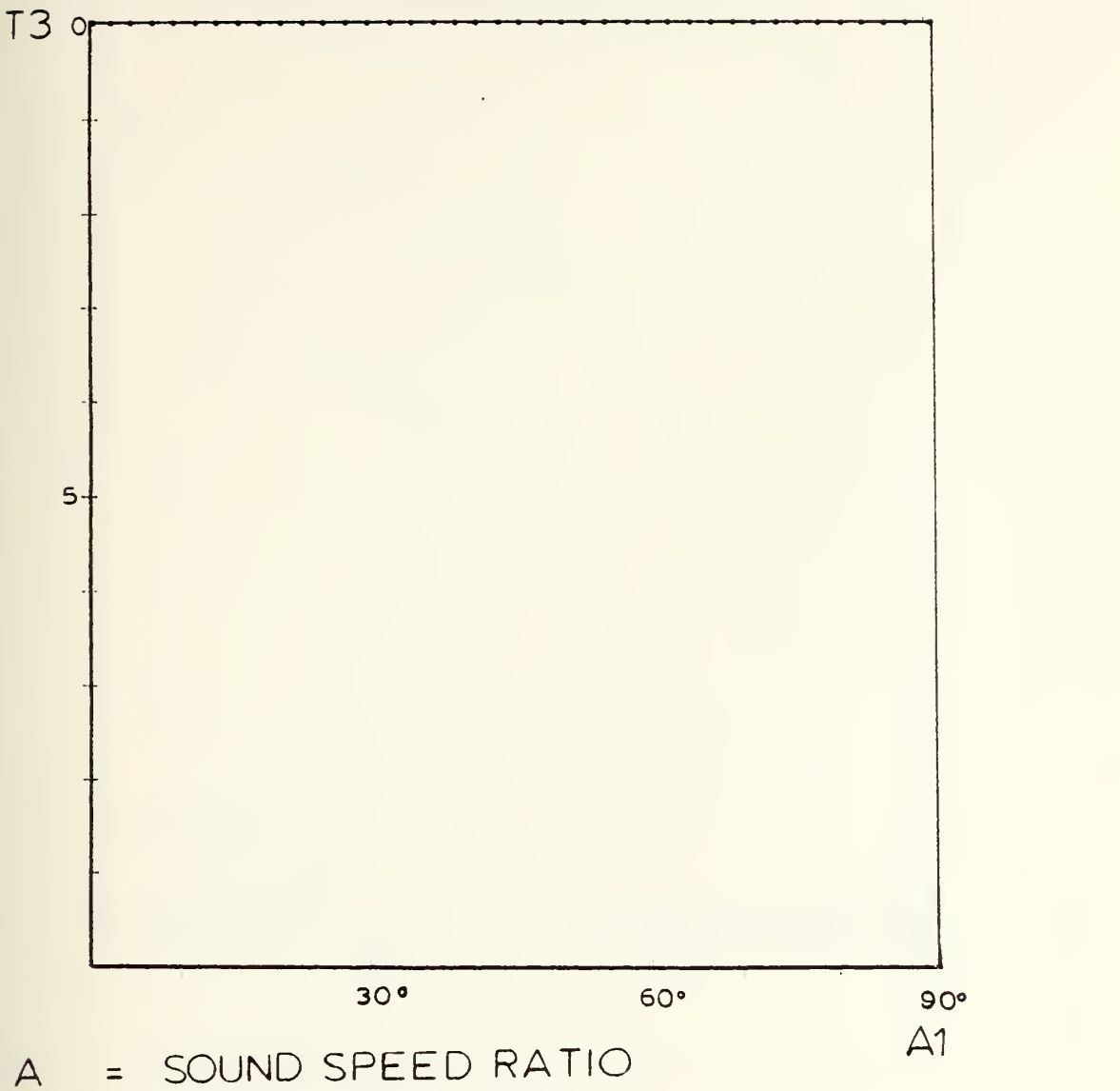

Figure 11. Sound power transmission coefficient vs. incident angle, parameter A for constant L2 = 0

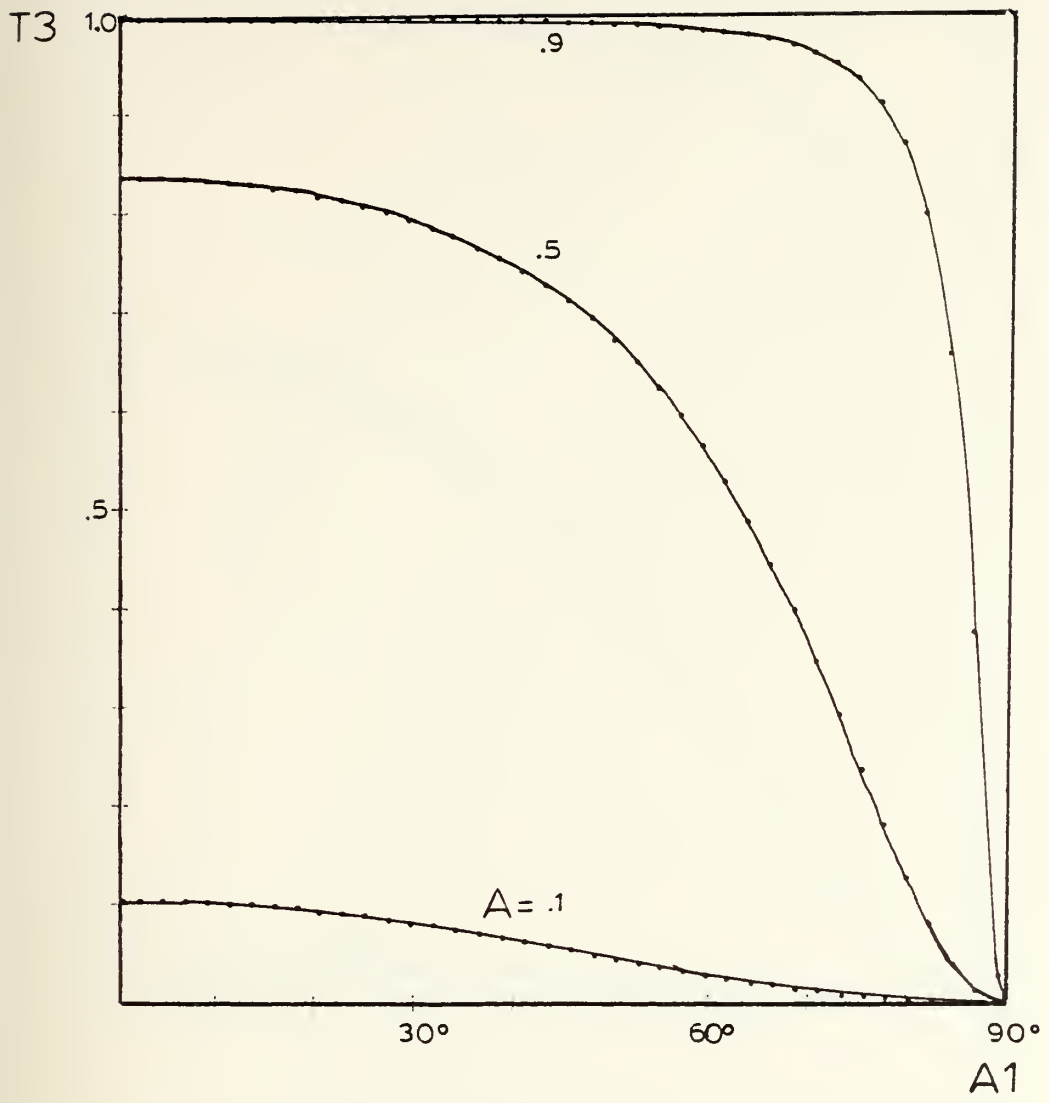

A = SOUND SPEED RATIO

A1 = INCIDENT ANGLE

L2 = LAYER WIDTH/WAVELENGTH RATIO

T3 = SOUND POWER TRANSMISSION COEFFICIENT

Figure 12. Sound power transmission coefficient vs. incident angle, parameter A for constant L2 = .1

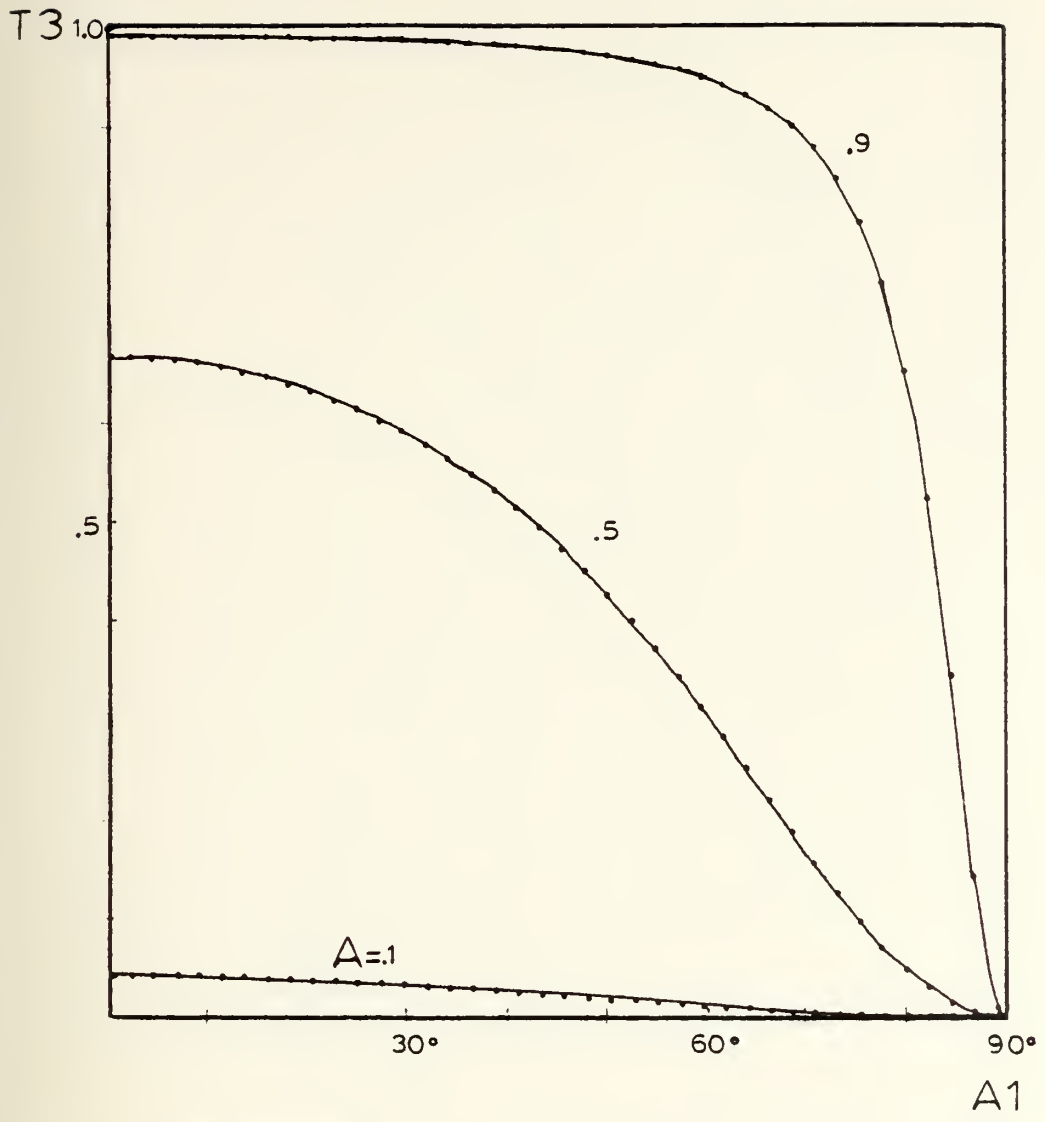

A = SOUND SPEED RATIO

A1 = INCIDENT ANGLE

L2 = LAYER WIDTH/WAVELENGTH RATIO

T3 = SOUND POWER TRANSMISSION COEFFICIENT

Figure 13. Sound power transmission coefficient vs. incident angle, parameter A for constant L2 = .2

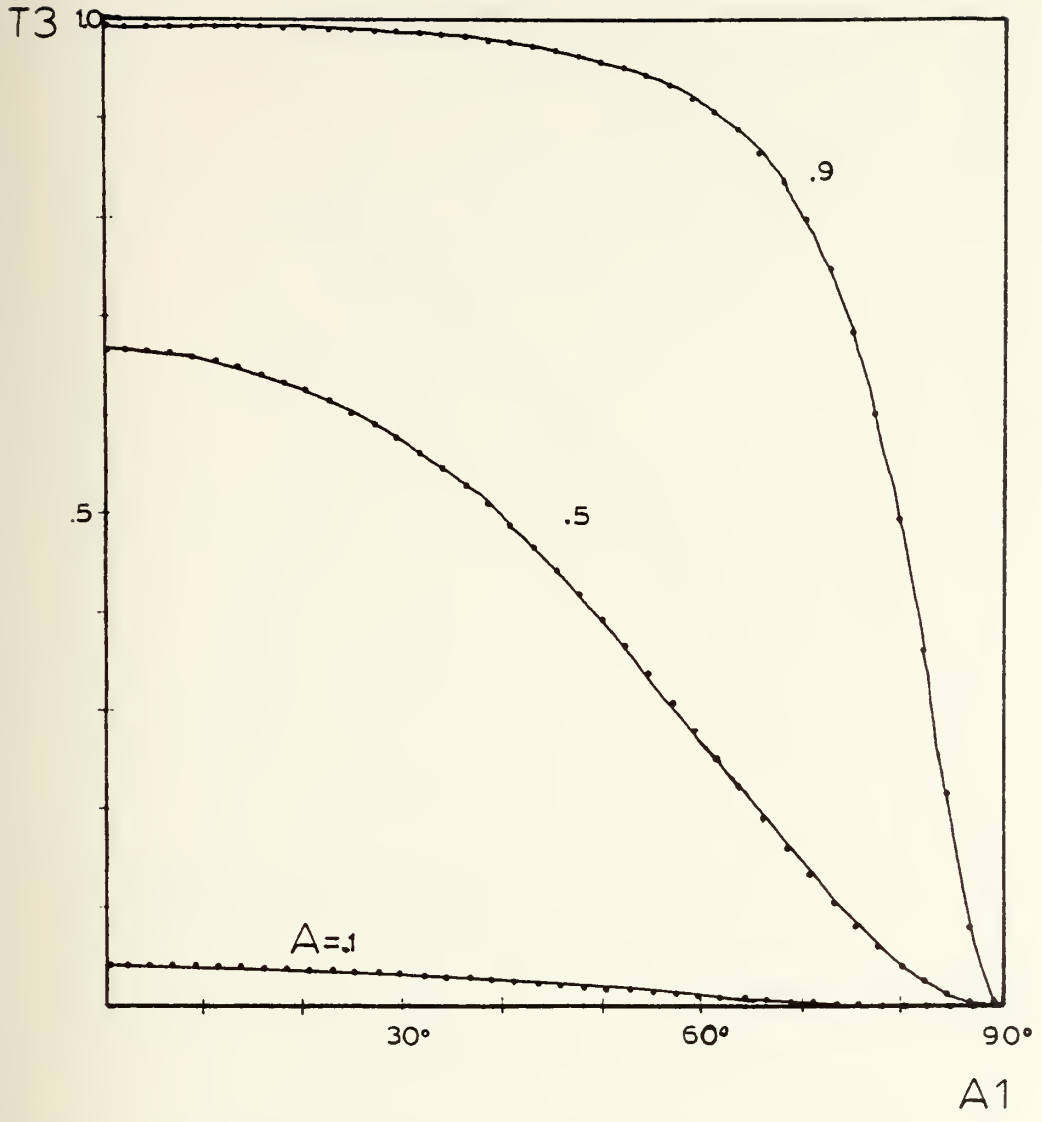

A = SOUND SPEED RATIO

A1 = INCIDENT ANGLE

L2 = LAYER WIDTH/WAVELENGTH RATIO

T3 = SOUND POWER TRANSMISSION COEFFICIENT

Figure 14. Sound power transmission coefficient vs. incident angle, parameter A for constant L2 = .3

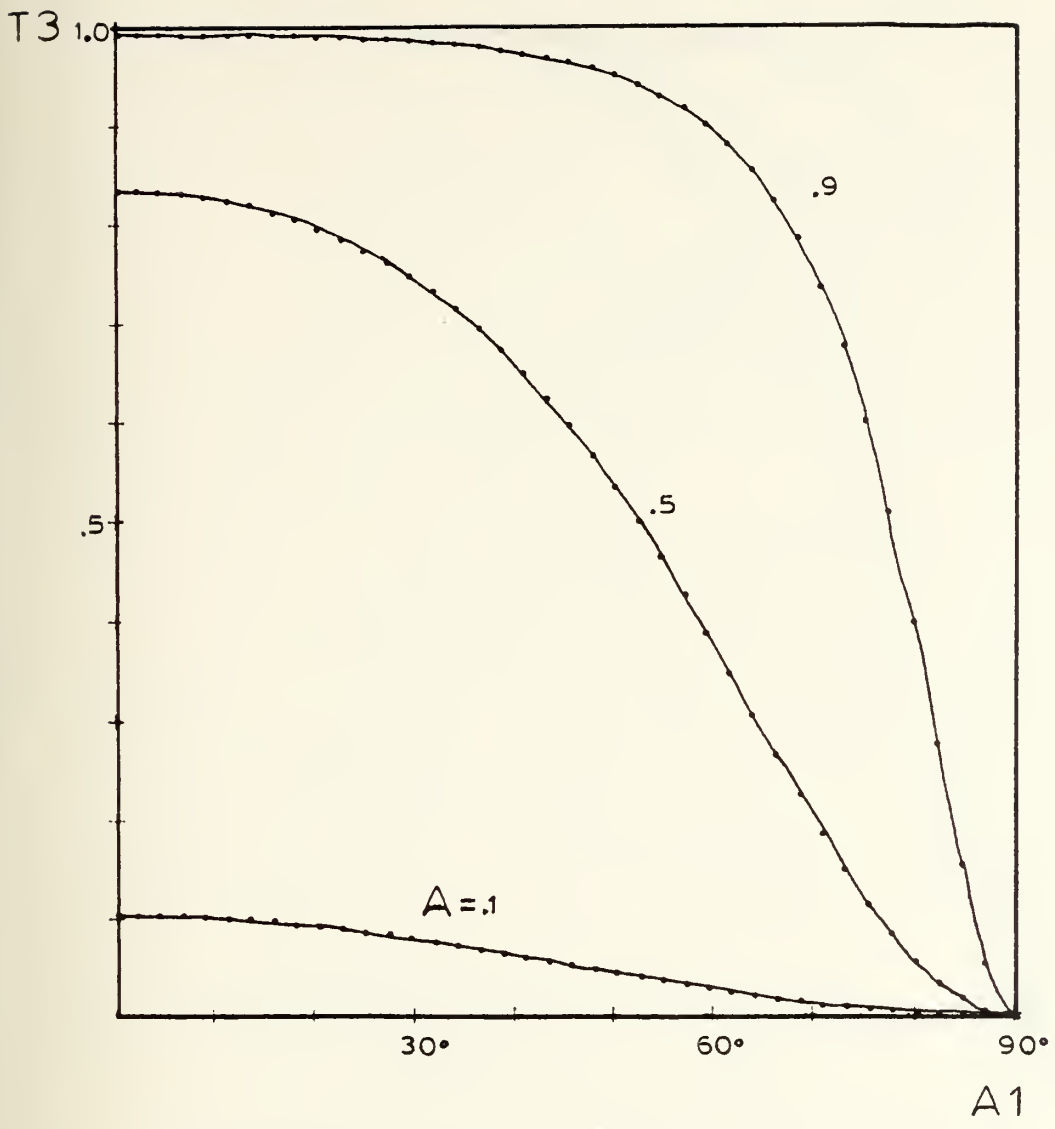

A = SOUND SPEED RATIO

A1 = INCIDENT ANGLE

L2 = LAYER WIDTH/WAVELENGTH RATIO

T3 = SOUND POWER TRANSMISSION COEFFICIENT

Figure 15. Sound power transmission coefficient vs. incident angle, parameter A for constant L2 = .4

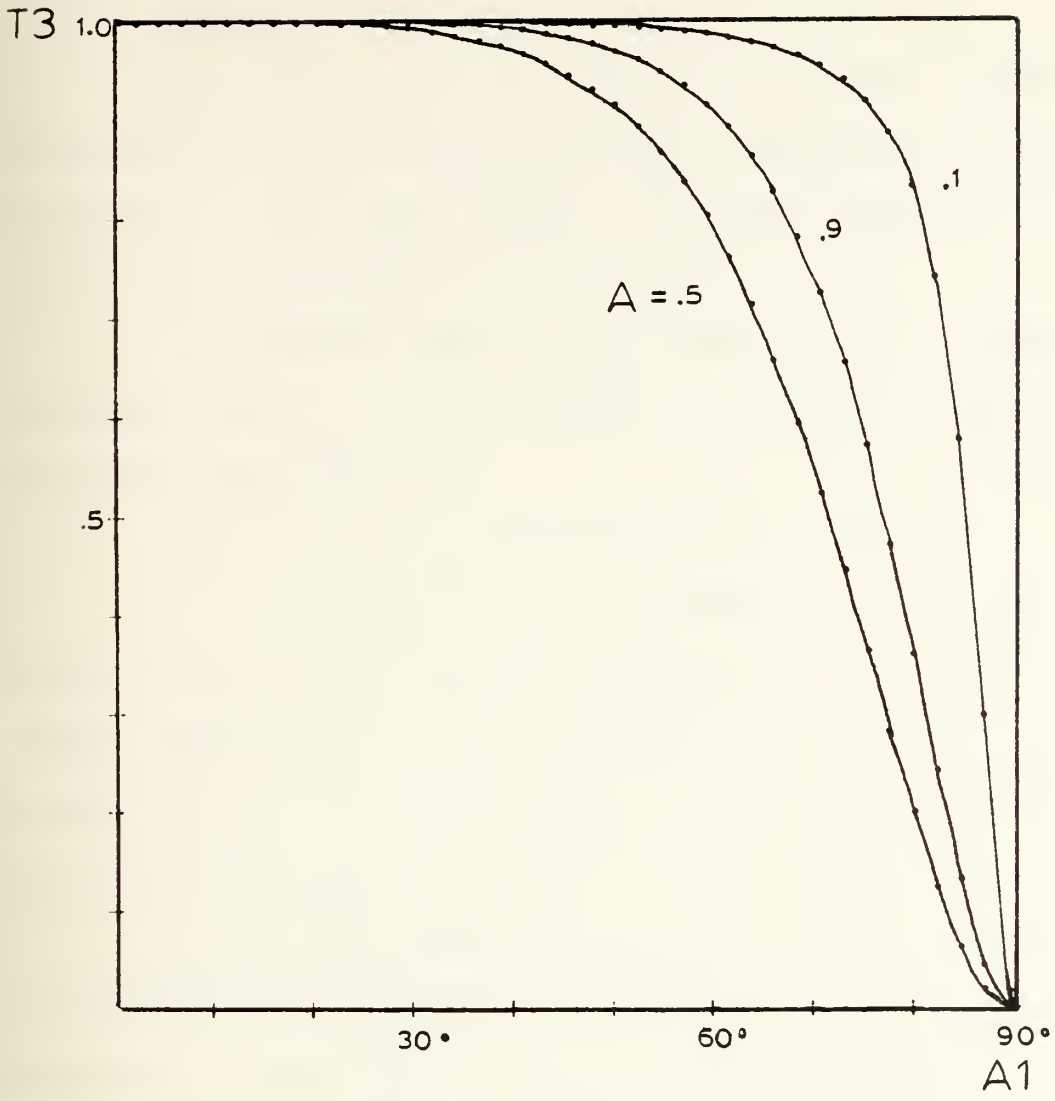

A = SOUND SPEED RATIO

A1 = INCIDENT ANGLE

L2 = LAYER WIDTH/WAVELENGTH RATIO

T3 = SOUND POWER TRANSMISSION COEFFICIENT

Figure 16. Sound power transmission coefficient vs. incident angle, parameter A for constant L2 = .5

5. Option 3

As in the plots for option 2, the sound power transmission coefficient is plotted against the angle of incidence. This time, though, the sound speed ratio is plotted as a parameter. See Figures 17 to 22.

The maximum sound transmitted occurs at normal incidence and the minimum always occurs as the angle of incidence approaches 90^{o}.

The following observations can be made:

a. The significance of a change in the sound speed ratio is very clear in this option. If Figure 18 (sound speed ratio = 0.1) is compared to Figure 22 (sound speed ratio = 0.5), a dramatic decrease of attenuation is seen to occur.

b. At low angles of incidence, values expected for attenuation are relatively constant. At high angles of incidence, attenuation values are changing rapidly, indicating less confidence for a given predicted layer width.

6. Option 4

This option plots the sound power transmission coefficient against the normalized layer ratio. The angle of incidence is the parameter which is varied for constant values of sound speed ratios (Figures 23 to 29). Again it is seen that values for the sound power transmission coefficient cycle between maxima and minima. The minimum

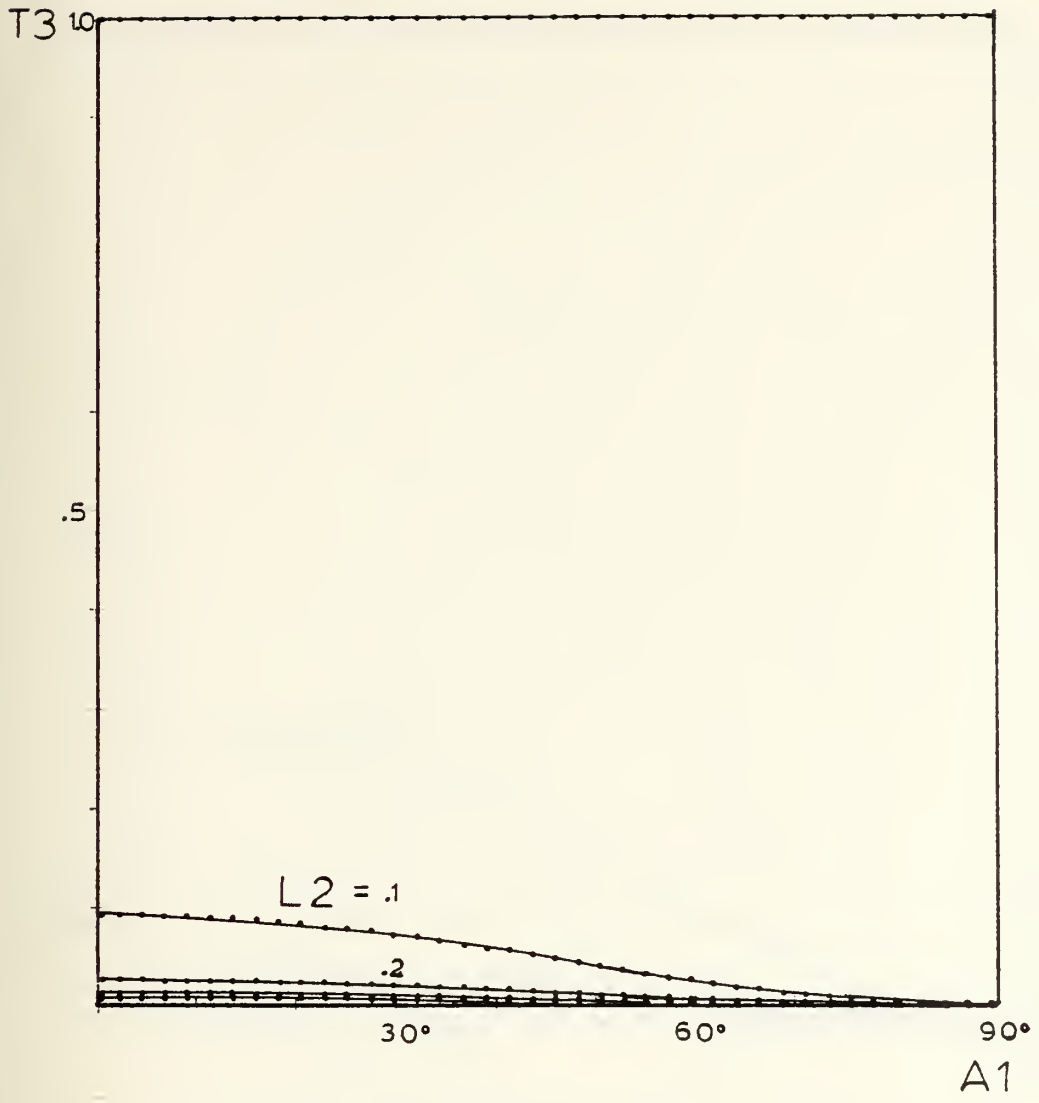

A = SOUND SPEED RATIO

A1 = INCIDENT ANGLE

L2 = LAYER WIDTH/WAVELENGTH RATIO

T3 = SOUND POWER TRANSMISSION COEFFICIENT

Figure 17. Sound power transmission coefficient vs. incident angle, parameter L2 for constant A = .05

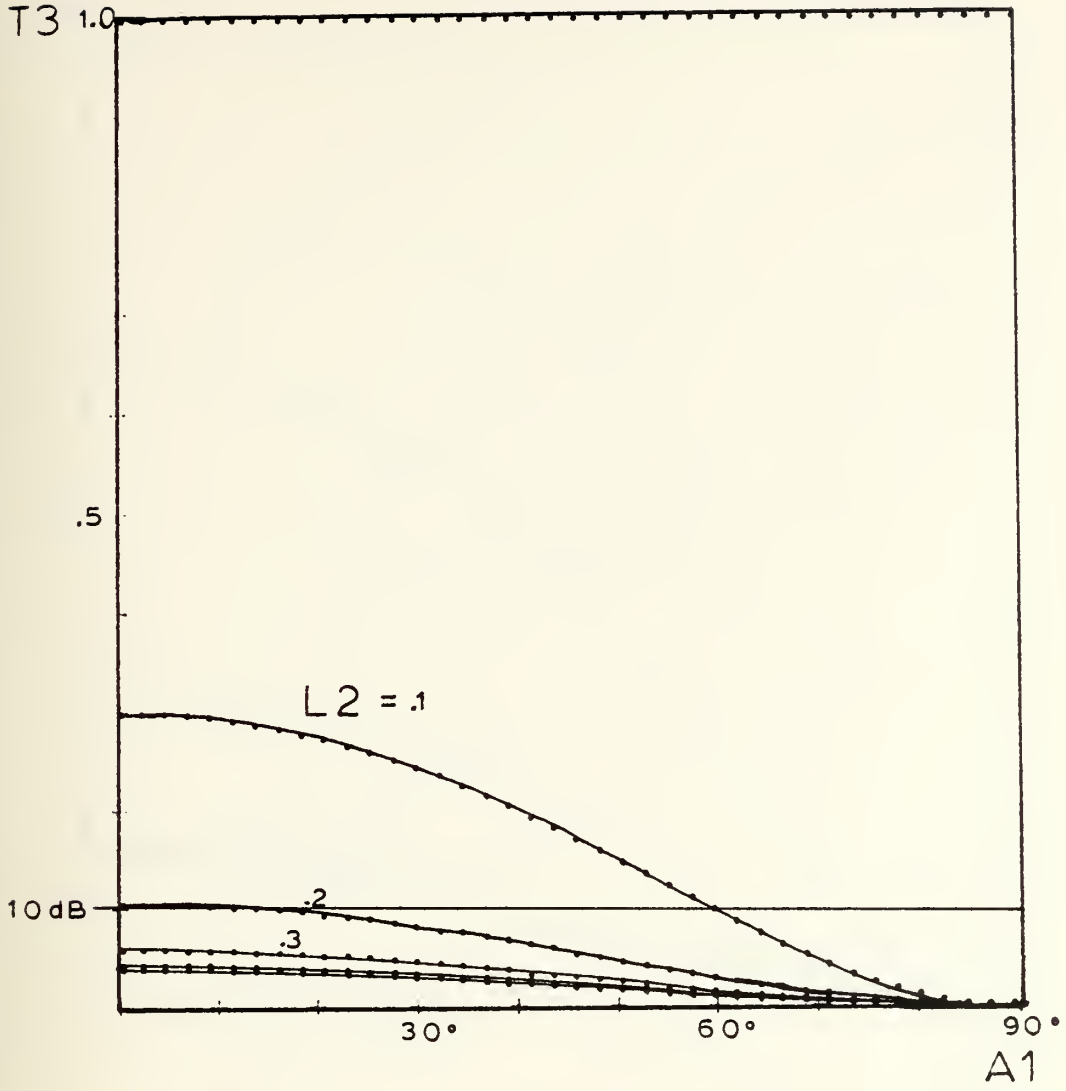

A = SOUND SPEED RATIO

A1 = INCIDENT ANGLE

L2 = LAYER WIDTH/WAVELENGTH RATIO

T3 = SOUND POWER TRANSMISSION COEFFICIENT

Figure 18. Sound power transmission coefficient vs. incident angle, parameter L2 for constant A = .1

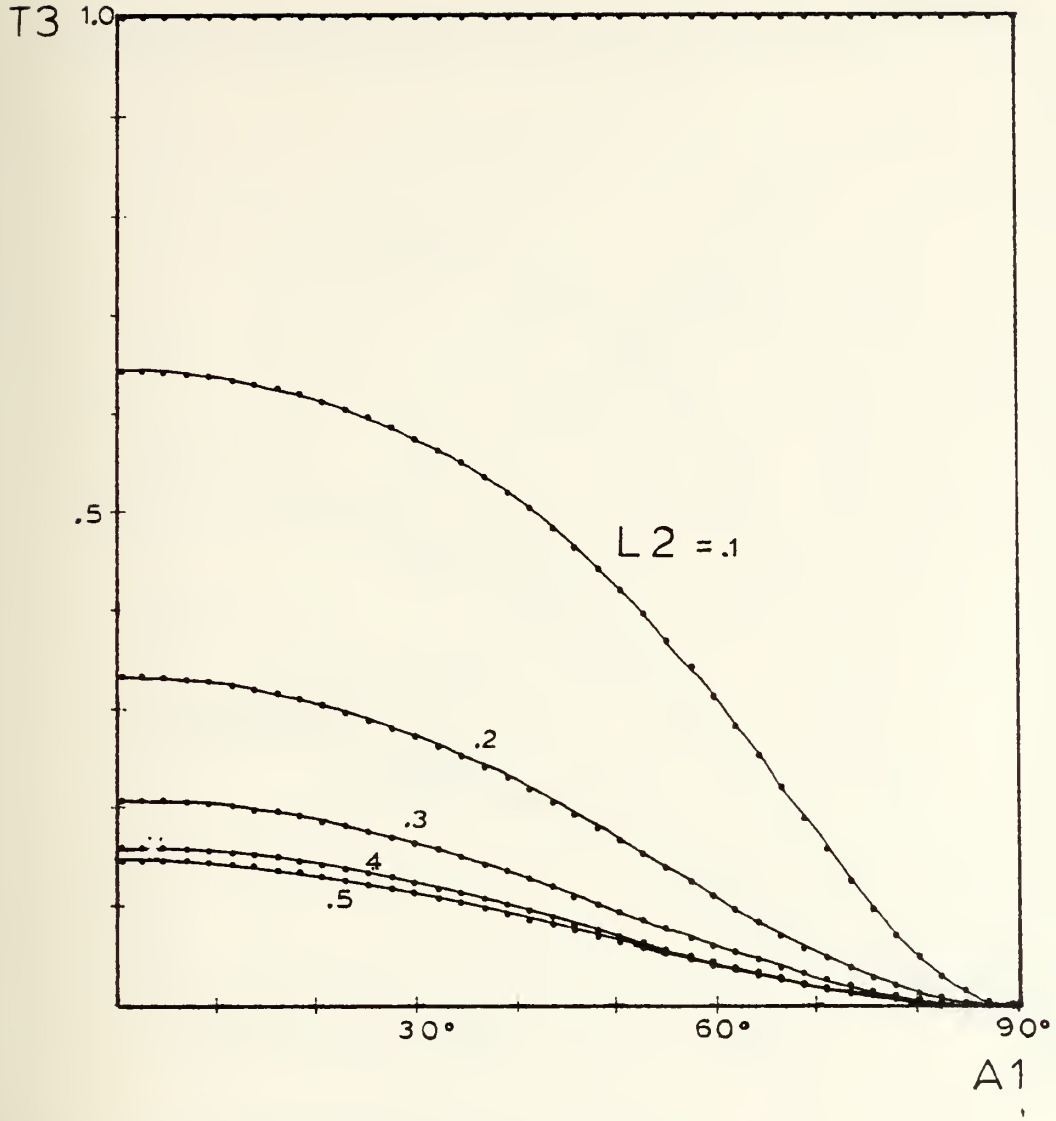

A = SOUND SPEED RATIO

A1 = INCIDENT ANGLE

L2 = LAYER WIDTH/WAVELENGTH RATIO

T3 = SOUND POWER TRANSMISSION COEFFICIENT

Figure 19. Sound power transmission coefficient vs. incident angle, parameter L2 for constant A = .2

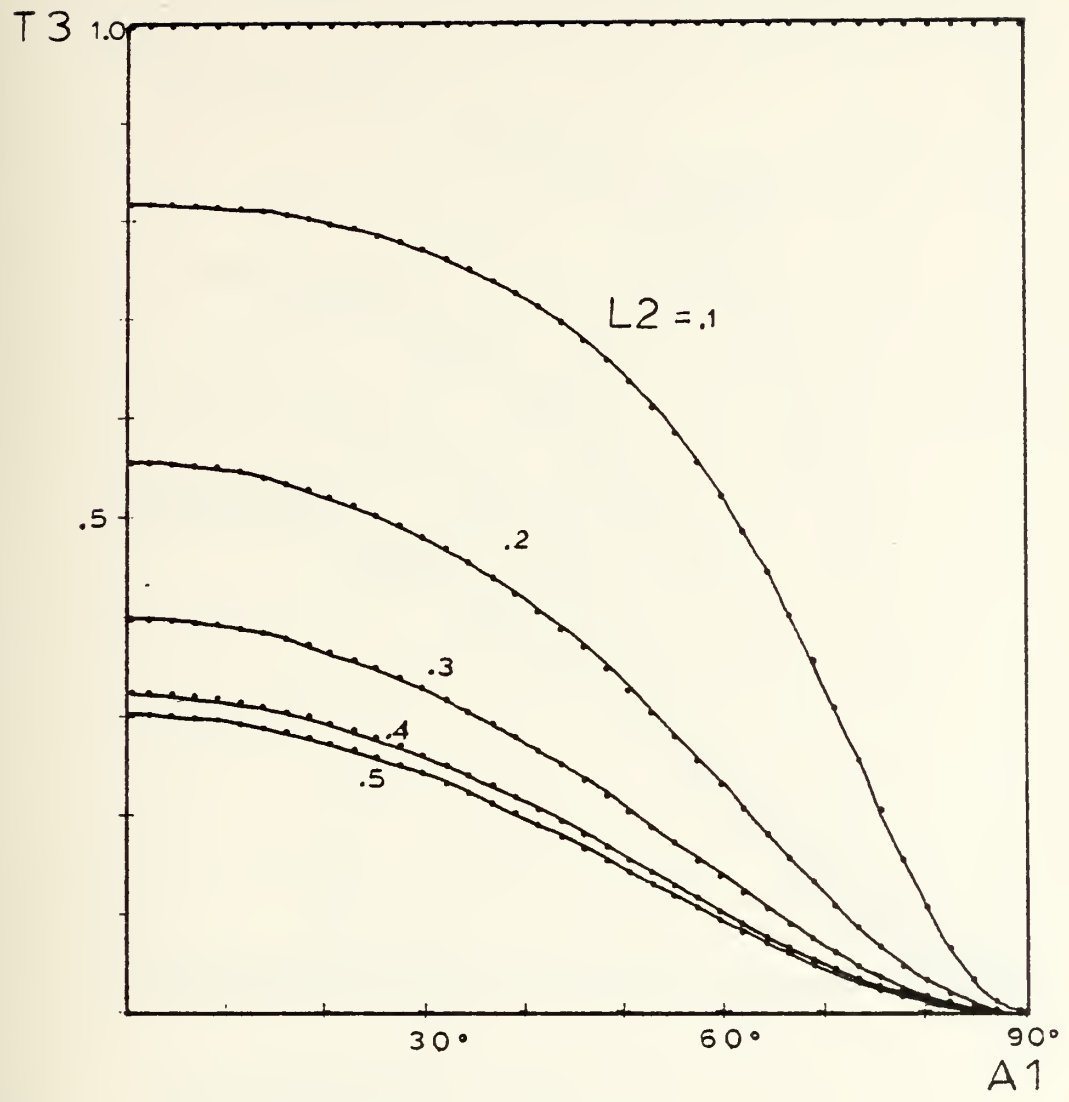

A = SOUND SPEED RATIO

A1 = INCIDENT ANGLE

L2 = LAYER WIDTH/WAVELENGTH RATIO

T3 = SOUND POWER TRANSMISSION COEFFICIENT

Figure 20. Sound power transmission coefficient vs. incident angle, parameter L2 for constant A = .3

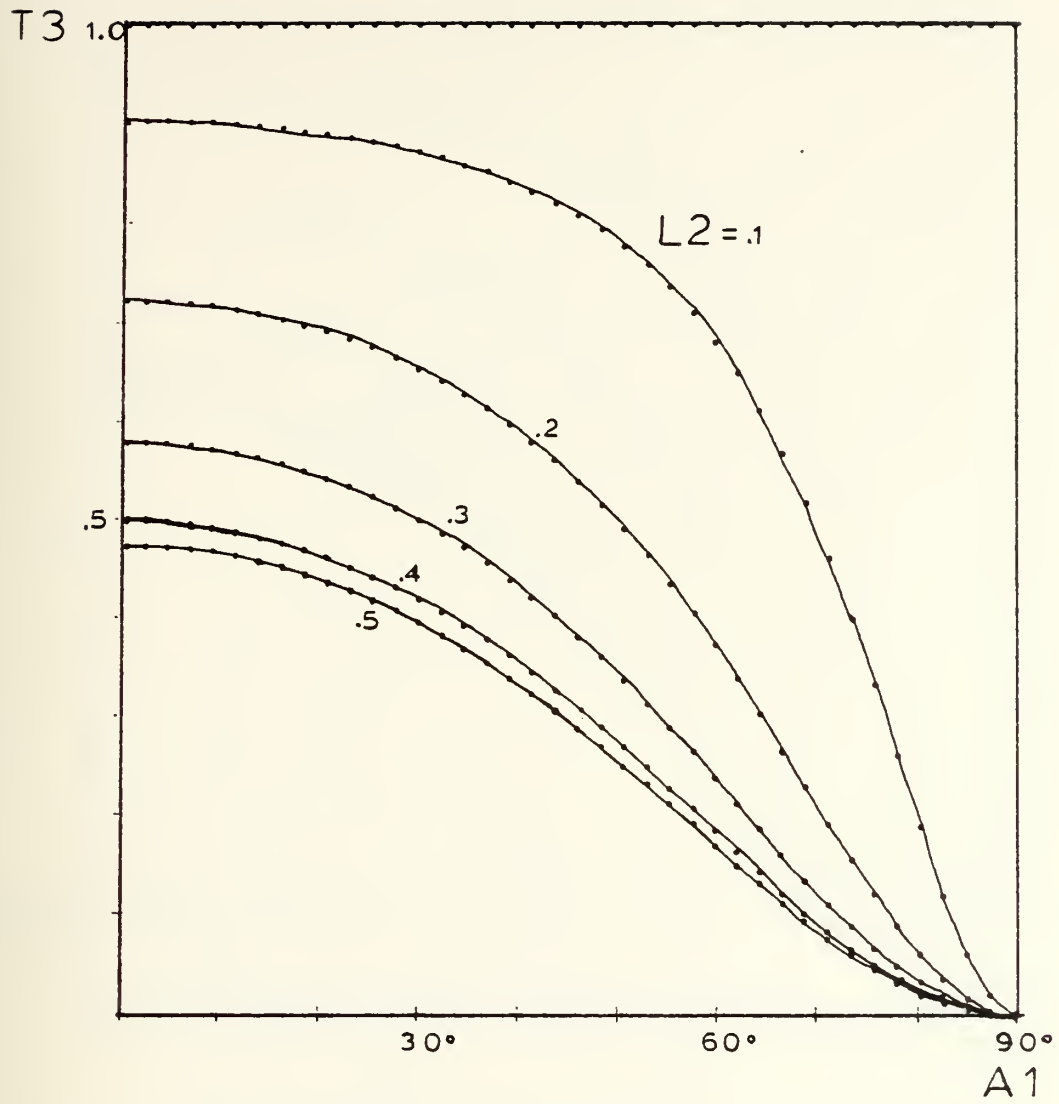

A = SOUND SPEED RATIO

A1 = INCIDENT ANGLE

L2 = LAYER WIDTH/WAVELENGTH RATIO

T3 = SOUND POWER TRANSMISSION COEFFICIENT

Figure 21. Sound power transmission coefficient vs. incident angle, parameter L2 for constant A = .4

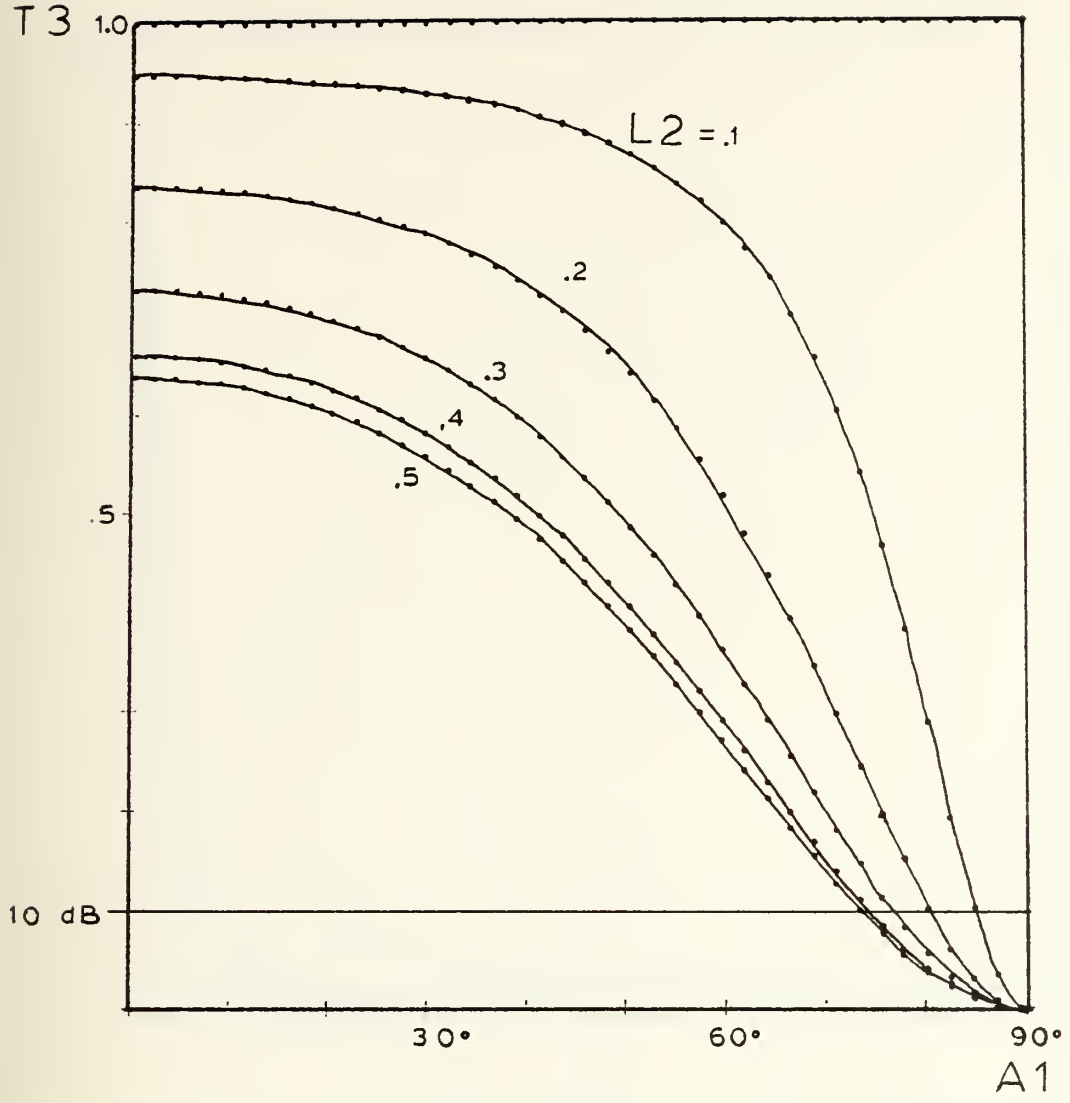

A = SOUND SPEED RATIO

A1 = INCIDENT ANGLE

L2 = LAYER WIDTH/WAVELENGTH RATIO

T3 = SOUND POWER TRANSMISSION COEFFICIENT

Figure 22. Sound power transmission coefficient vs. incident angle, parameter L2 for constant A = .5

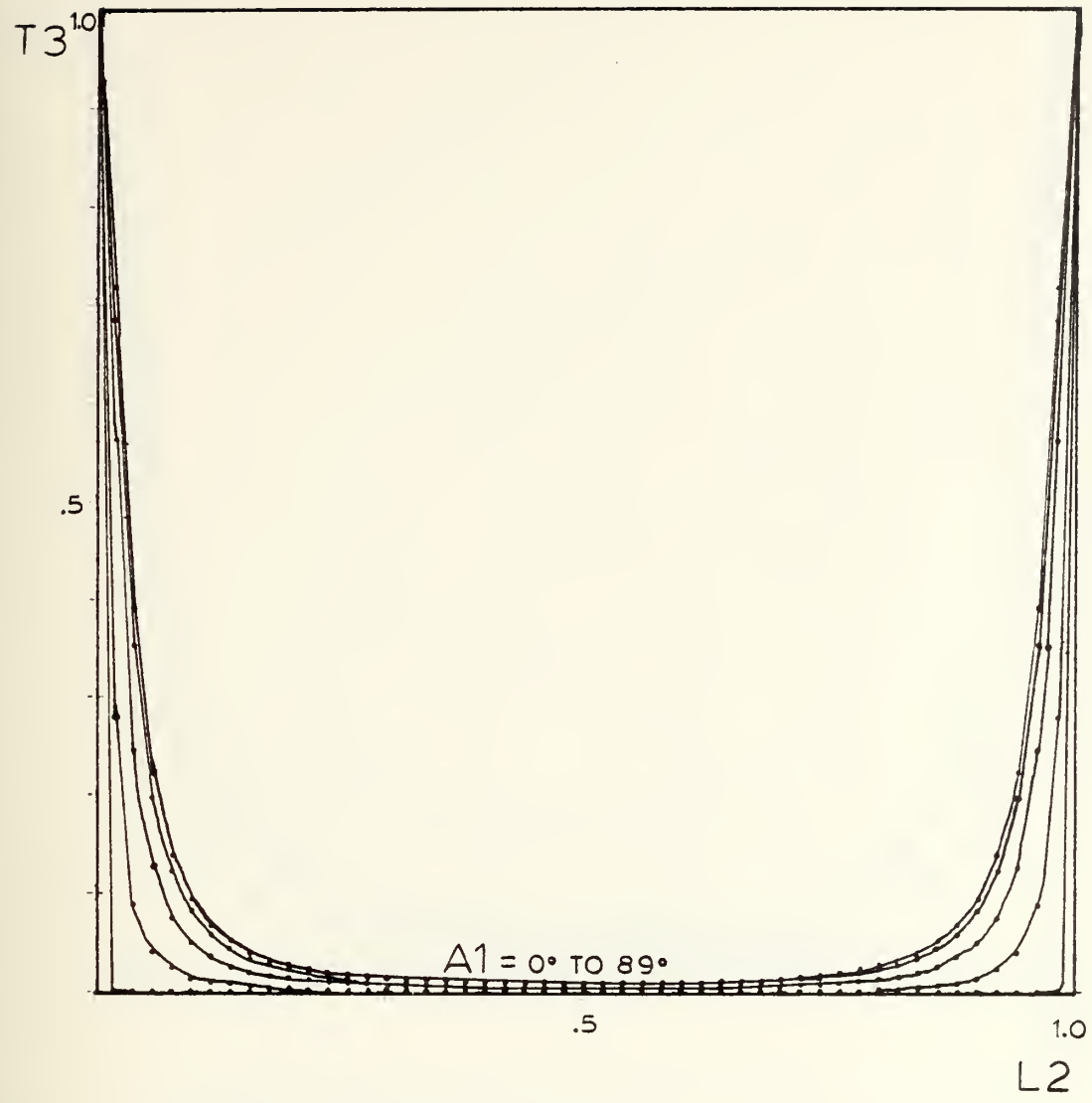

A = SOUND SPEED RATIO

A1 = INCIDENT ANGLE

L2 = LAYER WIDTH/WAVELENGTH RATIO

T3 = SOUND POWER TRANSMISSION COEFFICIENT

Figure 23. Sound power transmission coefficient vs. layer ratio, parameter A1 for constant A = .05

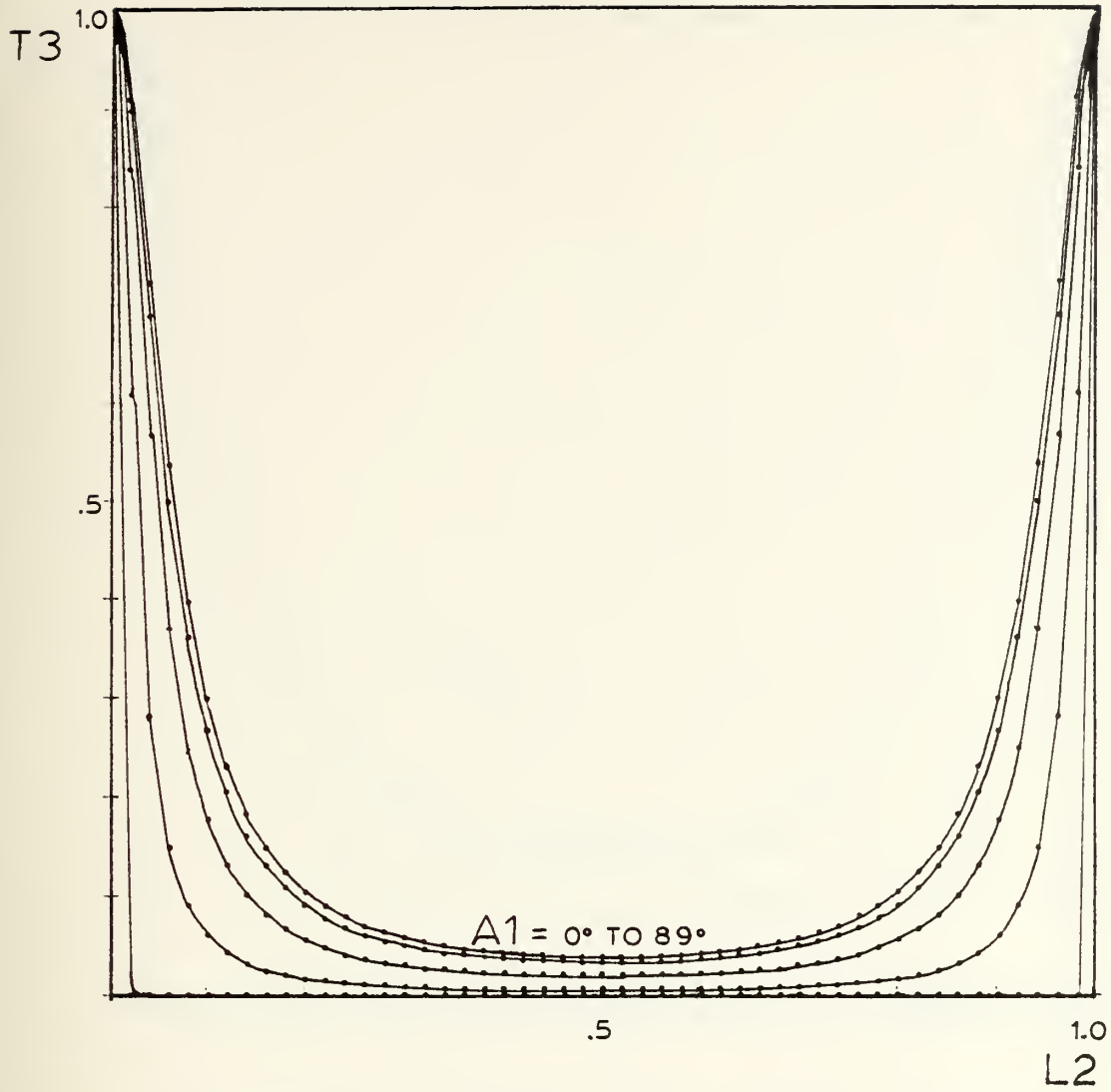

A = SOUND SPEED RATIO

A1 = INCIDENT ANGLE

L2 = LAYER WIDTH/WAVELENGTH RATIO

T3 = SOUND POWER TRANSMISSION COEFFICIENT

Figure 24. Sound power transmission coefficient vs. layer ratio, parameter A1 for constant A = .1

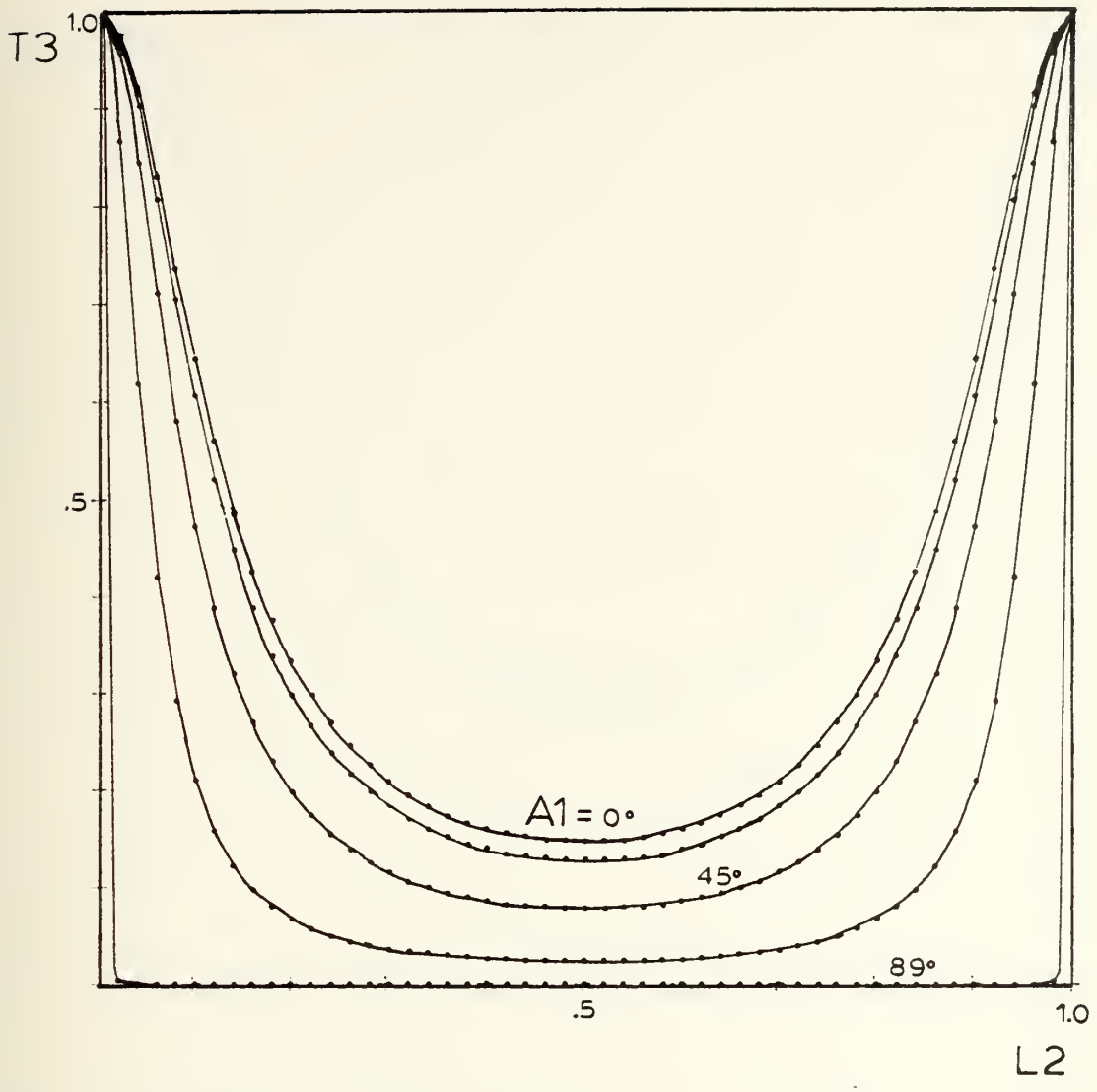

A = SOUND SPEED RATIO

A1 = INCIDENT ANGLE

L2 = LAYER WIDTH/WAVELENGTH RATIO

T3 = SOUND POWER TRANSMISSION COEFFICIENT

Figure 25. Sound power transmission coefficient vs. layer ratio, parameter A1 for constant A = .2

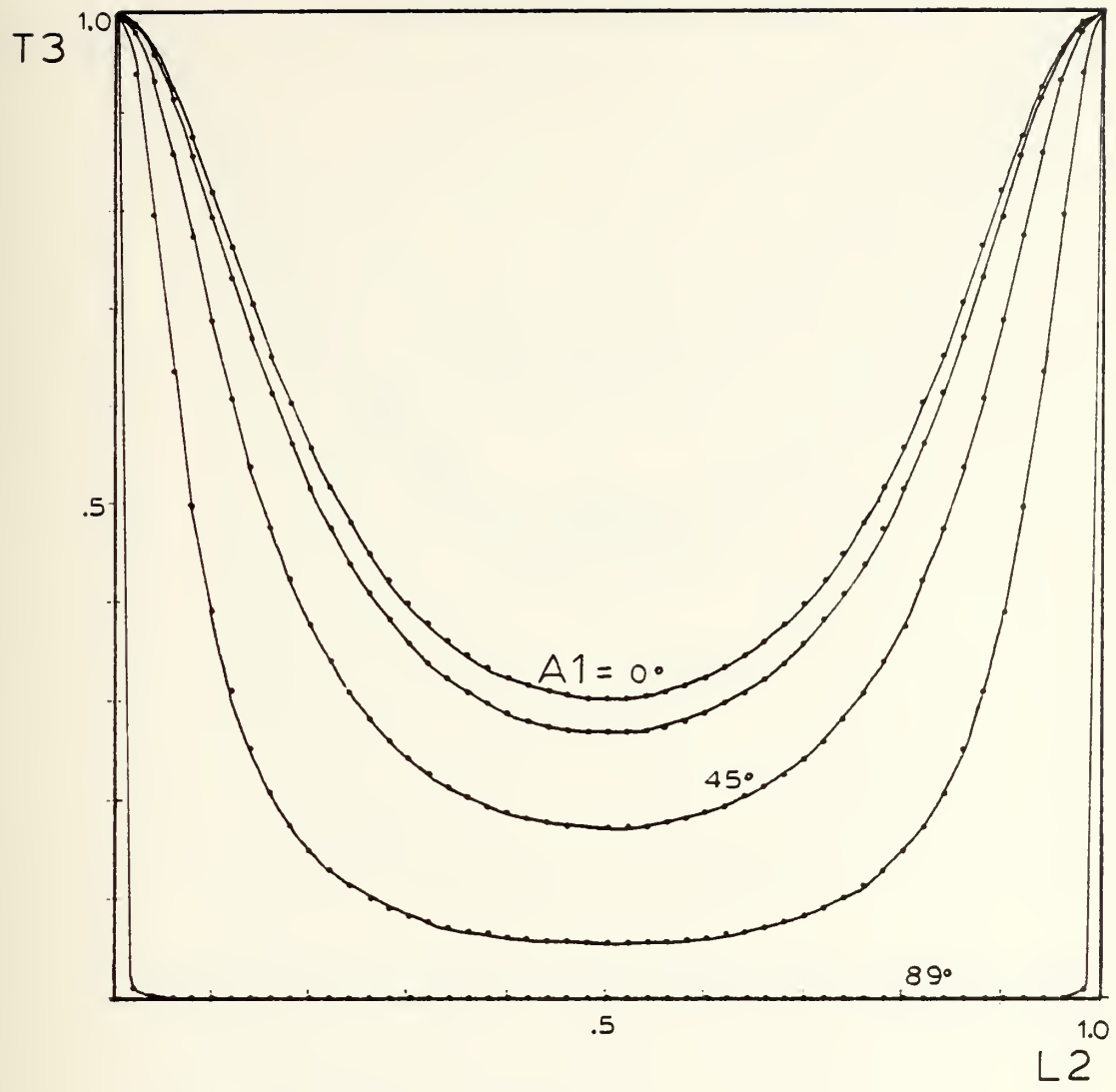

A = SOUND SPEED RATIO

A1 = INCIDENT ANGLE

L2 = LAYER WIDTH/WAVELENGTH RATIO

T3 = SOUND POWER TRANSMISSION COEFFICIENT

Figure 26. Sound power transmission coefficient vs. layer ratio, parameter A1 for constant A = .3

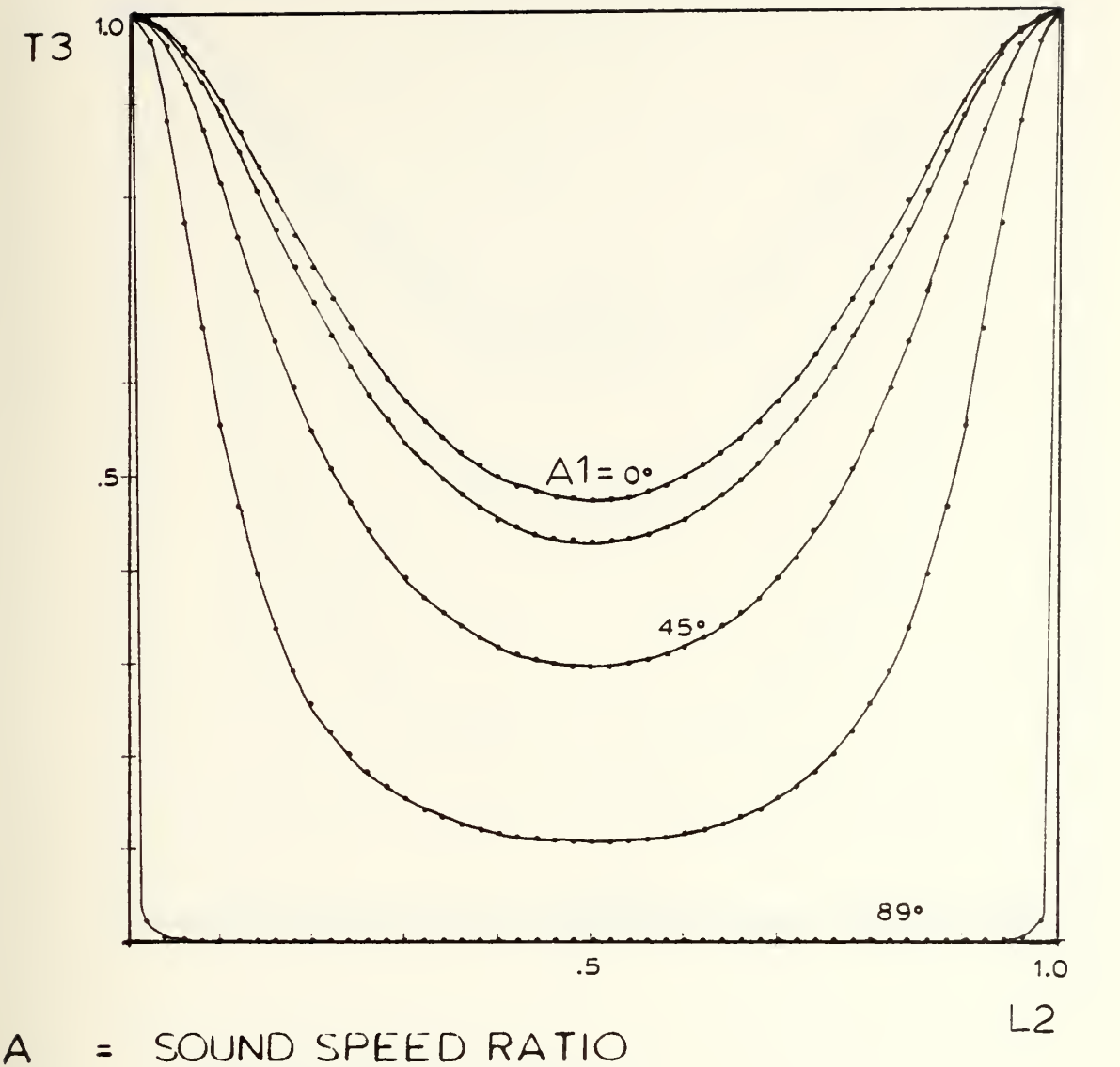

A = SOUND SPEED RATIO

A1 = INCIDENT ANGLE

L2 = LAYER WIDTH/WAVELENGTH RATIO

T3 = SOUND POWER TRANSMISSION COEFFICIENT

Figure 27. Sound power transmission coefficient vs. layer ratio, parameter A1 for constant A = .4

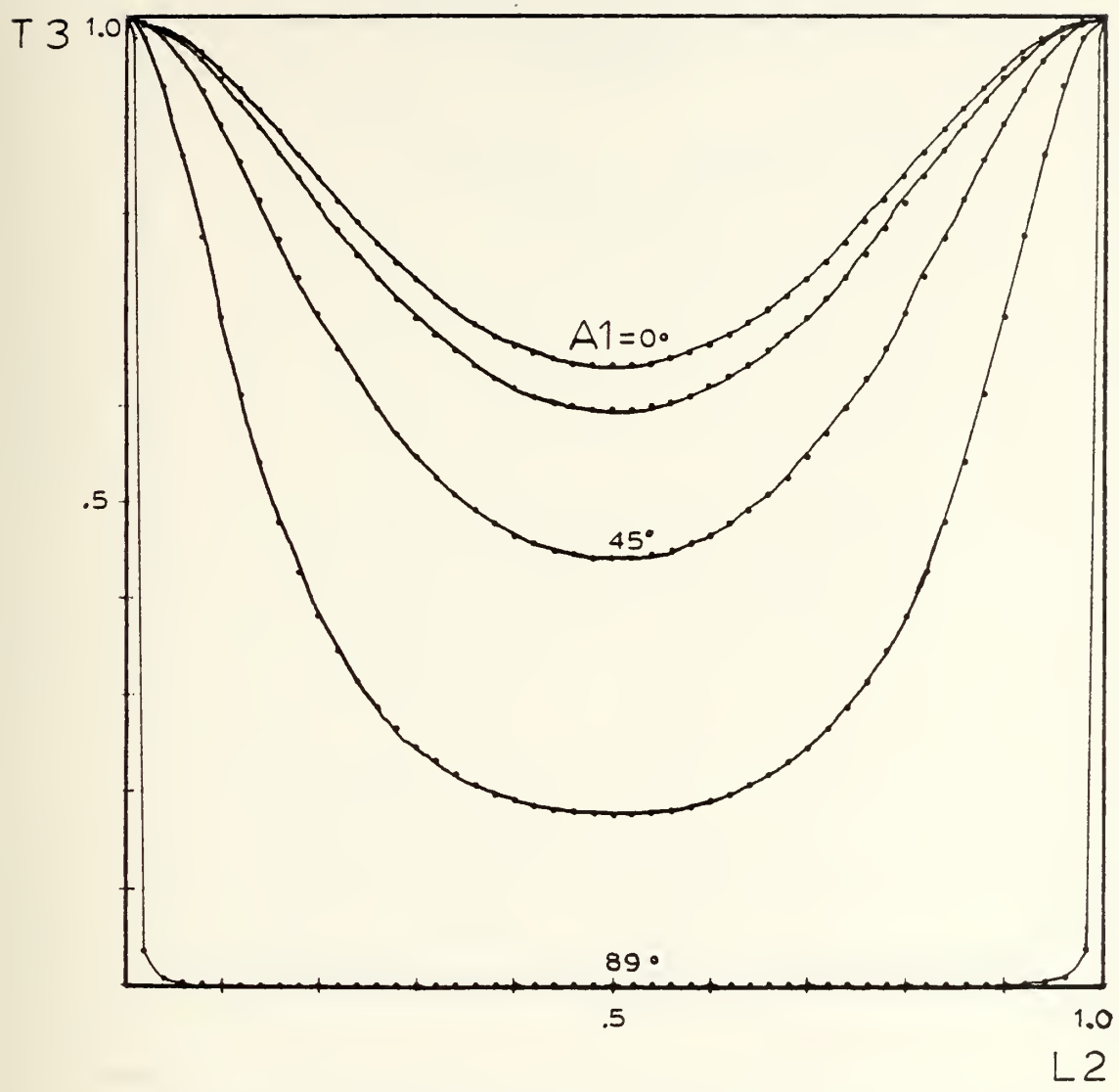

A = SOUND SPEED RATIO

A1 = INCIDENT ANGLE

L2 = LAYER WIDTH/WAVELENGTH RATIO

T3 = SOUND POWER TRANSMISSION COEFFICIENT

Figure 28. Sound power transmission coefficient vs. layer ratio, parameter A1 for constant A = .5

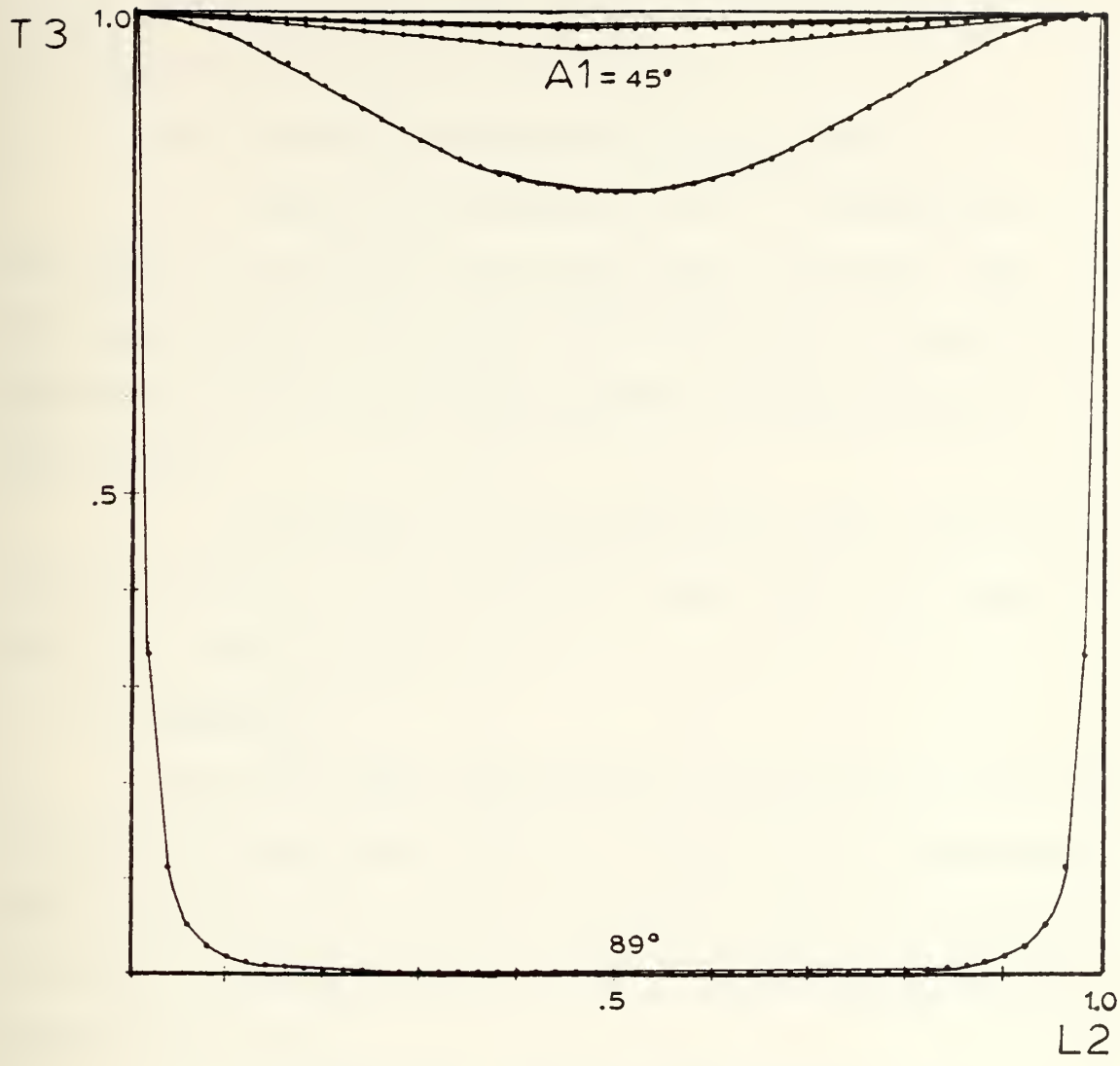

A = SOUND SPEED RATIO

A1 = INCIDENT ANGLE

L2 = LAYER WIDTH/WAVELENGTH RATIO

T3 = SOUND POWER TRANSMISSION COEFFICIENT

Figure 29. Sound power transmission coefficient vs. layer ratio, parameter A1 for constant A = .9

values occur at layer ratios which correspond to odd multiples of one-quarter wavelength.

The following observations can be made:

a. Changes in attenuation due to variations in the angle of incidence are very slight for angles less than approximately 45^{o}, but the attenuation in uniformly predictable and by far the greatest at angles greater than 80^{o}-85^{o}.

b. Variations in the sound speed ratio cause far greater effects on the attenuation when the sound speed ratio is greater than 0.2.

7. Option 5

The sound power transmission coefficient is plotted against the sound speed ratio in this option. The bubble layer ratio is kept constant while the angle of incidence is varied. A much different view of the data is seen in Figures 30 - 34.

The following observations can be made:

a. The best attenuation occurs at very low sound speed ratios as was also seen in options 1 and 2.

b. There is a significant amount of attenuation gained for angles of incidence past 75^{o}.

8. Option 6

In this option, the sound power transmission coefficient is plotted against the sound speed ratio with

the parameter of layer ratio varied for constant values of angles of incidence in Figures 35 to 38.

The following observation can be made:

a. Layer width ratio curves vary only slightly indicating that layer width is not an important parameter. In addition, there is still approximately 10 percent of the layer ratio range ($L2 < .05$) virtually unaffected by sound speed ratio or angle of incidence.

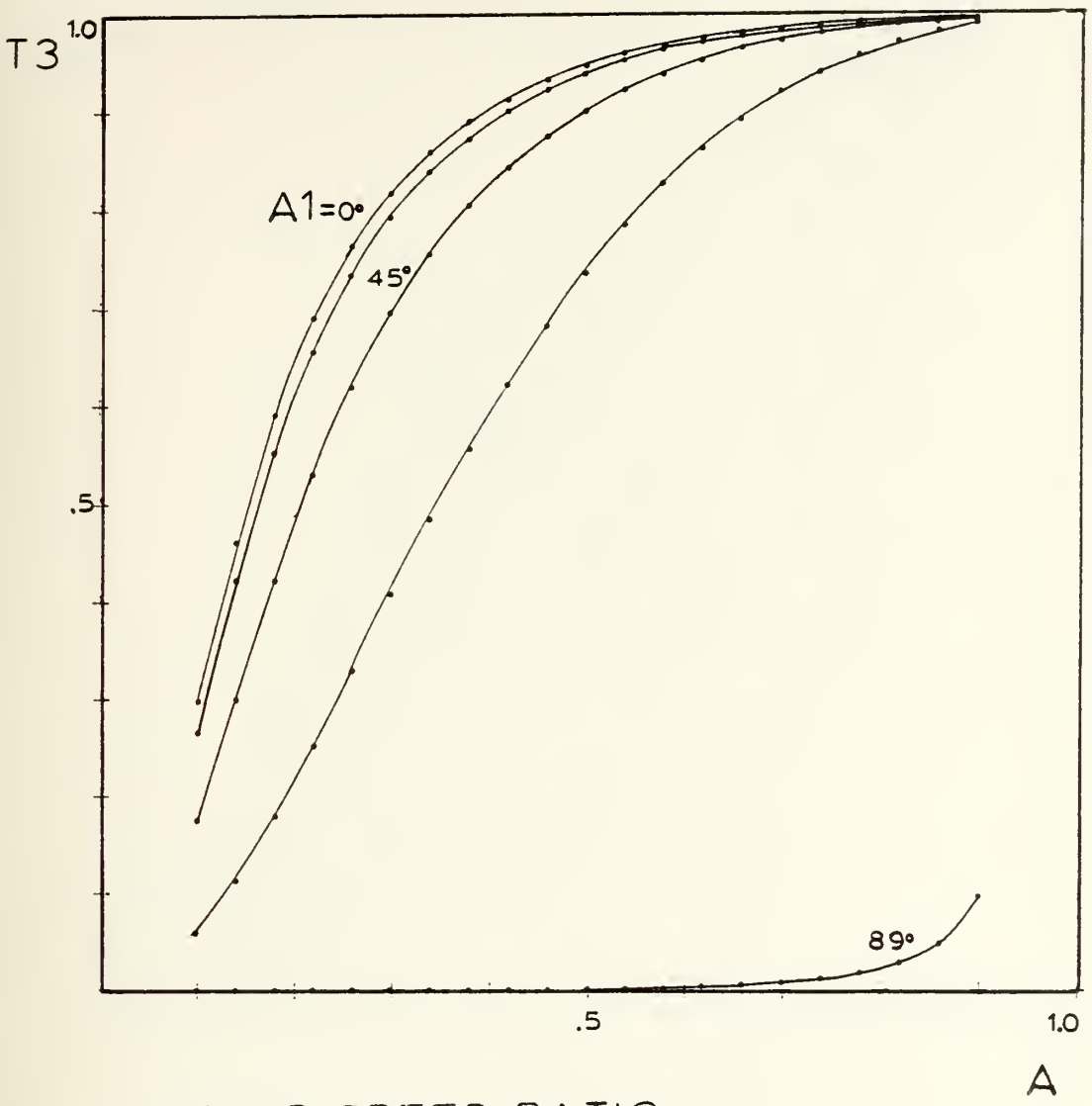

A = SOUND SPEED RATIO

A1 = INCIDENT ANGLE

L2 = LAYER WIDTH/WAVELENGTH RATIO

T3 = SOUND POWER TRANSMISSION COEFFICIENT

Figure 30. Sound power transmission coefficient vs. sound speed ratio, parameter A1 for constant L2 = .05

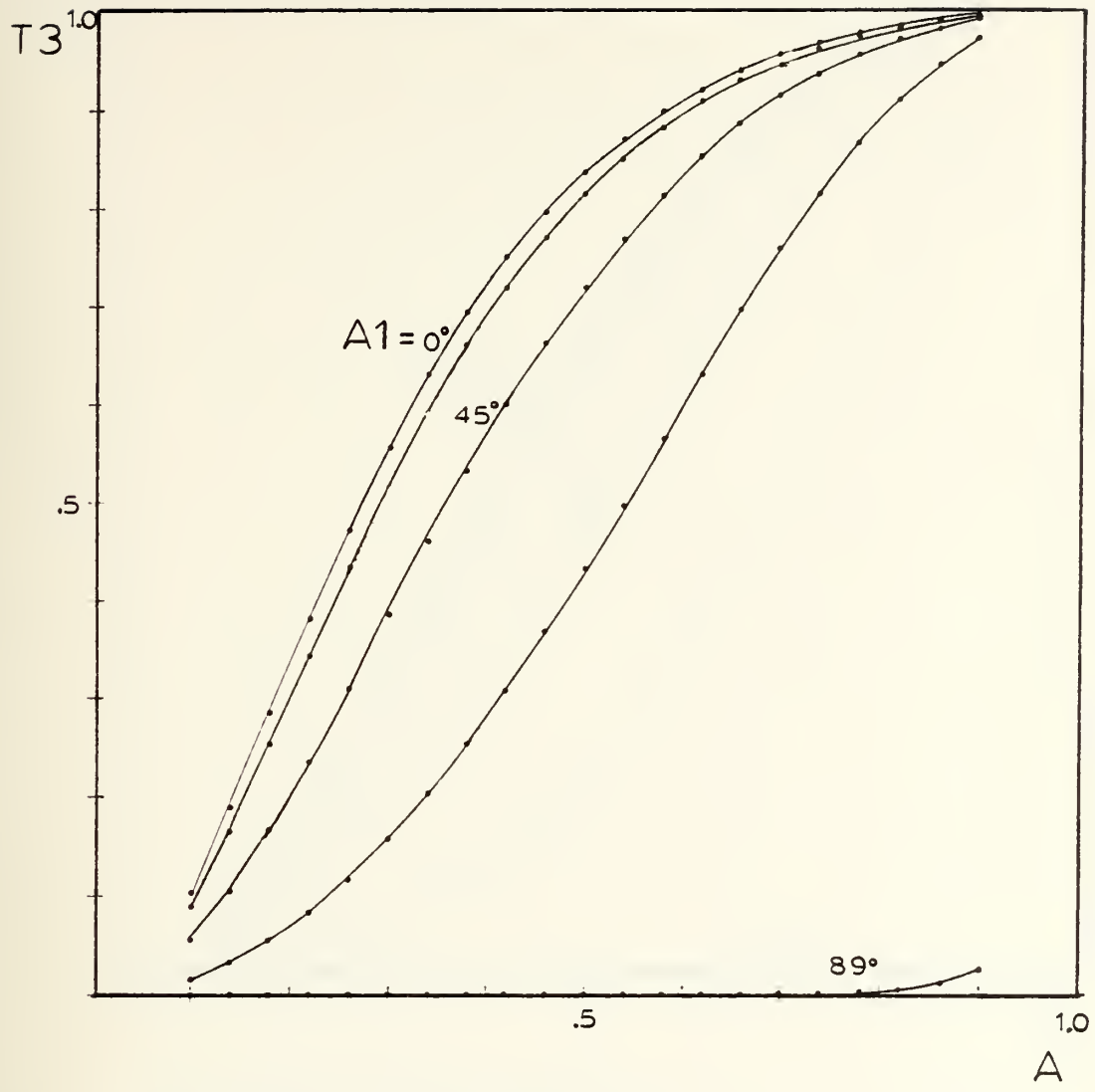

A = SOUND SPEED RATIO

A1 = INCIDENT ANGLE

L2 = LAYER WIDTH/WAVELENGTH RATIO

T3 = SOUND POWER TRANSMISSION COEFFICIENT

Figure 31. Sound power transmission coefficient vs. sound speed ratio, parameter A1 for constant L2 = .1

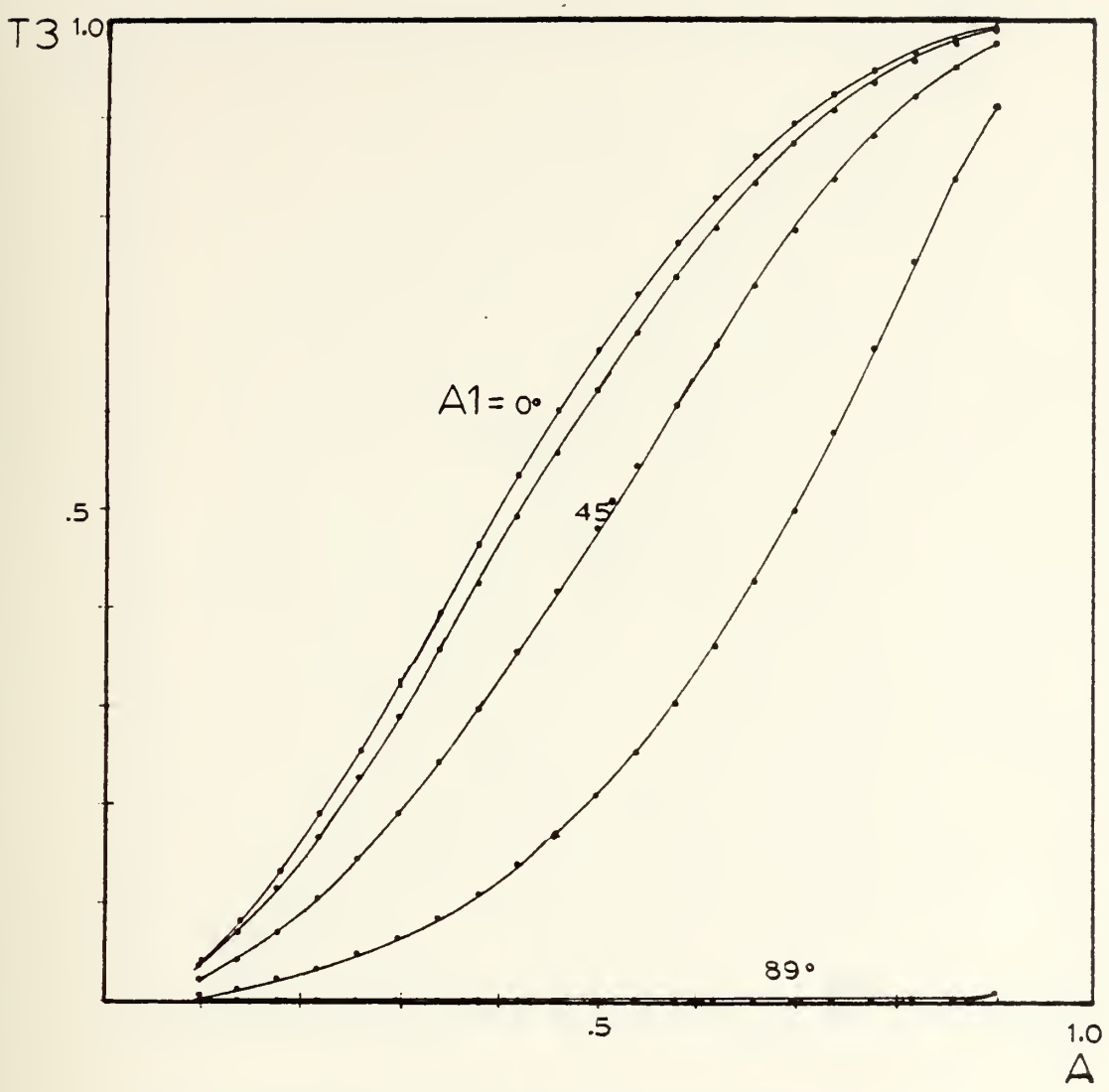

A = SOUND SPEED RATIO

A1 = INCIDENT ANGLE

L2 = LAYER WIDTH/WAVELENGTH RATIO

T3 = SOUND POWER TRANSMISSION COEFFICIENT

Figure 32. Sound power transmission coefficient vs. sound speed ratio, parameter A1 for constant L2 = .2

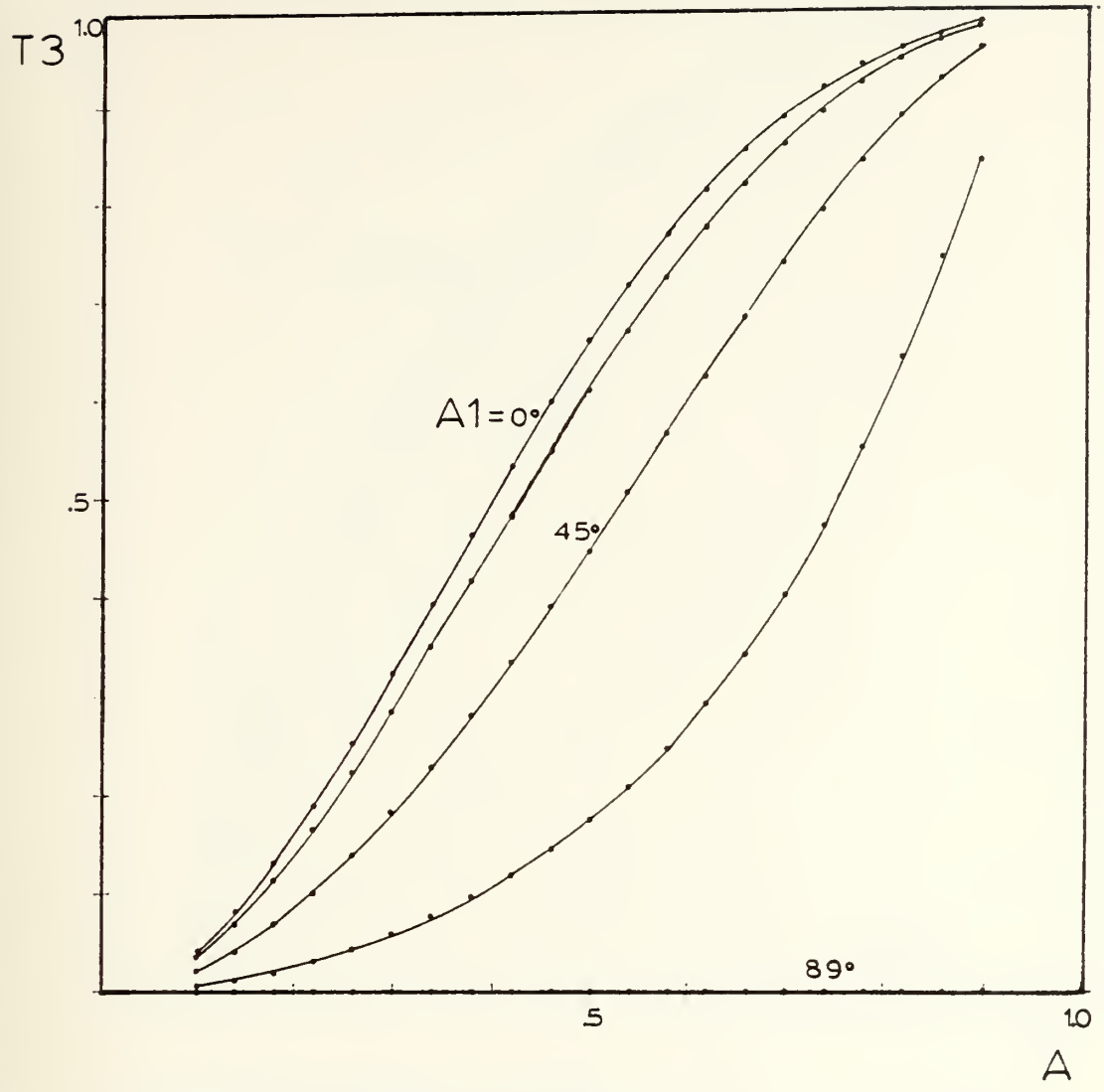

A = SOUND SPEED RATIO

A1 = INCIDENT ANGLE

L2 = LAYER WIDTH/WAVELENGTH RATIO

T3 = SOUND POWER TRANSMISSION COEFFICIENT

Figure 33. Sound power transmission coefficient vs. sound speed ratio, parameter A1 for constant L2 = .3

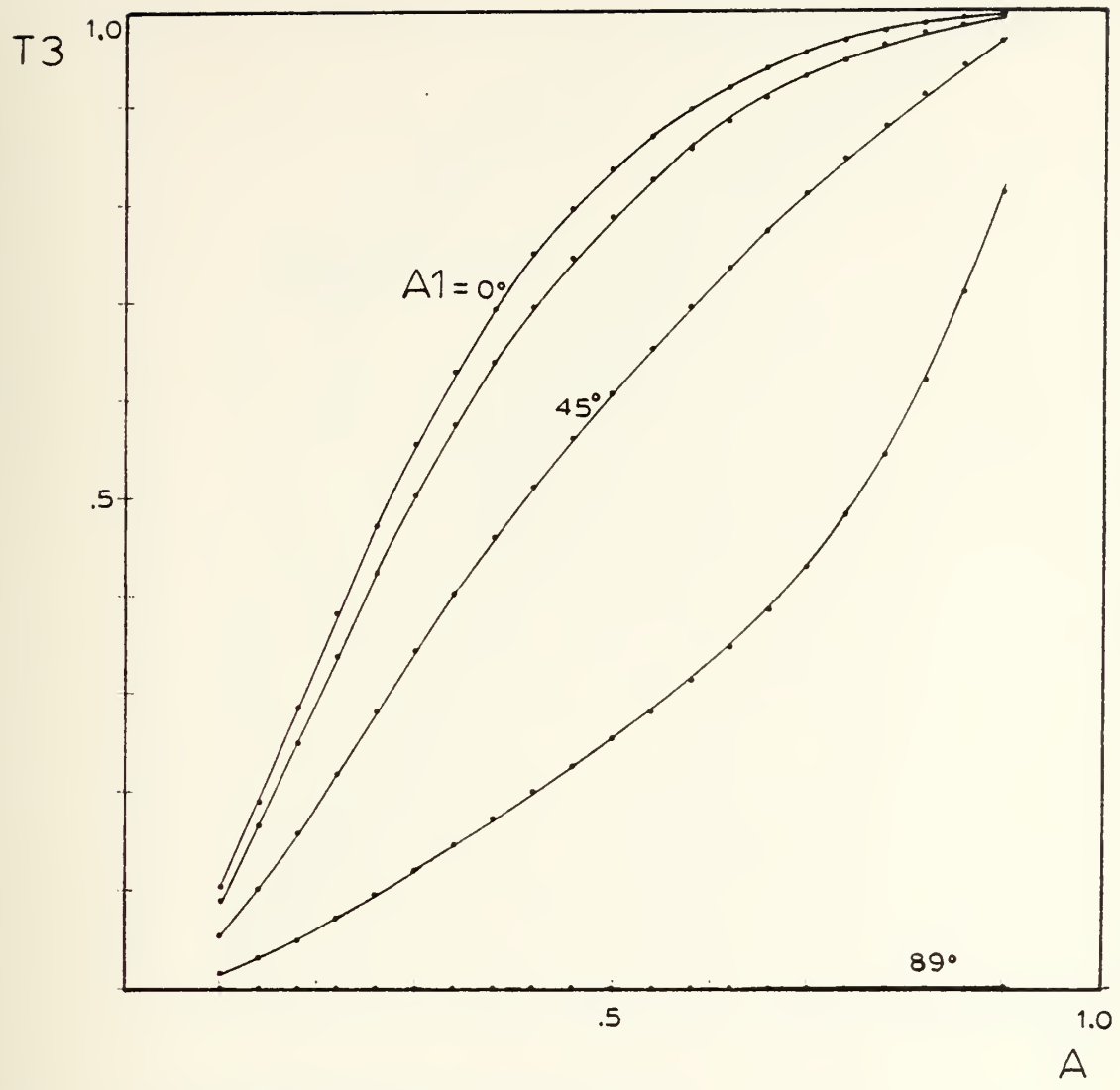

A = SOUND SPEED RATIO

A1 = INCIDENT ANGLE

L2 = LAYER WIDTH/WAVELENGTH RATIO

T3 = SOUND POWER TRANSMISSION COEFFICIENT

Figure 34. Sound power transmission coefficient vs. sound speed ratio, parameter A1 for constant L2 = .4

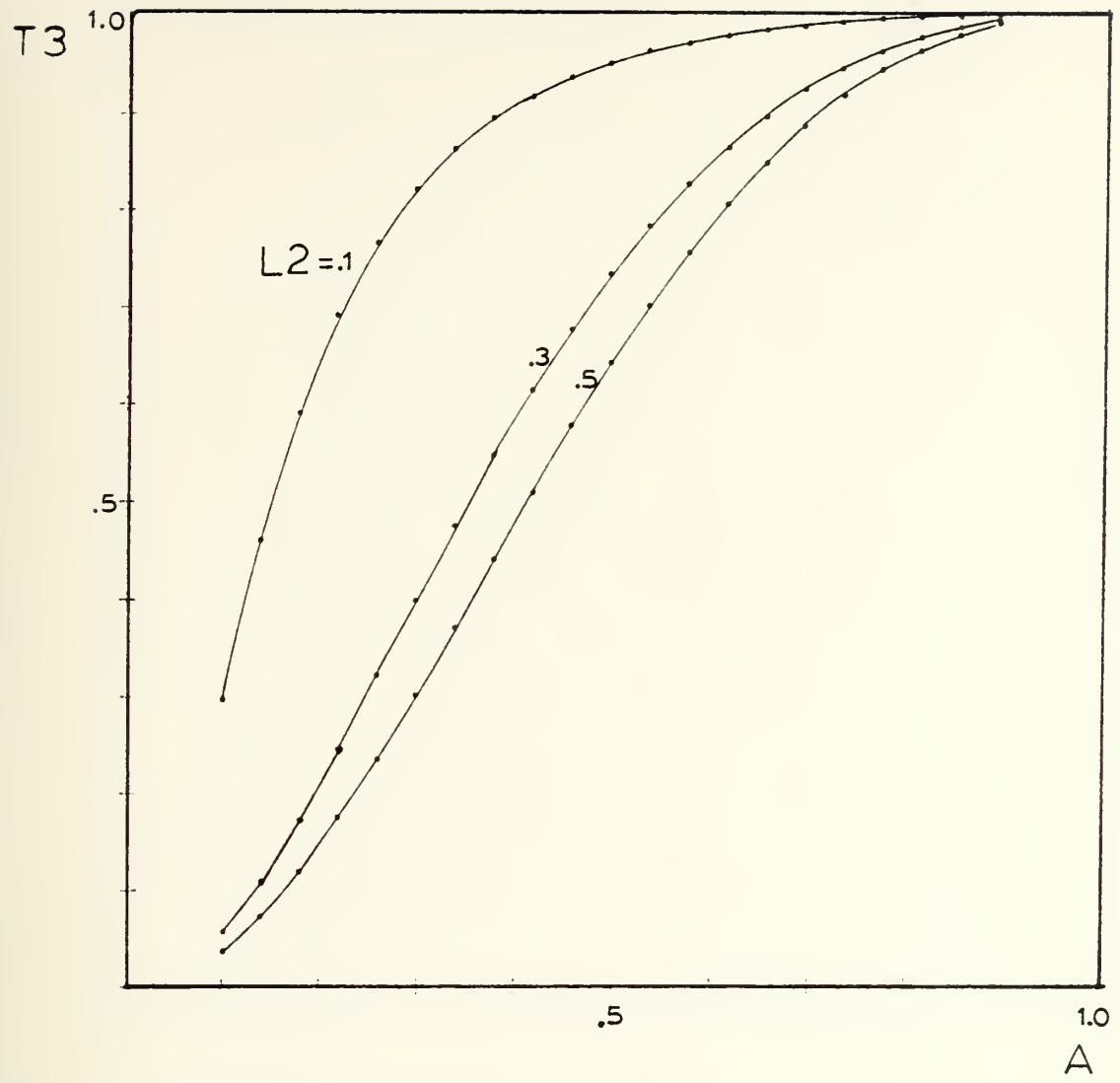

A = SOUND SPEED RATIO

A1 = INCIDENT ANGLE

L2 = LAYER WIDTH/WAVELENGTH RATIO

T3 = SOUND POWER TRANSMISSION COEFFICIENT

Figure 35. Sound power transmission coefficient vs. sound speed ratio, parameter L2 for constant A1 = 0°

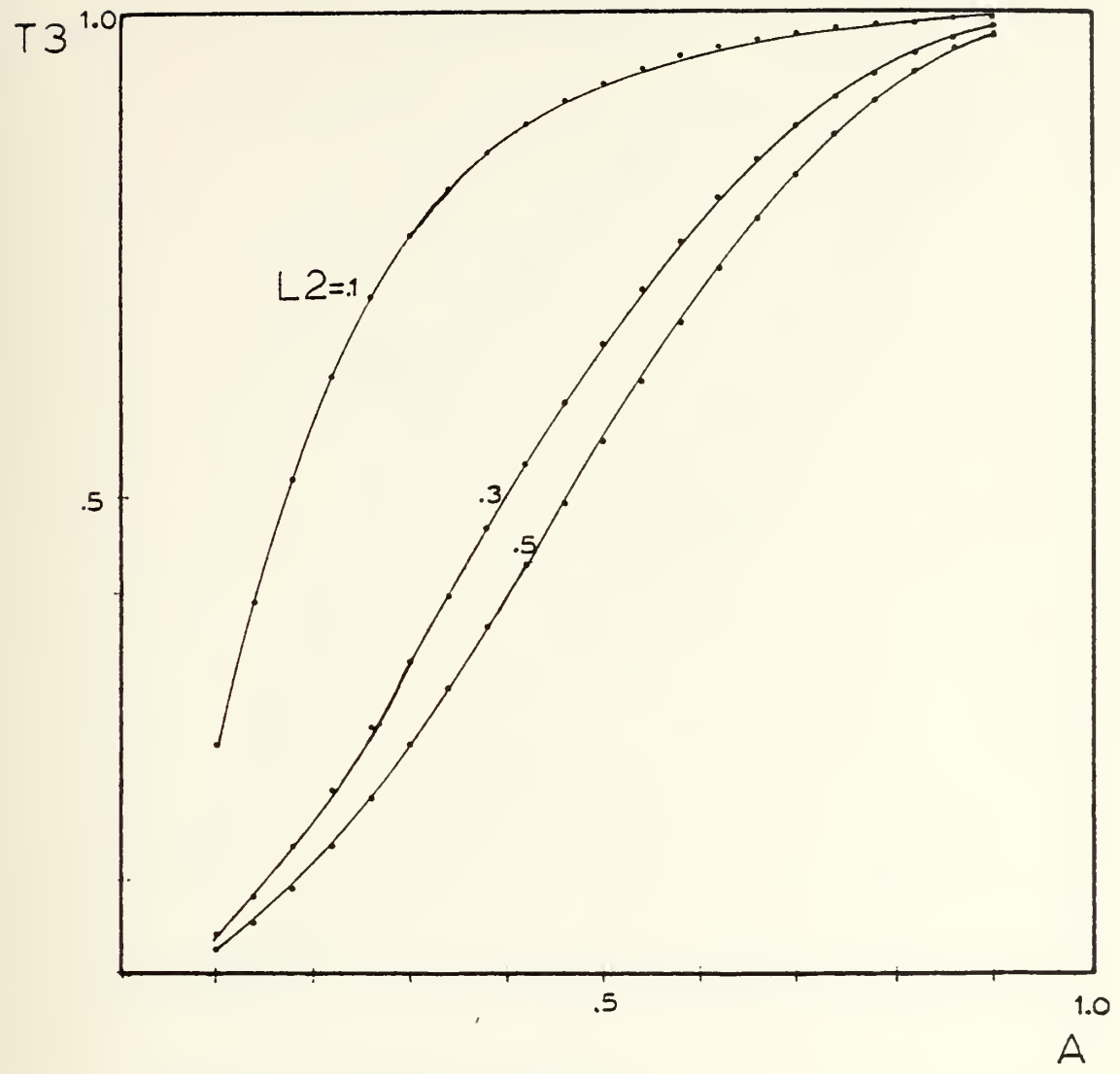

A = SOUND SPEED RATIO

A1 = INCIDENT ANGLE

L2 = LAYER WIDTH/WAVELENGTH RATIO

T3 = SOUND POWER TRANSMISSION COEFFICIENT

Figure 36. Sound power transmission coefficient vs. sound speed ratio, parameter L2 for constant A1 = 30°

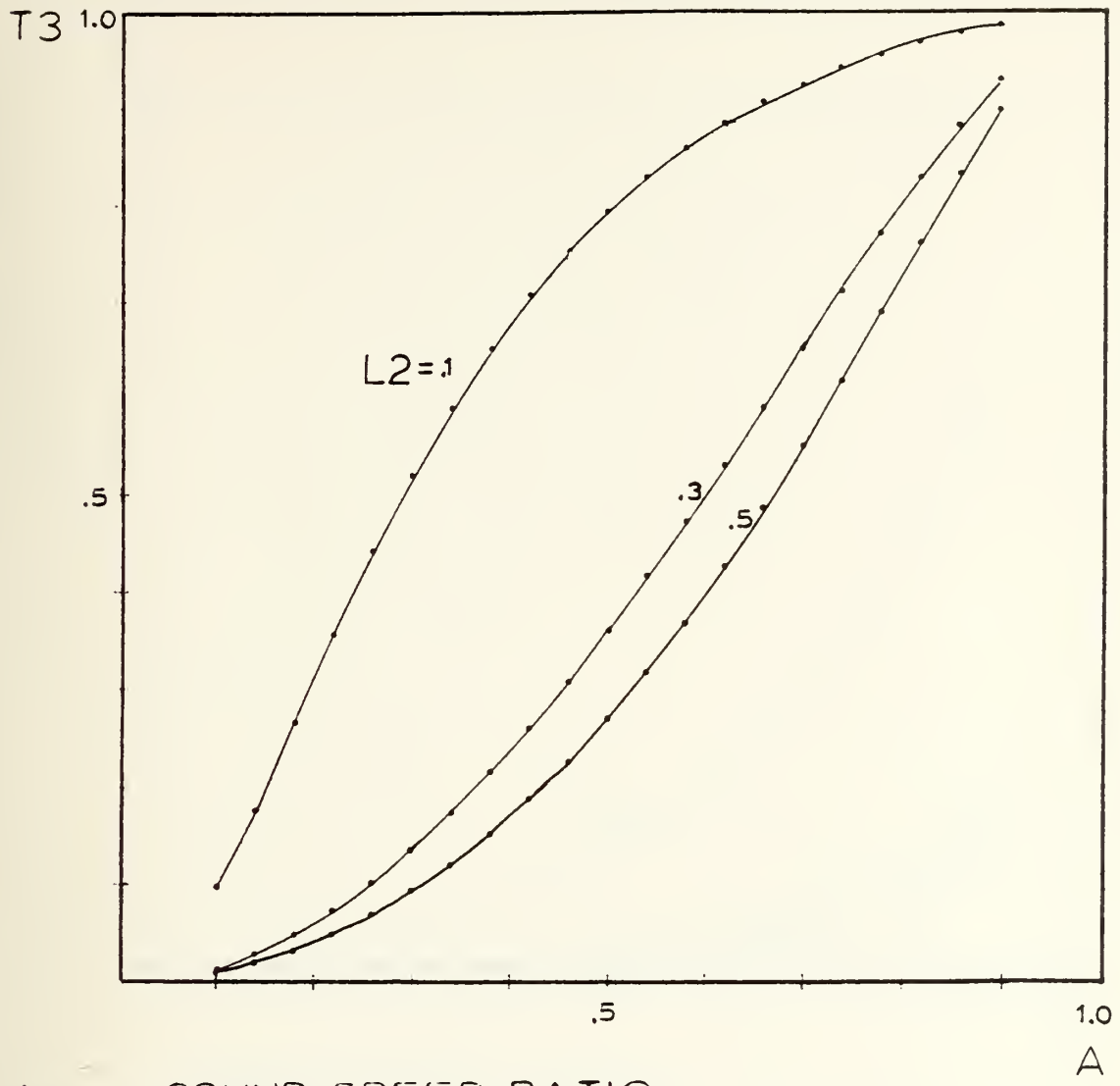

A = SOUND SPEED RATIO

A1 = INCIDENT ANGLE

L2 = LAYER WIDTH/WAVELENGTH RATIO

T3 = SOUND POWER TRANSMISSION COEFFICIENT

Figure 37. Sound power transmission coefficient vs. sound speed ratio, parameter L2 for constant A1 = 60^{o}

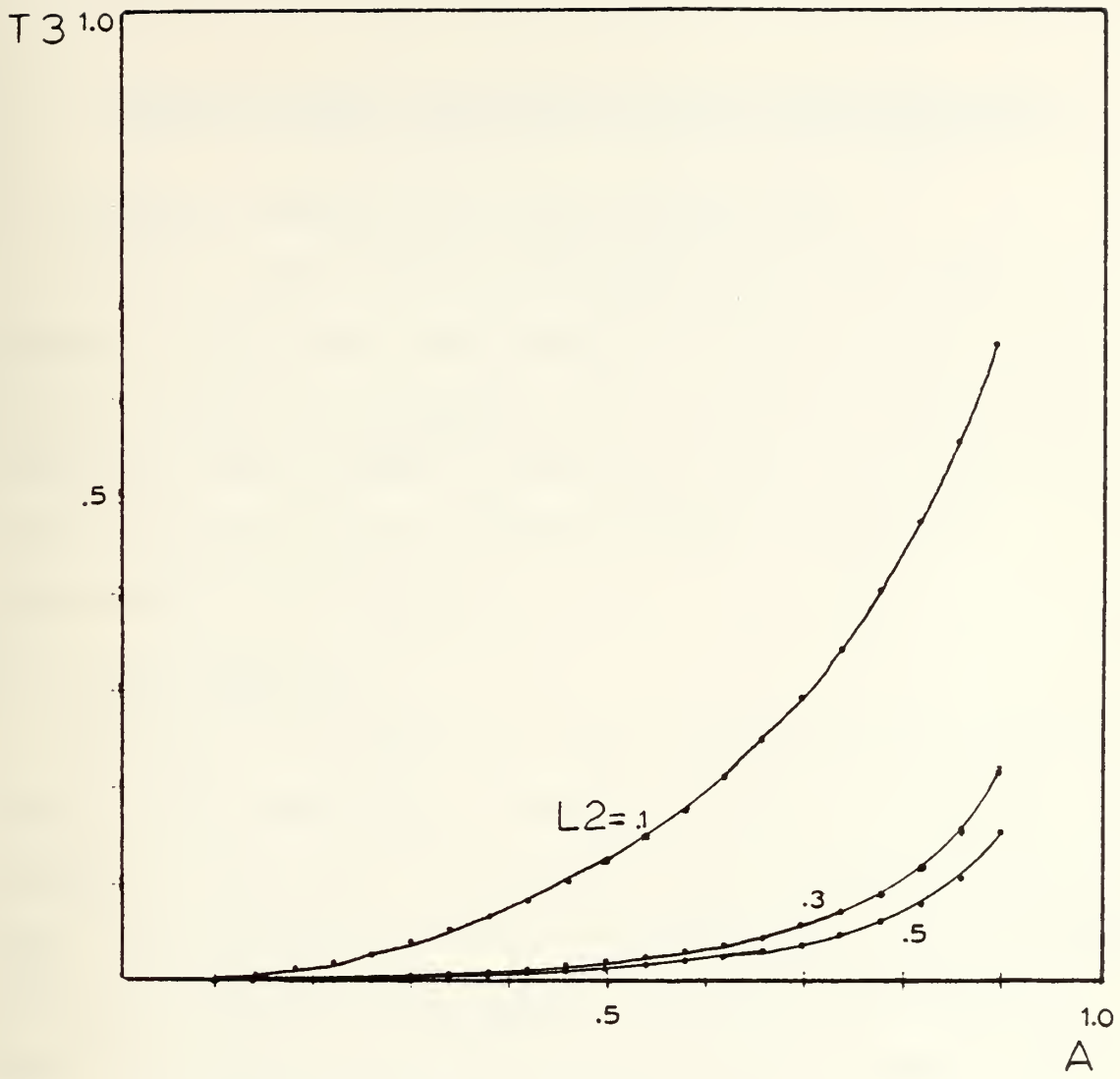

A = SOUND SPEED RATIO

A1 = INCIDENT ANGLE

L2 = LAYER WIDTH/WAVELENGTH RATIO

T3 = SOUND POWER TRANSMISSION COEFFICIENT

Figure 38. Sound power transmission coefficient vs. sound speed ratio, parameter L2 for constant A1 = 85°

V. BUBBLE SCREEN APPROXIMATIONS AND RECOMMENDATIONS

A. FREQUENCY BANDS WITH LITTLE ATTENUATION

Options 1 and 6 shows that there will be at least 10 percent of the layer ratio range virtually unaffected by a bubble screen. So for any given spectrum, there will be frequency bands of small attenuation which occur when the screen thickness is an integer multiple of one-half wavelengths in the layer.

B. LAYER SPREADING

Answers to questions on layer-width spreading were not found in the literature. Forcing parameters which are present in Carr Inlet which would cause a bubble screen to lose its simulated parallel interfaces with the surrounding media are bubble interactions, turbulent bubble motion, and inlet currents. In order to understand these effects, it might be better to conduct an experimental study at Carr Inlet and not a theoretical study because predictability rapidly disappears due to turbulent effects when bubbles grow larger than 1 to 2 cm.

However, an estimate of the layer spreading may be taken from a linear extrapolation of the observed laboratory results of Carstenson and Foldy. [Ref. 52] Their screen spread up to 6 in. for a rise of 10 ft. Figure 39 shows

DEPTH (IN FEET)	THICKNESS
10	.5
100	5.
200	10.
300	15.
400	20.
500	25.
600	30.

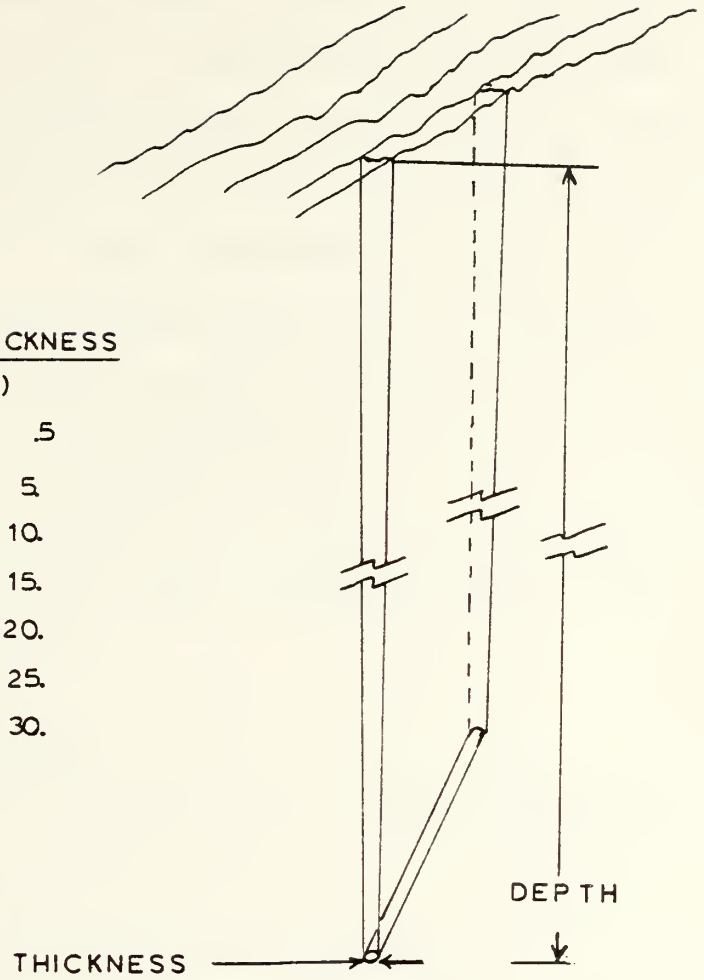

Figure 39. Bubble screen spreading effect

approximate layer thicknesses for a linear extrapolation. The corresponding screen volume increase in this case is a factor of 60 from 600 ft. to the surface. At the same time, the bubbles formed at 600 ft. are expanding their volume due to decreased hydrostatic pressure by a factor of about 18 atmospheres. So for this hypothetical case, the fraction volume of air to water changes by a factor of about one-third. This could cause a change of speed of sound of 200 - 300 m/s.

When considering an approximation like this, the number of unknowns involved indicate the uncertainty inherent in projecting any laboratory layer spreading data to the dimensions of Carr Inlet.

C. EXPERIMENTAL SCALING

The factors to be considered for proper scaling of laboratory experiments are:

1. Pressure change during bubble ascent
2. Height, length, thickness of the bubble layer
3. Angle of incidence and frequency of incident sound
4. Path lengths of sound

Of these factors, the pressure change is the most difficult to scale because volume expansion of the bubble would cause a significant change in the speed of sound.

On site experiments at Carr Inlet appear to be the only viable method to test the results of this sensitivity analysis.

D. RECOMMENDATIONS AND ALTERNATIVES

The purpose of this thesis was to investigate the benefits of a bubble screen which may offer some isolation from underwater noise interference at Carr Inlet. As a result of this sensitivity analysis and further investigation, the following recommendations are made:

1. An alternate screen position as shown in Figure 40.

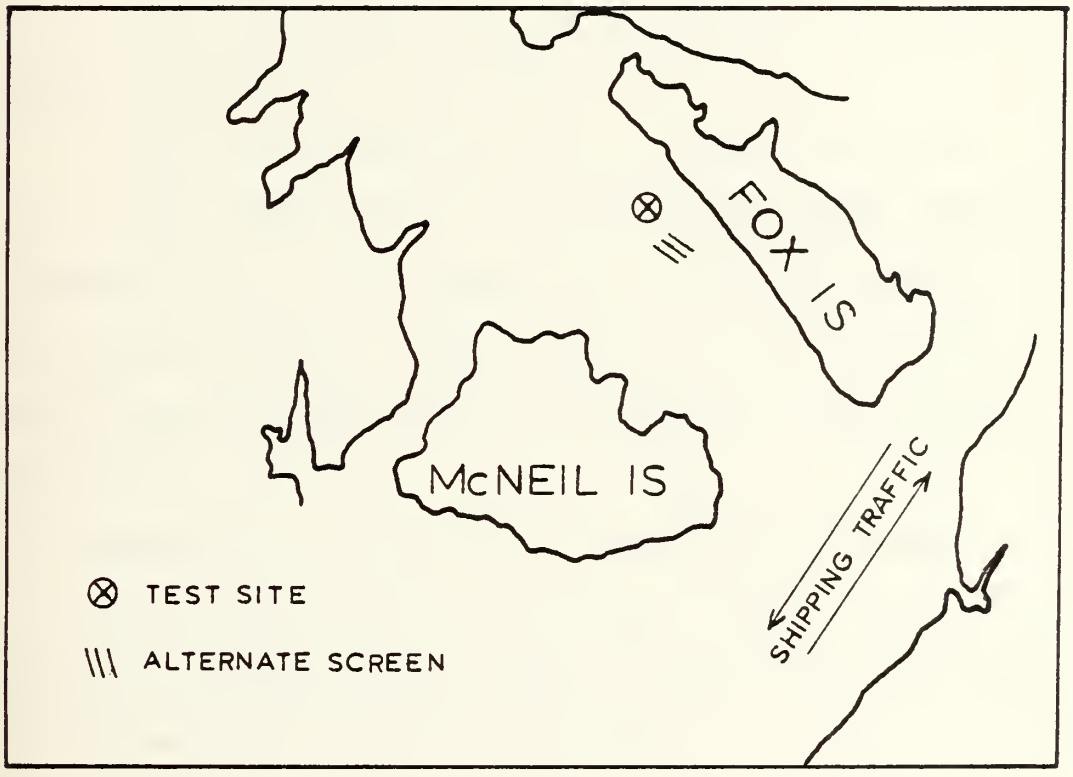

Figure 40. Alternate bubble screen position

a. The advantages of this position are:

(1) Only a fraction of the piping (one estimate for piping to cross the inlet for a uniform screen required either a large number of in line pressure regulators or almost 100 km of piping).

(2) Shallower depth allowing less dispersion of bubble layer.

(3) Exploitation of the high attenuation predicted in this sensitivity at steep angles of incidence.

b. The disadvantages include:

(1) Increased noise interference when screen is placed closer to the test site.

(2) Low frequency sound still not affected.

(3) Diffraction of sound around edges reduces any attenuation. Further study for any perforated pipe bubble screen mechanism should include pipe suspension or anchoring devices, pipe cleaning methods and compressor requirements.

2. Conduct an on-site layer spreading experiment.

3. As an alternative to the bubble screen solution, investigate the benefits of adaptive beam forming to null out bothersome interference directions.

VI. CONCLUSIONS

A. The insulating capability of a bubble screen at Carr Inlet is a function of the angle and frequency of incident sound energy and the width and speed of sound of the bubble layer. Of these parameters, the angle of incidence and the speed of sound in the layer are the most important to consider.

B. There will be approximately 10 percent of the frequency spectrum over which virtually no attenuation of sound will occur no matter what speed of sound could reasonably be acheived in the bubble layer.

C. The maximum consistent attenuation which could be expected is approximately 10 dB at bubble concentrations greater than about 5×10^{-3}.

These conclusions are based on the assumption that the air-water mixture in the layer is an ideal, homogeneous fluid. As a next step in the improvement of this model, the case of a lossy medium should be incorporated to include the effects of absorption of a bubble screen.

APPENDIX A: BUBBLE SCREEN POSITION AT CARR INLET.

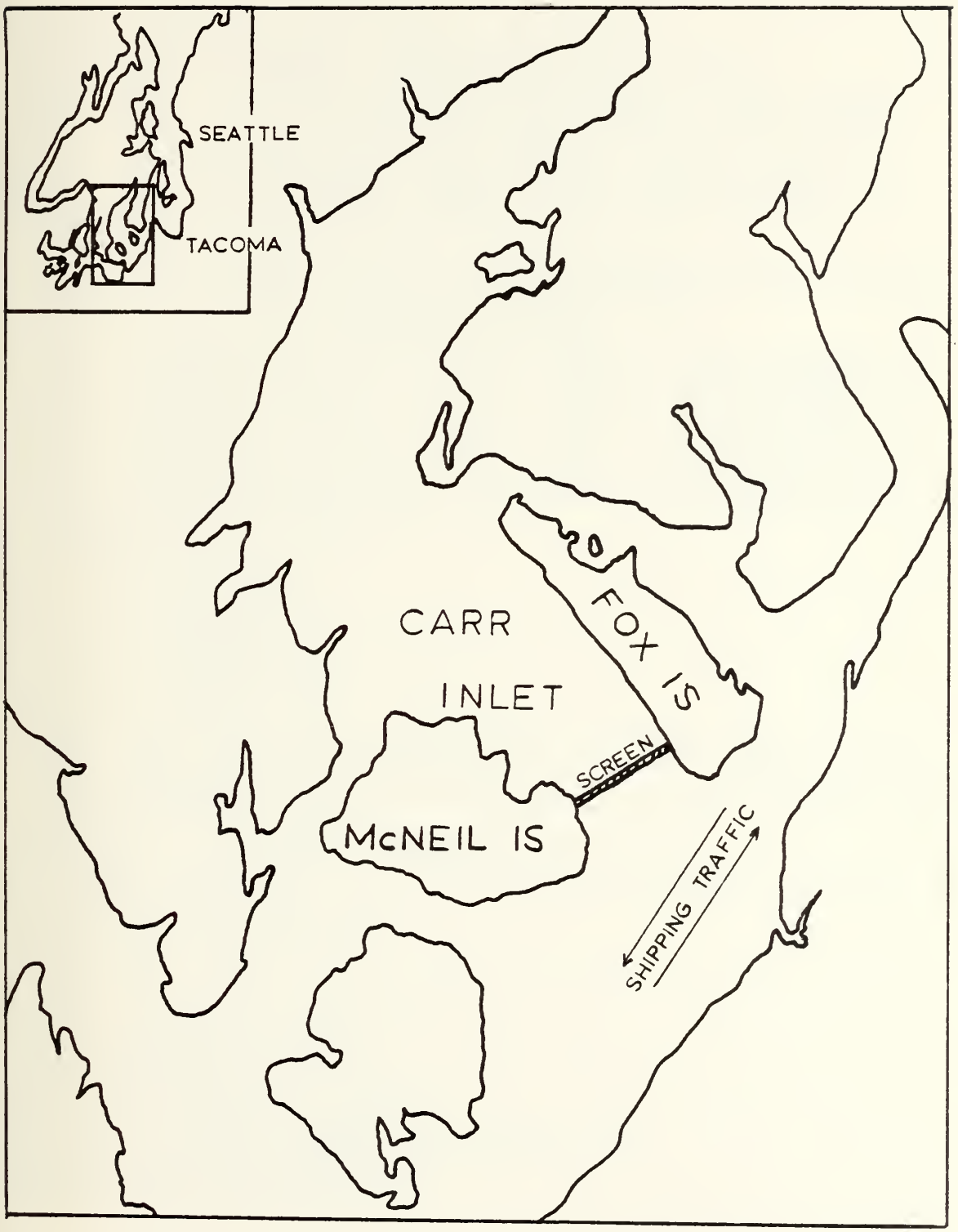

COMPUTER PROGRAM

```
10 REM ; PROGRAM NAME....."OPT6".....
20 REM ; PURPOSE...PLOTS THE POWER TRANSMISSION COEFFICIENT
(T3) FOR A PLANE WAVE INCIDENT ON A BUBBLE SCREEN LAYER IN
WATER.  THE DESIRED OUTPUT DISPLAY IS SELECTED FROM ONE OF
THE OPTIONS BELOW
30 REM ; .....DEFINITION OF VARIABLES.....
40 REM ; "A" IS ACOUSTIC IMPEDANCE RATIO = R2/R1
50 REM ; "A1"   IS THE INCIDENT ANGLE MEASURED FROM NORMAL
60 REM ; "A2" IS THE ANGLE OF TRANSMISSION IN THE SCREEN
70 REM ; "C" IS THE SOUND SPEED RATIO=C2/1500="A" APPROX
80 REM ; "C2" IS THE SOUND SPEED IN THE BUBBLE LAYER
90 REM ; "L" IS THE RATIO, BUBBLE SCREEN WIDTH/WAVELENGTH
100 REM ; "L1" IS THE NORMALIZING FACTOR FOR L
110 REM ; "L2" = L/L1
120 REM ; "T3" IS THE SOUND POWER TRANSMISSION COEFF(OFFICER)
130 REM ; "S" IS THE SELECTED PLOTTING OPTION
140 REM ; .....PLOTTING OPTIONS.....
150 REM ; OPTION 1 IS T3 VS L2 FOR CONST A1 AND PARAMETER A
160 REM ; OPTION 2 IS T3 VS A1 FOR CONST L AND PARAMETER A
170 REM ; OPTION 3 IS T3 VS A1 FOR CONST A AND PARAMETER L2
180 REM ; OPTION 4 IS T3 VS L2 FOR CONST A AND PARAMETER A1
190 REM ; OPTION 5 IS T3 VS A FOR CONST L AND PARAMETER A1
200 REM ; OPTION 6 IS T3 VS A FOR CONST A1 AND PARAMETER L2
210 INPUT "OPTION NUMBER =",S
215 SELECT R
220 IF S = 1 THEN 300
230 IF S = 2 THEN 570
240 IF S = 3 THEN 840
250 IF S = 4 THEN 1100
260 IF S = 5 THEN 1380
270 IF S = 6 THEN 1700
280 REM ; .....SUBROUTINE OPTION 1.....
290 REM ; THIS SUBROUTINE PLOTS T3 VS  L2 (A1 CONST), PAR A
300 INPUT "INCIDENT ANGLE IN RADIANS(EA 10 DEG=.174 RAD)=",A1
310 SELECT PRINT 213(64)
320 PRINT "     INCIDENT ANGLE=",A1
330 PRINT "     T3(0-1.0) VS L2(0-1.0), PARAMETER A(.1-.9)"
340 SELECT PRINT 413
350 PLOT (10) (0,-50,"+")
360 PLOT (10) (50, 0, "+")
370 PLOT (-500, 0,)
380 FOR A = .1 TO .9 STEP .4
390 H=0: V=0: H1=0: V1=0
400 A2 = ARCSIN(A*SIN(A1))
410 M1 = A*COS(A1)/COS (A2)
420 M2 = (1/A)*COS(A2)/COS(A1)
430 L1 = 1/(2*SQR(1-A*A*SIN(A1)*SIN(A1)))
440 FOR L2 = 0 TO 1 STEP .02
450 B2 = 2*#PI*L2*L1*COS(A2)
```

```
460 D1 = COS(B2)*COS(B2)
470 D2 = SIN(B2)*SIN(B2)
480 T3 = 1/(D1+((M1+M2)*(M1+M2)/4*D2))
490 H = INT(L2*500): V = INT(T3*500)
500 PLOT((H-H1),(V-V1),HEX(FB))
510 H1 = H: V1 = V
520 NEXT L2
530 PLOT (-H,-V,)
540 NEXT A
550 GOTO 210
560 REM ; ..............SUBROUTINE OPTION 2.................
570 REM ; THIS SUBROUTINE PLOTS T3 VS A1 (L CONST), PARAM. A
580 INPUT "BUBBLE LAYER/WAVELENGTH=",L
590 SELECT PRINT 213(64)
600 PRINT "     BUBBLE LAYER/WAVELENGTH=",L
610 PRINT "     T3 (0-1.0) VS A1(0-89 DEG), PARAM A(.1-.9)
620 SELECT PRINT 413
630 PLOT (10) (0,-50,"+")
640 PLOT (10) (50,0,"+")
650 PLOT (-500,0,)
660 FOR A = .1 to .9 STEP .4
670 H=0: V=0: H1=0: V1=0
680 FOR A1 = 0 TO 1.56 STEP .04
690 A2 = ARCSIN(A*SIN(A1))
700 M1 = A* COS(A1)/COS(A2)
710 M2 = (1/A)*COS(A2)/COS(A1)
720 B2 = 2*#PI*L*COS(A2)
730 D1 = COS(B2)*COS(B2)
740 D2 = SIN(B2)*SIN(B2)
750 T3 = 1/(D1+((M1+M2)*(M1+M2)/4*D2))
760 H=INT(A1*286): V= INT(T3*500)
770 PLOT ((H-H1),(V-V1),HEX(FB))
780 H1 = H: V1 = V
790 NEXT A1
800 PLOT (-H,-V,)
810 NEXT A
820 GOTO 210
830 REM ; ..............SUBROUTINE OPTION 3.................
840 REM ; THIS SUBROUTINE PLOTS T3 VS A1 (CONST A), PARAM. L2
850 INPUT "IMPEDANCE RATIO (R2/R1)=",A
860 SELECT PRINT 213(64)
870 PRINT "     IMPEDANCE RATIO (R2/R1)=",A
880 PRINT "     T3 (0-1) VS A1(0-89 DEG), PARAM L2()-0.5)"
890 PLOT (10) (0,-50,"+")
900 PLOT (10)(50,0,"+")
910 PLOT (-500,0,)
920 FOR L2 = 0 TO .5 STEP .1
930 H=0: V=0: H1=0: V1=0
940 FOR A1 = 0 TO 1.56 STEP .04
950 L1 = 1/(2*SQR(1-A*A*SIN(A1)*SIN(A1)))
```

```
960 A2 = ARCSIN(A*SIN(A1))
970 M1 = A*COS(A1)/COS(A2)
980 M2 = (1/A)*COS(A2)/COS(A1)
990 B2 = 2*#PI*L2*L1*COS(A2)
1000 D1= COS(B2)*COS(B2)
1010 D2 = SIN(B2)*SIN(B2)
1020 T3 = 1/(D1+((M1+M2)*(M1+M2)/4*D2))
1030 H = INT(A1*286): V = INT(T3*500)
1040 PLOT ((H-H1),(V-V!),HEX(FB))
1050 H1 = H: V1 = V
1060 NEXT A1
1070 PLOT (-H,-V,)
1080 NEXT L2
1090 GOTO 210
1100 REM ; .............SUBROUTINE OPTION 4.................
1110 REM ; THIS SUBROUTINE PLOTS T3 VS L (CONST A), PARAM A1
1120 INPUT "IMPEDANCE RATIO (R2/R10=", A
1130 SELECT PRINT 213(64)
1140 PRINT "     IMPEDENCE RATIO(R2/R1)=",A
1150 PRINT "     T3(0-1) VS L2(0-1), PARAMETER A1(22 DEG INC)"
1160 SELECT PRINT 413
1170 PLOT (10) (0,-50,"+")
1180 PLOT (10) (50,0,"+")
1190 PLOT (-500,0,)
1200 FOR A1 = 0 TO 1.56 STEP .39
1210 H=0: V=0: H1=0: V1=0
1220 L1 = 1/ (2*SQR(1-A*A*SIN(A1)*SIN(A1)))
1230 FOR L2 = 0 TO 1. STEP .02
1240 A2 = ARCSIN(A*SIN(A1))
1250 M1 = A*COS(A1)/COS(A2)
1260 M2 = (1/A)*COS(A2)/COS(A1)
1270 B2 = 2*#PI*L2*L1*COS(A2)
1280 D1 = COS(B2)*COS(B2)
1290 D2 = SIN(B2)*SIN(B2)
1300 T3 = 1/(D1+((M1+M2)*(M1+M2)/4*D2))
1310 H = INT(L2*500): V = INT(T3*500)
1320 PLOT ((H-H1),(V-V1), HEX(FB))
1330 H1 = H: V1 = V
1340 NEXT L2
1350 PLOT (-H,-V,)
1360 NEXT A1
1370 GOTO 210
1380 REM ; .............SUBROUTINE OPTION 5.................
1390 REM ; THIS SUBROUTINE PLOTS T3 VS A (CONST L2), PARAM A1
1400 INPUT "BUBBLE LAYER/WAVELENGTH RATIO=",L
1410 SELECT PRINT 213(64)
1420 PRINT "     BUBBLE LAYER/WAVELENGTH RATIO=",L
1430 PRINT "     T2(0-1) VS A(0-1), PARAM A1(22 DEG INC)
1440 PLOT (10) (0,-50,"+")
1450 PLOT (10) (50,0,"+")
1460 PLOT (-500,0,)
```

```
1470 FOR A1 = 0 TO 1.56 STEP .39
1480 H=0: V=0: H1=0: V1=0
1490 FOR A = .1 TO .9 STEP .04
1500 A2 = ARCSIN(A*SIN(A1))
1510 M1 = A*COS(A1)/COS(A2)
1520 M2 = (1/A)*COS(A2)/COS(A1)
1530 B2 = 2*#PI*L*COS(A2)
1540 D1 = COS(B2)*COS(B2)
1550 D2 = SIN(B2)*SIN(B2)
1560 T3 = 1/(D1+((M1+M2)*(M1+M2)/4*D2))
1570 H = INT(A*500): V = INT(T3*500)
1580 PLOT ((H-H1),(V-V1),HEX(FB))
1590 H1=H: V1=V
1600 NEXT A
1610 PLOT (-H,-V,)
1620 NEXT A1
1630 GOTO 210
1700 REM ; ..............SUBROUTINE OPTION 6.................
1710 SELECT R
1720 REM ; THIS SUBROUTINE PLOTS T3 VS A (CONST A1), PARAM L2
1730 INPUT"ANGLE OF INCIDENCE=",A1
1740 SELECT PRINT 213(64)
1750 PRINT "ANGLE OF INCIDENCE=",A1
1760 PRINT "T3(0-1) VS A(0-1), PARAMETER L2(0-.5, .1 STEPS)"
1770 PLOT (10) (0,-50,"+")
1780 PLOT (10) (50,0,"+")
1790 PLOT (-500,0,)
1800 FOR L2 = 0 TO .5 STEP .1
1810 H=0: H1=0: V=0: V1=0
1820 FOR A = .1 TO .9 STEP .04
1830 L1 = 1/(2*SQR(1-A*A*SIN(A1)*SIN(A1)))
1840 A2 = ARCSIN(A*SIN(A1))
1850 M1 = A*COS(A1)/COS(A2)
1860 M2 = (1/A)*COS(A2)/COS(A1)
1870 L = L2*L1
1880 B2 = 2*#PI*L*COS(A2)
1890 D1 = COS(B2)*COS(B2)
1900 D2 = SIN(B2)*SIN(B2)
1910 T3 = 1/(D1+((M1+M2)*(M1+M2)/4*D2))
1920 H = INT(A*500): V = INT(T3*500)
1930 PLOT ((H-H1),(V-V1),HEX(FB))
1940 H1 = H: V1 = V
1950 NEXT A
1960 PLOT (-H,-V,)
1970 NEXT L2
1980 GOTO 210
1990 END
```

LIST OF REFERENCES

1. Minnaert, M., "On Musical Air Bubbles and the Sounds of Running Water," Philosophical Magazine, v. 16, 1933.

2. Carstenson, E. L., and Foldy, L. L., "Propagation of Sound Through a Liquid Containing Bubbles," Journal of the Acoustical Society of America, v. 19, May 1947.

3. Donaldson, W. J. and MacFarlane, B. N., Design of an Improved Acoustic System for Determination of the Concentration of Microbubbles in the Ocean, M.S. Thesis, Naval Postgraduate School, December 1969, p.13.

4. Carstenson and Foldy, "Propagation of Sound", p.496.

5. Medwin, H., Oceanic Acoustic Modeling: Part 2, Acoustical Probing for Microbubbles at Sea, proceedings of a Conference at SACLANT ASW RESEARCH CENTER on 8-11 September 1975, p.6-15.

6. Ibid, p.6-2.

7. MacPherson, J. D., "The Effect of Gas Bubbles on Sound Propagation in Water," Proceedings of the Physical Society of London, v. 70, 1957.

8. Ibid, p.85.

9. Carstenson and Foldy, "Propagation of Sound", p.483.

10. Fox, F. E., Curley, S. R., and Larson, G. S., "Phase Velocity and Absorption Measurements in Water Containing Air Bubbles," Journal of the Acoustical Society of America, v. 27, May 1955.

11. Datta, R. L., Napier, D. H., and Newitt, D. M., "The Properties and Behavior of Gas Bubbles Formed at a Circular Orifice," Institute of Chemical Engineers, Transactions, v. 23, 1950.

12. Van Krevelen, D. W., and Hoftijzer, P. T., "Studies of Gas Bubble Formation," Chemical Engineering Progress, v. 46, January 1950.

13. Verschoor, H., "Some Aspects of the Motion of a Swarm of Gas Bubbles Rising through a Vertical Liquid Column," Institution of Chemical Engineers Transactions, v. 28, 1950.

14. Pattle, R. E., "The Aeration of Liquids, Part II. Factors in the Production of Small Bubbles," Institution of Chemical Engineers Transactions, v. 28, 1950, p.32.

15. Walters, J. K., and Davidson, J. F., "The Initial Motion of a Gas Bubble Formed in an Inviscid Liquid, Part I," Journal of Fluid Mechanics, v. 12, part 3, March 1962, p.408.

16. Walters, J. K. and Davidson, J. F., "The Initial Motion of a Gas Bubble Formed in an Inviscid Liquid, Part 2," Journal of Fluid Mechanics, v. 17, Part 3, November 1963, p.321.

17. Bachhuber, C., and Sanford, C., "The Rise of Small Bubbles in Water," Journal of Applied Physics v. 45, no. 6, June 1974, p. 2567.

18. Leblond, P.H., "Gas Diffusion from Ascending Gas Bubbles," Journal of Fluid Mechanics, v. 35, part 4, 1969.

19. Datta, Napier and Newitt, "The Properties and Behavior of Gas Bubbles," p.17.

20. Van Krevelen and Hoftijzer, "Studies of Gas Bubble Formation," p.30.

21. David Taylor Model Basin Report 805, Criterion for the Design of Bubble Screening Systems, by S. F. Crump, February 1957.

22. Clift, R., Grace, J. R., and Weber, M. E., Bubbles, Drops, and Particles, Academic Press, 1978.

23. Pattle, R. E., "The Aeration of Liquids, Part I," Institution of Chemical Engineers Transactions, v. 28, 1950.

24. Pattle, "The Aeration of Liquids, Part II."

25. Datta, Napier and Newitt, "The Properties and Behavior of Gas Bubbles," p.20.

26. Clift, Grace and Weber, Bubbles, p.72.

27. Soo, S. L., Fluid Dynamics of Multiphase Systems, Blaisdell, 1967, p.121.

28. Strasberg, M., "Gas Bubbles as Sources of Sound in Liquids," Journal of the Acoustical Society of America, v. 28, January 1956, p.25.

29. Clift, Grace and Weber, Bubbles, p.38.

30. Van Krevelen and Hoftijzer, "Studies of Gas Bubble Formation."

31. Strasberg, "Gas Bubbles as Sources," p.23.

32. Ibid, p.23.

33. Ibid, p.24.

34. Ibid, p.25.

35. Meyer, E., and Tamm, K., "Eigenschwinging und Dämpfung von Gasblasen in Flüssigkeiten," Akustische Zeitschrift, v. 4, May 1939, also TMB Translation Report 109, Natural Vibration and Damping of Gas Bubbles in Liquids, April 1943.

36. Foldy, L. L., Propagation of Sound Through a Liquid Containing Bubbles: Part I, General Theory, OSRD 3601, NDRC, 6.1-Sr 1130-1378, Project NS-141, USRL, 25 April 1944.

37. NDRC Summary Technical Report Division 6, v. 8, Physics of Sound in the Sea, ed. R. WILDT, 1946.

38. Carstenson and Foldy, "Propagation of Sound," p.501.

39. Wood, A. B., A Textbook of Sound, Mac Millan, 1941, p.362.

40. NDRC Report no. 6, 1-sr20-918 (1943), by L. Spitzer, Jr., 1943.

41. Silberman, E. , "Sound Velocity and Attenuation in Bubbly Mixtures Measured in Standing Wave Tubes," Journal of the Acoustical Society of America, v. 29, August 1957, p.930.

42. Campbell, I. J., and Pitcher, A. S., Supplement to the Proceedings Joint Admiralty-U.S. Navy Meeting on Hydroballistics, 1955.

43. Wood, A Textbook of Sound, p.362.

44. Silberman, "Sound Velocity and Attenuation", p.930.

45. Officer, C. B., Introduction to the Theory of Sound Transmission, McGraw-Hill, 1958.

46. Brekhovskikh, L. M., Waves in Layered Media, Academic Press, 1960.

47. University of Washington Department of Oceanography Special Report no. 19, Oceanographic Survey of Carr Inlet, Part XVII - Summary Report, by Barnes, C. A., Collins, E. E., and Paquette, R. G., August 1955.

48. Silberman, "Sound Velocity and Attenuation,"p.925.

49. Wood, A Textbook of Sound, p.362.

50. Silberman, "Sound Velocity and Attenuation," p.930.

51. Officer, Introduction to the Theory of Sound Transmission, p.224.

52. Carstenson and Foldy. "Propagation of Sound," p.482.

BIBLIOGRAPHY

Agranat, B. A., and Bashkirov, V.I., "Effect of Static Pressure on the Acoustical Properties of a Cavitating Liquid," Soviet Physics-Acoustics, v. 15, April-June, 1970.

Albers, V. M., Underwater Acoustics Handbook, Pennsylvania State University Press, 1960.

Bachhuber, C., and Sanford, C., "The Rise of Small Bubbles in Water," Journal of Applied Physics, v. 45, no. 6, June 1974.

Bobber, R. J., Underwater Electroacoustic Measurements, U.S. Government Printing Office, 1970.

Brekhovskikh, L. M., "Acoustics and the Ocean," Soviet Physics-Acoustics, v. 24, no. 5, September-October, 1978.

Brekhovskikh, L. M., Waves in Layered Media, Academic Press, 1960.

Buxcey, S., McNeil, J. E., and Marks, R. H., Acoustic Detection of Micro-Bubbles and Particulate Matter Near the Sea Surface, M.S. Thesis, Naval Postgraduate School, 1965.

Campbell, I. J., and Pitcher, A. S., Supplement to the Proceedings Joint Admiralty-U.S. Navy Meeting on Hydroballistics, 1955.

Carstenson, E. L., and Foldy, L. L., "Propagation of Sound Through a Liquid Containing Bubbles," Journal of the Acoustical Society of America, v. 19, May 1947.

Carstenson, E. L. and Foldy, L. L., Propagation of Sound Through Liquid Containing Bubbles, Part II, Experimental Results and Theoretical Interpretation, OSRD, 3872, NDRC 6.1-sr1130-1629, Project NS-141, USR1, 23 June 1944.

Clay, C. S., and Medwin, H., Acoustical Oceanography, Wiley, 1977.

Clift, R., Grace, J. R., and Weber, M. E., Bubbles, Drops, and Particles, Academic Press, 1978.

Crespo, A., "Sound and Shock Waves in Liquids Containing Bubbles," The Physics of Fluids, v. 12, November 1969.

Crighton, D. G., and Ffowcs Williams, J. E., "Sound Generation by Turbulent Two-Phase Flow," Journal of Fluid Mechanics, v. 36, part 3, 1969.

Crum, L. A., and Eller, A. G., "Motion of Bubbles in a Stationary Sound Field," Journal of the Acoustical Society of America, v. 48, no. 1, 1970.

Datta, R. L., Napier, D. H., and Newitt, D. M., "The Properties and Behavior of Gas Bubbles Formed at a Circular Orifice," Institute of Chemical Engineers Transactions, v. 23, 1950.

Davids, N., and Thurston, E. G., "The Acoustical Impedence of a Bubbly Mixture and Its Size Distribution Function," Journal of the Acoustical Society of America, v.22, January 1950.

David Taylor Model Basin Report R-177, The Effects of An Air-Bubble Screen on Pressures Due to Underwater Explosives, by J.J. Donoghue, August 1944.

David Taylor Model Basin Report 182, Migration of Underwater Gas Globes Due to Gravity and Neighboring Surfaces, by E. H. Kennard, December 1943.

David Taylor Model Basin Report 727, by B. Rosenberg, 1953.

David Taylor Model Basin Report 802, An Experimental Investigation of the Drag and Shape of Air Bubbles Rising in Various Liquids, by W. L. Haberman and R. K. Morton, September 1953.

David Taylor Model Basin Report 804, Diffusion of Air into Pulsating Air Bubbles, by L. Pode, March 1955.

David Taylor Model Basin Report 805, Criterion for the Design of Bubble Screening Systems, by S.F. Crump, February 1957.

David Taylor Model Basin Report 815, Experimental Study of Single Bubble Cavitation Noise, by M. Harrison, Rev. ed., November 1952.

David Taylor Model Basin Report 842 and 842A, A Brief Survey of Progress on the Mechanics of Cavitation, by P. Eisenberg, June 1953.

David Taylor Model Basin Report 1269, Hydronamic Sources of Noise, by H. M. Fitzpatrick and M. Strasberg, January 1959.

Devin, C. Jr., "Survey of Thermal Radiation, and Viscous Dampimg of Pulsating Air Bubbles in Water", Journal of the Acoustical Society of America, v. 31, December 1959.

Donaldson, W. J. and MacFarlane, B. N., Design of an Improved Acoustic System For Determination of the Concentration of Microbubbles in the Ocean, M.S. Thesis, Naval Postgraduate School, December 1969.

Drumheller, D. S. and Bedford, A. "A Theory of Bubbly Liquids," Journal of the Acoustical Society of America, v. 66, July 1979.

Epstein, P. S. and Plesset, M. S., "On the Stability of Gas Bubbles in Liquid-gas Solutions," Journal of Chemical Physics, v. 18, November 1950.

Fay, H. J., Ship Protection, U. S. Patent 1,416,955, 23 May 1922.

Foldy, L. L., Propagation of Sound Through a Liquid Containing Bubbles: Part I, General Theory, OSRD 3601, NDRC, 6.1-Sr 1130-1378, Project NS-141, USRL, 25 April 1944.

Fox, F. E., Curley, S. R., and Larson, G. S., "Phase Velocity and Absorption Measurements in Water Containing Air Bubbles," Journal of the Acoustical Society of America, v. 27, May 1955.

Garrettson, G. A., "Bubble Transport Theory with Application to the Upper Ocean," Journal of Fluid Mechanics, V. 59, part 1, 1973.

Gavigan, J. J., Watson, E. E., and King, W. F., "Noise Generation by Gas Jets in a Turbulent Wake," Journal of the Acoustical Society of America, v. 56, October 1974.

Gavrilov, L. R., "Free Gas Content of a Liquid and Acoustical Techniques for its Measurement," Soviet Physics-Acoustics, v. 15, no. 3, January-March 1970.

Glotov, V. P., Kolobaev, P. A., and Neuimin, G. G., "Investigation of the Scattering of Sound by Bubbles Generated by an Artificial Wind in Sea Water and the Statistical Distribution of Bubble Size," Soviet Physics-Acoustics, v.7, no. 4, April-June 1962.

Hartunian, R. A. and Sears, W. R., "On the Instability of Small Gas Bubbles Moving Uniformly in Various Liquids," Journal of Fluid Mechanics, v.3, part 1, October 1957.

Hiestand, F. H., Bubble Distribution in the Upper Ocean, M.S. Thesis, Naval Postgraduate School, December 1971.

Hsieh, Din-Yu and Plesset, M. S., "On the Propagation of Sound in a Liquid Containing Gas Bubbles," Physics of Fluids, V.4, no. 8, August 1961.

Huffmann, Zveare, Sound Speed Dispersion, Attenuation and Infeered Microbubbles in the Upper Ocean, M.S. Thesis, Naval Postgraduate School, December 1974.

Hydronautics Inc. Report 231-12, Growth of a Turbulent Wake in Density Stratified Media., by W. P. VanDeWatering, November 1966.

Hydronautics Inc. Report 231-24, Experiments on Turbulent Wakes in a Stable Density Stratified Environment, by W. P. VanDeWatering, February 1969.

Junger, M. C., and Cole, J. E. III, "Bubble Swarm Acoustics Insertion Loss of a Layer on a Plate," Journal of the Acoustical Society of America, v. 68, July 1980.

Kapustina, O. A., "Effect of Radiation Pressure on Rate of Ascent of Gas Bubbles in a Liquid," Soviet Physics-Acoustics, v. 14, January - March 1969.

Kieffer, S. W., "Sound Speed in Liquid-Gas Mixtures: Water-Air and Water-Steam," Journal of Geophysical Research, v. 82, no. 20, July 1977.

Kinsler, L. E., and Frey, A. R., Fundamentals of Acoustics, Wiley 2nd edition, 1962.

Klein, E., "Underwater Sound and Naval Acoustic Research Applications Before 1939," Journal of the Acoustical Society of America, v. 43, May 1968.

Laird, D. J. and Kendig, P.M., "Attenuation of Sound in Water Containing Air Bubbles," Journal of Acoustical Society of America, v. 24, no. 1, January, 1952.

Leblond, P. H., "Gas Diffusion from Ascending Gas Bubbles," Journal of Fluid Mechanics, v. 35, part 4, 1969.

Lieberman, "Air Bubbles in Water," Journal of Applied Physics, v. 28, 1957.

MacPherson, J. D., "The Effect of Gas Bubbles on Sound Propagation in Water," Proceedings of the Physical Society of London, v. 70, 1957.

McWilliam, D., and Duggins, R. K., "Speed of Sound in Bubbly Liquids," Proceedings Institution of Mechanical Engineers, v. 184, part 3C, 1969.

Medwin, H., Oceanic Acoustic Modeling: Part 2, Acoustical Probing for Microbubbles at Sea, proceedings of a Conference at SACLANT ASW RESEARCH CENTER on 8-11 September 1975.

Medwin, H., "Counting Bubbles Acoustically: A review," Ultrasonics, January 1977.

Meyer, E., and Tamm, K., "Eigenschwinging und Dämpfung von Gasblasen in Flüssigkeiten," Akustische Zeitschrift, v. 4, May 1939, also TMB Translation Report 109, Natural Vibration and Damping of Gas Bubbles in Liquids, April 1943.

Minnaert, M., "On Musical Air Bubbles and the Sounds of Running Water," Philosophical Magazine, v. 16, 1933.

Muhle, C. and Heckl, M., "Sound Radiation by Submerged Exhaust", NAVSHIPSTRANS 1321, 1972.

Naugol'nykh, K.A., and Rybak, S. A., "Wave Interaction in a Liquid Containing Gas Bubbles," Soviet Physics-Acoustics, v. 20, no. 1 July-August 1974.

NDRC Report no. 6, 1-sr20-918 (1943), by L. Spitzer, Jr., 1943.

NDRC Summary Technical Report Division 6, v. 8. Physics of Sound in the Sea, ed. R. WILDT, 1946.

Officer, C. B., Introduction to the Theory of Sound Transmission, McGraw-Hill, 1958.

Pattle, R. E., "The Aeration of Liquids, Part I," Institution of Chemical Engineers Transactions, v. 28, 1950.

Pattle, R. E., "The Aeration of Liquids, Part II. Factors in the Production of Small Bubbles," Institution of Chemical Engineers Transactions, v. 28, 1950.

Principles and Applications of Underwater Sound, Originally issued as NDRC Summary Technical Report of Division 6, v. 7, 1946. Reprinted by Department of the Navy, Washington, D. C., 1968.

Plesset, M. S., and Hsieh, Din-Yu, "Theory of Gas Bubble Dynamics in Oscillating Pressure Fields," Physics of Fluids, V. 3, November-December 1960.

Prosperetti, A. P., "Thermal Effects and Damping Mechanisms in the Forced Radial Oscillating of Gas Bubbles in Liquids," Journal of the Acoustical Society of America, V. 61, 1977.

Ross, D., Mechanics of Underwater Noise, Pergamon Press, 1976.

St. Anthony Falls Hydraulic Laboratory Report 82, A Study of the Influence of Microbubbles on Hydrodynamic Flow Noise, by J. M. Killer and S. D. Crist, April 1966.

St. Anthony Falls Hydraulic Laboratory Report 120, An Evaluation of Acoustic Techniques for Measuring Gas Bubble Size Distributions in Cavitation Research, by F. R. Schiebe and J. M. Killer, May 1971.

Scherf, W. W., Amplitude Modulation of a Stationary Acoustic Field by Cavitation Bubbles, MS Thesis, Naval Postgraduate School, December 1971.

Silberman, E., "Sound Velocity and Attenuation in Bubbly Mixtures Measured in Standing Wave Tubes," Journal of the Acoustical Society of America, v. 29, August 1957.

Soo, S. L., Fluid Dynamics of Multiphase Systems, Blaisdell, 1967.

Strasberg, M., "Gas Bubbles as Sources of Sound in Liquids," Journal of the Acoustical Society of America, v. 28, January 1956.

U.S. Naval Academy Report 278, Nucleation, Stabilization and Growth of Microbubbles in Water, by L. A. Crum, October 1978.

University of Washington Department of Oceanography Special Report no. 19, Oceanographic Survey of Carr Inlet, Part XVII-Summary Report, by Barnes, C. A., Collins, E. E., and Paquette, R. G., August 1955.

Urick, R. J., Principles of Underwater Sound, McGraw-Hill, 1972.

Vajda, T. C., Bubble Distribution in a Quiescent Ocean Calculated from the Bubble Transport Equation, M.S. Thesis, Naval Postgraduate School, June 1972.

Van Krevelen, D. W., and Hoftijzer, P. T., "Studies of Gas Bubble Formation," Chemical Engineering Progress, v. 46, January 1950.

Van Wijngaarden, L., "On the Equations of Motion for Mixtures of Liquid and Gas Bubbles," Journal of Fluid Mechanics, v. 33, part 3, 1968.

Verschoor, H., "Some Aspects of the Motion of a Swarm of Gas Bubbles Rising Through a Vertical Liquid Column," Institution of Chemical Engineers Transactions, v. 28, 1950

Walters, J. K. and Davidson, J. F., "The Initial Motion of a Gas Bubble Formed in an Inviscid Liquid, Part I," Journal of Fluid Mechanics, v. 12, part 3, March 1962.

Walters, J. K. and Davidson, J. F., "The Initial Motion of a Gas Bubble Formed in an Inviscid Liquid, Part 2," Journal of Fluid Mechanics, v. 17, Part 3, November 1963.

White, W., "The Behavior of Air Bubbles in Acoustic Fields," M.S. Thesis, Naval Postgraduate School, 1963.

Williams, B. and Foster, L, Gas Bubbles in the Sea: A Review and Model Proposals, Proceedings of a Conference at SACLANT ASW Research Center, 8-11 September 1975.

Wood, A. B., A Textbook of Sound MacMillan, 1941.

Zwick, S.A. "Growth of Vapor Bubbles in a Rapidly Heated Liquid," The Physics of Fluids, v. 3, September - October 1960.

INITIAL DISTRIBUTION LIST

		No. Copies
1.	Defense Technical Information Center Cameron Station Alexandria, Virginia 22314	2
2.	Library, Code 0142 Naval Postgraduate School Monterey, California 93940	2
3.	Department Chairman, Code 61 Department of Physics and Chemistry Naval Postgraduate School Monterey, California 93940	1
4.	Professor O. B. Wilson, Code 62Wi Naval Postgraduate School Monterey, California 93940	1
5.	Professor J. V. Sanders, Code 61Sd Naval Postgraduate School Monterey, California 93940	4
6.	LT C. T. Kelley 1812 Longmeadow Drive Montgomery, Alabama 36101	1
7.	LT K. W. Marr 2636 N. 7th Street Sheboygan, Wisconsin 53081	3
8.	Commander, Puget Sound Naval Shipyard ATTN: Carr Inlet Acoustic Range, Code 246 Bremerton, Washington 98310	10

193692
Thesis
M3525 Marr
c.1 On the design of an acoustically isolating bubble screen for the Carr Inlet Acoustic Range.